

**EVALUATION OF FILTER CAKE MINERALOGY
IN A HORIZONTAL WELL**

BY

BADR SALEM BA GERI

A Thesis Presented to the
DEANSHIP OF GRADUATE STUDIES

KING FAHD UNIVERSITY OF PETROLEUM & MINERALS

DHAHRAN, SAUDI ARABIA

In Partial Fulfillment of the
Requirements for the Degree of

MASTER OF SCIENCE

In

PETROLEUM ENGINEERING

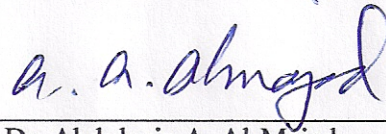
May 2012

KING FAHD UNIVERSITY OF PETROLEUM & MINERALS

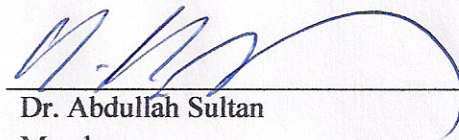
Dhahran, Saudi Arabia

This thesis, written by Mr. BADR SALEM BA GERI under the direction of his Thesis Advisor and approved by his Thesis Committee, has been presented to and accepted by the Dean of the College of Graduate Studies, in partial fulfillment of the requirements for the degree of MASTER OF SCIENCE in Petroleum Engineering.

Thesis Committee



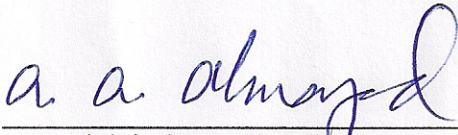
Dr. Abdulaziz A. Al-Majed
Thesis Advisor



Dr. Abdullah Sultan
Member



Dr. Anwar Ul-Hamid
Member



Dr. Abdulaziz A. Al-Majed
Department Chairman

Dr. Salam A. Zummo
Dean, College of Graduate Studies

Date: 30/5/12



DEDICATION

This thesis is dedicated to

MY BELOVED MOTHER & FATHER,

MY WIFE, MY CHILD, MY BROTHERS & SISTERS

ACKNOWLEDGMENTS

In the name of Allah, Most Gracious, Most Merciful. All praise is to Almighty Allah who gave me courage, knowledge and ability to complete this work and blessing of Allah be upon his prophet Mohammed.

I wish to express my deep appreciation and thanks to Dr. Abdulaziz A. Al-Majed, thesis advisor, Dr. Abdullah Sultan and Dr. Anwar Ul-Hamid for providing their invaluable help and guidance through this work. I also esteem the support extended by Dr. Saleh H. Mutairi of Saudi Aramco.

Acknowledgment is due to King Fahd University of Petroleum & Minerals and Saudi Aramco for the Research Assistantship. My sincere appreciation is extended to all faculty and staff of the Petroleum Engineering Department for the contribution to this work.

I am also indebted to the following help: Mr. Mansour Al-Dhafeer, Mr. Abdul Samad Iddrius, Mr. Mohammad Ali Sanito, Mr. Wesam Al-Alqam, Mr. Sarmad Zafar and Mr. Abdul Rashid, for their priceless in PETE Department, RI and CENT laboratories.

Special thanks are due to all my colleagues and friends who help me in my work and made my stay at the University memorable and source of valuable experience.

Finally, I am indebted to Eng. A. A. Bugshan & HEFHD for their extreme moral support throughout my master program career and also for their encouragement.

Table of Contents

DEDICATION	II
ACKNOWLEDGMENTS	III
LIST OF TABLES	VIII
LIST OF FIGURES	IX
THESIS ABSTRACT	XII
ARABIC ABSTRACT.....	XIII
CHAPTER 1	1
INTRODUCTION	1
CHAPTER 2	6
2.1 LITERATURE REVIEW	6
2.2 AN OVERVIEW OF FILTER CAKE PROPERTIES.....	15
2.2.1 Filter Cake Build up Mechanisms.....	15
Static Filtration Mechanism	16
Dynamic Filtration Mechanism	17
2.2.2 Filter Cake Properties	18
Filter Cake Thickness	18
Filter Cake Porosity	21
Filter Cake Permeability	23

Filter Cake Structure Analysis	32
Other properties of Filter Cake	36
CHAPTER 3	44
3.1 STATEMENT OF THE PROBLEM	44
3.2 OBJECTIVE & APPROACH.....	46
CHAPTER 4	47
EXPERIMENTAL SETUP & PROCEDURE.....	47
4.1 Drilling Fluid Properties	47
4.1.1 Drilling Fluid Density	49
4.1.2 Drilling Fluid Rheological Characteristics.....	51
4.2 Static Filtration Tests	53
4.3 Filter Cake Properties	55
4.3.1 Filter Cake Thickness	55
4.3.2 Filter Cake Minerology	56
A) Scanning Electron Microscopy (SEM)	56
B) X-Ray Diffraction (XRD)	56
4.4 Internal Filter Cake Evaluation	59
CHAPTER 5	63
RESULTS AND DISCUSSION	63
5.1 Drilling Fluid Properties	63

5.1.1	Drilling Fluid Density	63
5.1.2	Drilling Fluid Rheological characteristics	66
5.2	External Filter Cake Properties	70
5.2.1	Filter Cake Thickness	70
5.2.2	Filter Cake Characterization	74
A)	Scanning Electron Microscopy (SEM) Analysis	74
B)	X-Ray Diffraction (XRD) Analysis	81
5.3	Internal Filter Cake Evaluation Using CT Scan.....	89
CHAPTER 6		93
IMPACT OF SAND		93
6.1	Impact of Sand on Drilling Fluid Properties	93
6.1.1	Drilling Fluid Density	94
6.1.2	Drilling Fluid Rheological Characteristics.....	96
6.2	Impact of Sand on External Filter Cake & Solids Invasion	99
6.3	A Model to Predict Filter Cake Sand Content	103
	Procedure to Predict Sand Content in the Filter Cake.....	108
6.4	A Model to Predict Filter Cake Thickness.....	109
CHAPTER 7		111
7.1	CONCLUSIONS.....	111
7.2	RECOMMENDATION	114

NOMENCLATURE	115
REFERENCE.....	119
APPENDIX-A (SEM RESULTS)	126
APPENDIX-B (XRD RESULTS)	142
APPENDIX-C (CT SCAN RESULTS).....	158
VITAE	163

LIST OF TABLES

Table 2. 1: Permeability/Porosity Empirical Relationship for Various Filter cakes by (Khatib 1994)	25
Table 5. 1: Drilling Fluid Density	64
Table 5. 2: Drilling Fluid Rheological Characteristics	69
Table 5. 3: The Summary of SEM Results of Whole Filter Cake Samples	79
Table 5. 4: Quantitative Analysis of the Filter Cake (Sample 6) Using (XRD)	83
Table 5. 5: The Summary of XRD Results of Whole Filter Cake Samples	88

LIST OF FIGURES

Figure 1. 1: Schematic Diagrams of the Well.....	5
Figure 2. 1: Laser Apparatus for Filter Cake Thickness Measurement (M.d. Amanullah and C.P. Tan, 2001).	38
Figure 2. 2: Dial Gauge for Filter Cake Thickness Measurement (M.d. Amanullah and C.P. Tan 2001).	39
Figure 2. 3: (Martinez et al. 2000) Method to Determine the Permeability of Filter Cake	40
Figure 2. 4: (Tiller 2002) Method to Determine the Permeability of Filter Cake	41
Figure 2. 5: (Li et al. 2005) Method to Determine the Permeability, Typical Volume of Filtrate vs Time Curve	42
Figure 2. 6: (Dangou and Chandler 2009) Change in the Dynamic Filtration Flow Rate with the Shear Rate and Filtration	43
Figure 4. 1: A Schematic of Horizontal Well Shows the Collection Point of Drilling Fluid Samples.....	48
Figure 4. 2: Balance Arm for Determining the Drilling Fluid Density, (lb/gal), (Darley and Gray 1988)	50
Figure 4. 3: Schematic Diagram of the Viscometer (Darley and Gray 1988)	52
Figure 4. 4: Assembled High Pressure High Temperature Cell.....	54
Figure 4. 5: Scanning Electron Microscope (SEM).....	60
Figure 4. 6: X-ray Diffraction (XRD).....	61

Figure 4. 7: CT scanner.....	62
Figure 5. 1: Changes of Drilling Fluid Density with Horizontal Measured Depth.....	65
Figure 5. 2: Changes of Drilling Fluid Density with Horizontal Length.....	65
Figure 5. 3: Changes in Drilling Fluid Apparent Viscosity, Plastic Viscosity, and Yield Point with Horizontal Measured Depth	67
Figure 5. 4: Changes in Drilling Fluid Apparent Viscosity, Plastic Viscosity, and Yield Point with Horizontal Length.....	67
Figure 5. 5: Changes in Drilling Fluid Gel Strength (10 Minutes / 10 Seconds) with Measured Depth of Horizontal Section.....	68
Figure 5. 6: Changes in Drilling Fluid Gel Strength (10 Minutes / 10 Seconds) with Horizontal Length	68
Figure 5. 7: Filter Cake Sample Obtained from Fluid Loss Tests	72
Figure 5. 8: Changes in Filter Cake Thickness with Horizontal Measured Depth	73
Figure 5. 9: Changes in Filter Cake Thickness with Horizontal Length	73
Figure 5. 10: The Chemical Compositions of the Filter Cake (Sample 6) Using (SEM). 76	
Figure 5. 11: Two Different Locations (Spectrum 1&2) of Filter Cake (Sample 6) Using (SEM).....	77
Figure 5. 12: The Summary of SEM Results of the Main Four Elements.....	80
Figure 5. 13: The Phases Identification of the Filter Cake (Sample 6) Using (XRD).....	82
Figure 5. 14: The Minerlogy of Filter Cake Using XRD.....	85
Figure 5. 15: Shows the Three Regions Based on the Sand Content in Filter Cake.....	86
Figure 5. 16: The Relationship between the Lengths of Horizontal Section Drilled and Sand Percentage in Filter Cake	87

Figure 5. 17: The Internal Solid Invasions Using CT scan.....	90
Figure 5. 18: CT scan Number Result.	92
Figure 6. 1: Changes in Drilling Fluid Density with Sand Weight %	95
Figure 6. 2: Changes in Drilling Fluid Apparent Viscosity, Plastic Viscosity, and Yield Point with Sand Weight %	97
Figure 6. 3: Changes in Drilling Fluid Gel Strength (10 Minutes / 10 Seconds) with Sand Weight %	98
Figure 6. 4: Changes in Filter Cake Thickness with Sand Weight %	101
Figure 6. 5: Impact of Sand Particles Percentages on Internal Invasion Using CT scan	102
Figure 6. 6: Drilling Fluid Density and the Length of Horizontal Section Relationship	106
Figure 6. 7: Drilling Fluid Density and Sand Content Relationship.....	106
Figure 6. 8: Drilling Fluid Apparent Viscosity and the Length of Horizontal Section ..	107
Figure 6. 9: Drilling Fluid Apparent Viscosity and Sand Content Relationship	107
Figure 6. 10: Filter Cake Thickness and the Horizontal Section Length Relationship...	110
Figure 6. 11: Filter Cake Thickness and the Sand Content Relationship	110

THESIS ABSTRACT

Name of the student : **Badr Salem Ba geri**
Title of the study : **Evaluation of Filter Cake Mineralogy in a
Horizontal Well**
Major Field : **Petroleum Department**
Date of Degree : **May 2012**

Filter cake occurs intentionally during the drilling operations to prevent fluid losses to the formation and to allow good circulation for drilling fluids to the surface and is known to depend on a well-designed drilling mud fluids and additives. The filter cake must allow for minimum filtration and solid invasions to the formation and must also withstand high differential overbalance pressures. This work evaluated the filter cake properties such as filter cake thickness and mineralogy in the horizontal section of well during drilling sandstone formation.

This study focuses on the chemical composition of filter cake formed in the horizontal section, from its tip to its toe. High pressure fluid loss test were performed using real drilling fluid samples from the field which were collected during drilling of a horizontal section in a sandstone formation. The mineralogy of the external filter cake formed by fluid loss test is described in detail using both Scanning Electron Microscopy (SEM) and X-Ray Diffraction (XRD). CT scan also was used to evaluate the internal solids invasion.

The results show that for long horizontal sections in sandstone formations, the composition of the filter cake is not constant from its toe to heal and the sand percentage increases up to 50%. Since the small drilled solids, those are not properly removed, will be mixed with the drilling fluid during circulation and degrade the performance of the drilling fluid as well as become an integral part of the fabric of the filter cake. Moreover, this study investigates that as more feet of horizontal section of sandstone formation is drilled the sand percentage increases as well as the cake thickness increases. This internal invasion becomes critical when the sand percentage reaches higher than 40%, because the solids will invade into deeper zones.

MASTER OF SCIENCE DEGREE

KING FAHD UNIVERSITY OF PETROLEUM AND MINERALS
DHAHRAN, SAUDI ARABIA
May, 2012

ARABIC ABSTRACT

ملخص البحث

اسم الطالب	:	بدر سالم باجري
موضوع الدراسة	:	تقييم المكونات المعدنية لطبقة طين الحفر في بئر أفقي
التخصص	:	هندسة البترول
تاريخ التخرج	:	مايو 2012

تتكون طبقة طين الحفر اثناء حفر الأبار وذلك لبناء طبقة عازلة على جدار البئر تعمل على منع طين الحفر من التدفق إلى الطبقات النفطية. وعلية فإن تكوين هذه ال طبقة يعتمد وبشكل رئيسي على مكونات طين الحفر وما يحدث له من تغييرات اثناء حفر البئر. في هذا البحث عملنا على دراسة التركيب الكيميائي لهذه ال طبقة اضافة الى سماكتها خلال حفر الجزء الافقي من البئر. فتركزت هذه الدراسة على هذه الخصائص ومدى تغيرها في الجزء الأفقي من الطبقات الرملية. طين الحفر المستخدم في هذا البحث تم اخذه خلال حفر الجزء الأفقي من البئر. لدراسة مكونات ال طبقة يتم تكوين الكعكة اولاً عن طريق إجراء تجربة ترشيح طين الحفر تحت ضغط عالية بعد ذلك ثم استخدام جهاز المسح الميكروسكوبي الدقيق (SEM) وكذلك جهاز اشعة اكس (XRD) لدراسة مكونات هذه الطبقة. كما تم استخدام جهاز الاشعة المقطعية (CT scan) لفحص التدفق الداخلي للمواد الصلبة. اثبتت نتائج هذه البحث أن التركيب الكيميائي لطبقة طين الحفر المتكونة اثناء حفر الجزء الأفقي من البئر في الطبقات ال رملية ليس ثابتا حيث ازدادت نسبة المكونات الرملية في هذه الطبقة إلى مايقارب 50% وذلك نتيجة لتدوير قطع الصخور الدقيقة مع طين الحفر. كما اثبتت هذه الدراسة ايضا ان سماكة ال طبقة تزيد مع زيادة الطول المحفور من المقطع الافقي. كذلك الحال في نتائج الاشعة المقطعية حيث برهنت انه ومع ازدياد نسبة المكونات الرملية فان التدفق الداخلي للمواد الصلبة يشكل ضرورا حيث يصل الى عمق اكبر من مثيلة في العينات ذات المحتوى الرملي الاقل.

درجة الماجستير في علوم هندسة البترول
جامعة الملك فهد للبترول والمعادن
الظهران؛ المملكة العربية السعودية

CHAPTER 1

INTRODUCTION

It is commonly recognized that rotary drilling is used for almost all oil and gas well drilling done today. The hole is drilled by rotating a bit to which a down-ward force is applied. In drilling operations, it is of major importance to circulate drilling mud into the wellbore to clean the rock fragments from beneath the bit and carry them to the surface. This drilling fluid should also be able to control the loss through the porous formations to improve stability of wellbore and decrease risks of formation damage when contacting the reservoir. One of the drilling fluid's basic functions is to exert hydrostatic pressure over the permeable formation to prevent kicks since the drilling fluid pressure is normally kept above the formation pore pressure. This concept, called overbalanced drilling, is traditionally employed in most of drilling operations worldwide.

The drilling mud travels from the steel tank to the mud pump, from the pump through the drilling string to the bit, through the nozzles of the bit and up the annulus space between the drilling string and hole to surface, and through the contaminant removal equipment back to the suction tank. The drilling fluids are re-used in drilling operations to cut the cost. The contaminant removal equipment includes mechanical

devices for removing the solids and gases from the mud. The coarse rock cuttings are removed by the shale shaker. Additional separation of solids and gases from the mud occurs in the settling pit. In cases where finely ground solids in the mud become too great the hydro cyclones and decanting centrifuges are used. After these processes the mud recirculates into the well.

In overbalanced drilling operation, the drilling fluid invades the formation due to the positive pressure differential between the drilling fluid and formation pore pressure; this is more true in presence of permeable formations. Hence, the suspended solids in the mud are deposited on the face of the permeable formation to build a filter cake over the formation face, decreasing the rate of filtrate invasion, **Figure 1.1**. In addition to the deposition of drilling mud particles on the formation face around the wellbore, the small particles in the mud invade the formation causing an internal formation damage. Fortunately, the depth of particles invasion is usually small, ranging from less than an inch to a maximum of about 1 ft (Economides *et al.* 1994). Therefore, the mud particles should be larger than the pores (Abrams 1977). Arthur and others (1988) evaluated filter cake properties by investigating the relationship between the cake structure, as characterized by the cake compressibility, resistance, fluid loss, spurt loss and cake thickness, and the influence of pressure, temperature and mud components. Consequently, the fine drilling cuttings, which are not separated from the drilling mud while removing the solids by contaminant removal equipment, will influence the filter cake structure. Drill solids interaction with drilling fluid can produce dense, highly viscous fluid that impede and adversely affect filter cake cleanup (Burnett and Hodge 1996).

Two invasion mechanisms are notable in the well. The first, called static filtration, which occurs when the fluid pumping is interrupted and, from that point on, filtration occurs due to the positive difference between the hydrostatic pressure of the drilling fluid and the formation pore pressure. The filtration rates are controlled by the gradual growth of filter cake thickness with time. Continuous increase in thickness of filter cake with time will lead to decreasing the filtration rate and cake permeability which will greatly inhibit the growth of filter cake thickness itself.

The other invasion mechanism, called dynamic filtration, occurs when the fluid is pumped through the well. The pressure difference between the drilling fluid and reservoir pressure has the same role in this mechanism. The major difference between dynamic and static filtration can be described by saying that, in the dynamic process, the cake thickness is resultant from the dynamic equilibrium between solids particles deposition rate and the erosion rate due to the shear stresses generated by the fluid flow in the well bore. Therefore, the filtration rate to the formation tends to stabilize around a certain value while the cake thickness turns constant.

All in all, the advantages of building filter cake over the formation face with typical permeabilities ranging from 10^{-5} Darcies to 10^{-7} Darcies (Hanssen *et al.* 1999) will control fluid loss during drilling and completion operations. On the other side, filter cake causes productivity impairment at the formation face as extra skin (e.g., positive skin) which will reduce the performance of the well. Therefore, good understanding of filter cake structure leads to successful selection of drilling fluid that minimizes formations damage and selection of an effective recipe for removing the filter cake without exposure of the well to fluid loss through completion operations.

The two primary sources of solids are drilling mud chemical additives and formation cuttings. Formation cuttings are usually removed using sand solid control equipment because their presence will degrade the performance of the drilling fluid. These cuttings are ground into smaller particles if not properly removed. All current solid separation methods are either based on size exclusion or gravity. They ignore the chemical composition of the solids. For long horizontal wellbores penetrating clastic formations, the chemical composition and the physical properties of the mud play a significant role. Ground clastic fragments and debris are mixed with drilling mud during mud circulation. As so, these materials become an integral part of fabric of the filter cake.

The effect of introducing sand particles to the structure of the filter cake is significant from the filter cake removal point of view. The sand percentage might reach to 40% by weight of the mud solids making it prohibitively difficult to be removed with regular acids. Filter cake removers are designed to remove acid soluble particles such as calcium carbonate. The intrusion of sand to the fabric of the filter cake renders these treatments ineffective.

This study will focus on an aspect which was not fully covered in the literature: the chemical characteristics of filter cake (Mineralogy) formed in the horizontal section, from its tip to its toe. The knowledge gained about the sand content of the filter cake will help in the design of stimulation treatments to remove the filter cake.

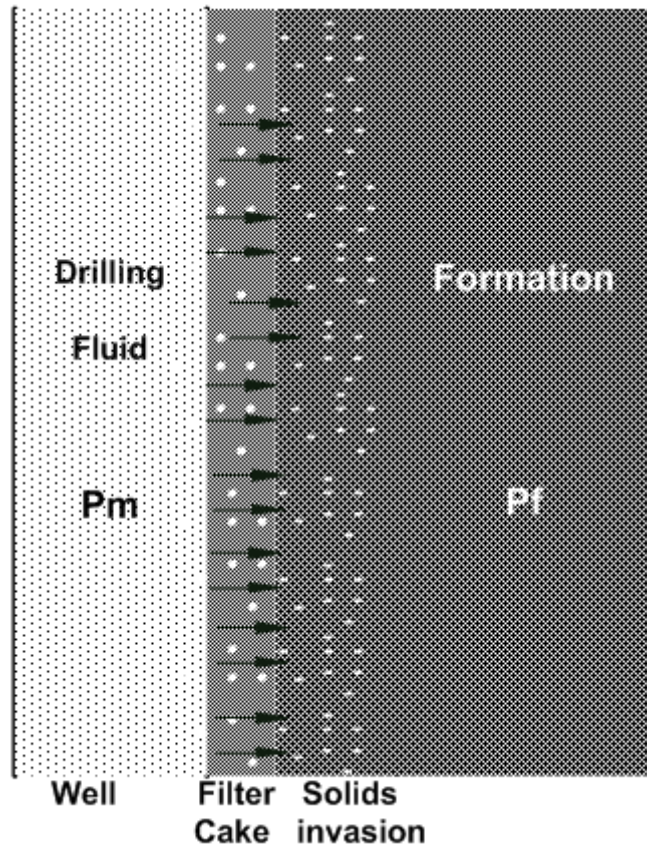


Figure 1. 1: Schematic Diagrams of the Well

CHAPTER 2

2.1 LITERATURE REVIEW

Abram (1977): performed a laboratory flow test on two different types of rock: high permeability (4-6 Darcy) unconsolidated Brezas River sand in radial model and low permeable (5-50 md) dolomite in linear model. He performed the test under 50 psi differential pressure and mud (water based) rate of 2-3 ft/min for 20 minutes. He emphasized the addition of bridging material to the drilling mud to minimize solids invasion and formation impairment. He defined two rules for selecting the size and concentration of the bridging additives. (i) The median particle size of the bridging additives should be equal to or slightly greater than 1/3 the median pore size of the formation. (ii) The concentration of the bridging solids must be at least 5% by volume of the solids in the final mud mixture. Experimental results with mud competent showed that impairment caused by invasion of mud particles occurred to a depth of less than 1 inch.

Iraj Ershaghi and Mehdi Azari (1980): in an attempt to minimize the extent of the laboratory data requirement to simulate the filter cake build up under borehole condition; the authors discussed a new model. The application of the new model results in

predicting the growth rate of filter cake and filtration volume for given zone once the drilling stops, and used it to study the effect of filtrate properties on the cumulative filtration under equal conditions. They pointed out that the model proposed by Ferguson and Klotz 1954 “gradually approaches a constant value of the mud filtration rate and an equilibrium filter cake is established during the dynamic phase of drilling against the porous formation”, therefore, the authors effort was mainly focused on understanding the subsequent filtration through the filter cake when the drilling stops. Their results showed that, the cake permeability and the filtrate viscosity were the most important factors controlling the filtration process using this model.

Peden et al. (1982): studied formation damage by circulating KCL-polymer and gypsum-lignosulfonate muds in the annulus across the core face. Scanning electron microscope (SEM) was used for qualitative evaluation of the damage. They concluded that the dynamic filtrate loss was significantly affected by the annular velocity and the permeability of the core. They also observed that the range of particle sizes in the mud was crucial to the effective depth of invasion of the mud particles. They recommended SEM as the most useful tool to support core flow experiments to identify the nature of damage.

Peden et al. (1984): used three fluid systems, a 9.7 ppg Calcium chloride brine and two water based Gypsum – lignosulphonate& KCL Polymer muds, to provide an overview of an experimental study on the dynamic and static filtration characteristic of drilling mud. They investigated the factors effected of fluid loss controlling such as annular velocity, fluid temperature, hole angle, shear rate and effect of the filter media. Filter medium consisted of four types of core plugs. Their results showed that the ability of mud to limit

spurt loss and filtration was improved by addition of bridging particles such as CaCO_3 , gypsum, Barites. Circulating drilling mud across the face of the core through annular space with different annular velocity conducted that equilibrium dynamic fluid loss rate increased with increasing annular velocity. They also found that in static filtration an increase in cake thickness and cake permeability. Their results described the difference in cake thickness and composition of the cake obtained in angled hole caused higher fluid loss for the high side than for the low side of the hole. Regarding the effect of temperature, they observed that temperature influenced dynamic fluid loss through parameters such as shear stress, filter medium and fluid undergoing filtration

Albert Hartmann et al. (1988): conducted a laboratory investigation to lead to a better understanding of the basic principles of filter cake build up and formation damage. The investigation was a combination of scanning electron microscopy “SEM” study of filter cake structures with evaluation of experimentally determined fluid loss data. The specimens were studied with SEM in both freeze-dried and frozen-hydrate stages. The study gave an SEM-aided description of filter cake of different drilling fluids with respect to the fluid loss data as well as thermal and chemical effects. Two freshwater and two salt water-base drilling fluid were used in the experiment. The drilling fluids were subjected to chemical or thermal prestressing or both. Fann viscosimeter was used to determine the rheological mud properties. Filter cake built up statically on filter paper, dynamically on Bentheim sandstone (porosity= 20 to 24%; permeability= 1.5 to 2.5 μm^2 ; average pore radius= $15 \pm 7 \mu\text{m}$). The results of honeycomb were visualized it showed that a significant relationship exists between the drilling fluid and filter cake.

Di Jiao and M.M. Sharma (1992): performed several laboratory tests on seven kinds of water based muds with different salinities and different dynamic filtration rates by circulating the muds across the face of Berea sandstone cores. They studied the effect of particle concentrations and particle size on the extent permeability impairment and depth of formation damage. Their results clearly showed that the low bentonite concentration (fresh water based mud with 2% bentonite) caused in more damage than the high bentonite concentration 4%, also, the dynamic filtration rate for the 2% bentonite concentration mud was more than twice as large as that the 4% bentonite mud. They emphasized addition of bridging material to the drilling mud to minimize solids invasion and formation impairment on account of mud cakes to become more impermeable. They concluded that, below the critical salt concentration required to prevent fines migration (approximately 5,000-10,000 ppm), fines migration became a potential damage mechanic.

Yidan et.al (1995): conducted an API static and dynamic filtration tests on filter papers and rock slices under a pressure drop of 7 bars. The aim of their work was to correlate the filtration behavior of water based muds with structural properties of the cake and in particular to compare filtration through paper filters and rock slices using suspension of bentonite as a base fluid. They studied the influence of addition of monovalent salt and water-soluble polymers. The cake was analyzed by cryo scanning electron microscopy which concluded as same structure on filter papers and rock slices. On rock slices they were able to visualize the structure of the internal cake and show a selective filtration of the polymer. Their experimental results proved that the addition of salt NaCl lead to an increase filtrate volume due to screening of the electrostatic repulsion between the clay

sheets with NaCl that induces some aggregate of the clay particles & result in a more permeable cake. Conversely, in presence of STP Polymer, filtrate volumes are much smaller due to build up of less permeable cake. It was found that, the dynamic filtration of clay suspension gave high filtration volumes and less filter cake thickness when compared static filtration.

Burnett and Hodge (1996): examined the role of drilling solids contained in drilling fluid in causing formation and completion damage and well screen plugging in horizontal open hole completion and to emphasize the important of minimizing solids, not only to maintain the desired drilling fluid rheology, but also to effect better filter cake clean up. Drilling solids are routinely kept in drilling fluids even at low concentration; represent a significant source of insoluble particulates that become incorporated in drilling fluid filter cake. They concluded in their work that drilling solids interaction with drilling fluid can produce dense, highly viscous fluid that impede and adversely affect filter cake cleanup. And damage occurs not from particulate invasion of the formation, but rather from surface damage at the formation face.

S.Z. Jilani et al. (2002): presented an experimental study performed to study the influence of overbalance pressure on the formation damage during the drilling operation. They introduced a new evaluation method to measure the invasion depth. An innovative ultrasonic technique was employed for this purpose in order to investigate the relationship between the overbalance pressure and the invasion depth. A leak-off apparatus was constructed to simulate the mud circulation process across the formation face during drilling operation. Berea sandstone cores were used for the experiment and the core samples were subjected to different overbalance pressure for various mud

contamination times under reservoir conditions and all other parameters, like mud composition, confining pressure, pore pressure and temperature were kept constant. They concluded that the invasion depth start increasing with the overbalance pressure only after the overbalance pressure reaches certain 'critical' values as well as the return permeability of cores decrease as the overbalance increase.

H.A. Nasr-EL-Din et al. (2007): presented a study focused on removing filter cake generated by water based drilling fluid in sandstone gas reservoir. The effects of the following parameters on filter cake removal were examined: soaking time, surfactant concentration and temperature. The base mud used in this study contained per bbl, 1.2 bbl Xanthan polymer, 2.0 bbl starch, 8.0 bbl CaCO₃ fine, 0.04 gal Deformer, 0.02 gal Biocide and 0.84gal Lubricant to reduce torque while drilling. Xanthan polymer and other drilling additive were typically field samples and were used without purification. Potato starch was used to prepare the drilling mud in this study and carbonate particles (sized 8 to 10 microns) were used as the bridging agent. To remove the filter cake generated by this drilling mud α -amylase was used to break starch. Several experimental were conducted using HPHT fluid loss cell to find out the nature of filter cake and the efficiency of the visco-elastic surfactant on filter cake degradation using enzyme solutions. The removal efficiency of filter cake using various cleaning solutions and soaking time was defined as the brine flow rate after the cleaning process, divided by the flow rate before cake deposition, both measured at the same down hole pressure. The result showed that 11 vol.% enzyme + 3 vol% surfactant at 135°C provided the best removal efficiency for 24 hour soaking time. For 48 hours soaking time at 141°C, 11 vol.% denotes enzyme + 6 vol.% surfactant the highest removal efficiency. At the end of the test, the filter cake was

separated and dried and then its mineralogy was determined by using X-ray diffraction 'XRD'.

A.S. Al-Yami et al. (2008): The authors highlighted three drilling fluid systems. Two drilling fluid systems, water base CaCO₃/Barite mud and Potassium Formate mud, used to drill the U-formation which can provide high drilling fluid mud density ($\pm 95 \text{ lb/ft}^3$) required for drilling those formations. The third drilling fluid, water base manganese tetraoxide Mn₃O₄ mud, was developed to overcome some of the problems associated with these two systems. The objectives of their study were to determine solid invasion and damage characteristics for the three drilling fluids. Coreflood tests were conducted, and then the cores were examined by environmental-scanning-electron-microscopic (ESEM) analysis to investigate solids invasion, solids type and location of damage. On the basis of the results obtained in their study, the three drilling fluids examined did damage the core plugs either through external filter cake, internal filter cake, or both. Water base manganese tetraoxide was recommended as the least damage occurred while testing it.

M.B. Al Otaibi et al. (2008): conducted a research on the performance of four different organic acids (acetic, formic, citric, and lactic) and enzymes. The objectives of their study were to assess the effectiveness of the cleaning fluids in removing formate drilling fluid filter cake, and to study the compatibility of formation brine and cleaning fluids with potassium formate brine. Synthetic formation brine fluid prepared in the lab was used in compatibility tests with potassium drilling fluid field system samples. Compatibility tests were tried first at room temperature for five different mixing ratios, secondly at reservoir temperature using hot plate (HTHP). The results showed that, the largest amount of precipitation was noticed at a 50:50 mixing ratio over a wide

temperature range. The solids precipitated on 1.2 μm filter paper separated and dried in the oven and then analyzed by using XRD and ESEM techniques which indicated that the potassium chloride was the main component in the solids. They observed that, the organic acids were not able to clean up the filter cake damage efficiently. Calcium carbonate particles were covered by the polymers and thus acted as a physical barrier that inhibited acid reaction with calcium carbonate particles, however, an enzyme acetic acid solution gave the highest removing efficiency compared to other cleaning fluids.

S.M. Elkatatny et, al. (2011) :used a new technique to characterize drilling fluid filter cake; computed tomography (CT scan) to study the homogeneity of the filter cake. The objectives of their work were to the filter cake properties such as thickness, porosity; permeability of filter cake formed from water based fluid by a new approach and compared the results with previous available models in the Literature. CT scan was used to measure the thickness and porosity of the filter cake. SEM was used to provide the morphology of the filter cake. Leica microscope was used to determine particle size distribution. They conducted HPHT filter press under static conditions (225 $^{\circ}$ F and 300 psi) to perform the filtration process. Based on experimental results, they concluded that filter cake was heterogeneous and contained two layers with different properties such as thickness, porosity, and permeability; external layer and internal layer. The porosity in the external layer was zero, while the porosity of thin internal layer was found to be in the range from 10 to 20%. Previous models of filter cake buildup assumed that the filter cake was homogenous and contained one layer, which affected greatly the filtration process. This will also greatly impact the design of the chemical treatment for a filter cake removal. Li et al. (2005) model was a good method to determine filter cake permeability

takes into account the change in the filter disk properties and the thickness of the filter cake. Finally, they recommend using CT to characterize drilling fluid filter cake properties such as thickness, permeability and porosity.

2.2 AN OVERVIEW OF FILTER CAKE PROPERTIES

Filter cake occurs intentionally during the drilling operations to prevent fluid losses to the formation and to allow good circulation for drilling fluids to the surface and is known to depend on a well-designed drilling mud fluids and additives. The filter cake must allow for minimum filtration and solid invasions to the formation and must also withstand high differential overbalance pressures.

This chapter involves filter cake build up mechanisms and the most important filter cake properties such as filter cake thickness, porosity, permeability and filter cake minerology for both oil-based and water-based drilling muds. Moreover, it provides measuring methods for these filter cake properties and range of accuracy in each method. It describes the effect of each property on drilling operation and health of the drilled well.

The survey was found to provide a comprehensive reference for filter cake properties and methods. The reader can easily use this paper to benchmark his/her produced data or select the right method.

2.2.1 Filter Cake Build up Mechanisms

In an overbalanced drilling, there are two notable mechanisms for filter cake build up, static and dynamic filtration mechanisms, both of them depend upon the conditions in the well. There are several models in the literature for filtration analysis such as

(Outmans 1963; Ershaghi and Azari 1980; Hassen 1980; Peden *et al.* 1982; Peden *et al.* 1984; Jiao and Sharma 1993). The objective of this part is to give the reader a quick overview idea about the filter cake build up Mechanisms.

Static Filtration Mechanism

The first filtration mechanism, called static filtration, which occurs when the fluid pumping is interrupted and, from that point on, filtration occurs due to the positive difference between the hydrostatic pressure of the drilling fluid and the formation pore pressure. The filtration rates are controlled by the gradual growth of filter cake thickness with time. Continuous increase in thickness of filter cake with time will lead to decreasing the filtration rate and cake permeability which will greatly inhibit the growth of filter cake thickness itself.

The volume of static filtration is described by (Hassen 1980) in the equation below under constant temperature and pressure

$$V = C \sqrt{t} + \text{spurt loss, (2.1)}$$

Where

V = filtration volume, ml

t =time, hr

C =static filtrate volume coefficient

The constant “C” can be obtained from the static test. This mechanism is directly affected by drilling fluid composition, drilling fluid pressure, formation pressure and formation properties such as permeability, porosity and grain size distribution.

Dynamic Filtration Mechanism

The other filtration mechanism, called dynamic filtration, occurs when the fluid is pumped through the well. The pressure difference between the fluid and reservoir pressure has the same role in this mechanism. The major difference between dynamic and static filtration is that, in the dynamic process, the cake thickness is resultant from the dynamic equilibrium between solids particles deposition rate and the erosion rate is due to the shear stresses generated by the fluid flow in the well bore. Therefore, the filtration rate to the formation tends to stabilize around a certain value while the cake thickness turns constant. This balance between filter cake formation and erosion is give by (Hassen 1980) as:

$$u_f = \frac{c}{\sqrt{t}} + 3600b\gamma, \dots\dots\dots (2.2)$$

Where

u_f = filtrate velocity ml/cm².hr

γ =shear rate at the well, s⁻¹

C = dynamic filtrate volume coefficient

t =time, hr

C can be obtained from laboratory dynamic fluid loss test, and b is a constant accounting for the mechanical stability of the filter cake; (Hassen 1980) reported values of b from 2×10^{-8} to $5 \times 10^{-5} \text{ cm}^3/\text{cm}^2$.

In addition to, this mechanism is directly affected by drilling fluid composition, drilling fluid pressure, formation pressure and formation properties such as permeability, porosity and grain size distribution. It is also affected by the circulation rate of drilling fluids, drill string rotation speed and size distribution of solid content in the drilling fluid.

2.2.2 Filter Cake Properties

After the static or dynamic filtration test is run according to the standard API procedure, the excess drilling fluid will be decanted and the filter cake will be carefully removed from the API cell and then washed gently. The properties of filter cake such as thickness, porosity, permeability and mineralogy are some of the parameters used to assess the cake building properties of a drilling fluid system. For this reason, the way that the measurement of cake properties followed is an essential part for a qualitative assessment of a fluid system. These properties are critical factors in production and reservoir engineering.

Filter Cake Thickness

Jiao and Sharma (1993) observed that filter cake thickness was a sensitive function of the mud rheology, the mud shear rate and the permeability of the rock. Dangou and Chandler (2009) concluded that the cake thickness was also a function of shear rate in dynamic filtration. Their results show that as the shear rate increase the cake thickness

decrease. Furthermore, the filter cake thickness is a critical factor in many drilling and reservoir engineering problems. Forming soft and thick filter cake increase the potential of differential sticking and make the openhole more and more difficult (Amanullah and Tan 2001). Thus, filter cake thickness is an important input parameter in numerical modeling of differential pressure sticking. Isambourg and Matri (1999) showed how the magnitude of pulling force necessary to free a stuck pipe changes with the change in filter cake thickness. For this reason, accurate filter cake thickness measurement is essential.

The most commonly used method to measure the filter cake thickness is the direct method by using vernier caliper or ruler. The traditional method need direct contact with the filter cake to measure its thickness and the accuracy of this method ± 0.1 mm (Cook E.L. 1954). Amanullah and Tan (2001) measured the filter cake thickness using the **Laser** apparatus and **Digital Dial Gauge**. Since the cake thickness will be used for estimation of certain drilling and reservoir engineering parameters, any slight error in the cake thickness measurement may lead to a completely wrong conclusion.

The Laser Method, (Figure 2.1): The Laser method was proposed as non-contact method of filter cake measurements. It has been developed to eliminate inaccuracies associated with the conventional direct contact methods and to present high precision and accuracy measurements of the cake thickness. A seventeen spot measurement layout was adopted to provide a reliable average of the cake thickness. The measured thickness values have a standard deviation of less than 0.025 mm and a coefficient of variation of less than 1%. The device is portable, easy to operate and suitable for quick thickness

measurement. The output of this advice is between 4 mA to 20 mA. Hence, a calibration equation or chart is used to convert the results to mm.

Dial Gauge Method,(Figure 2.2): The Dial Gauge method is an electronic measuring device with a soft touch to prevent significant cake damage. The cake plus the filter paper thickness are measured at several spots on the cake. The thickness of the cake is determined from the average measurement by subtracting the filter paper thickness. The measuring range of the transducer is 10 mm with a resolution of 0.001 mm. However, the dial gauge measured cake thickness values show somewhat lower or higher values than the laser measured thickness values. This indicates that the technician has measured higher or lower values on the basis of his assumption as to when the dial gauge foot has touched the top of the mud cake. Hence, the authors concluded that the dial gauge measured thickness values are highly influenced by the skill of the technician to take reading at the right time.

In addition to these equipments, there are some unpopular tools which were highlighted in the literature such as a flat foot penetrometer (Amanullah 1996), nuclear magnetic resonance imaging (NMRI), CAT scan and ultra-sonic. They are not popular because their unsuitability for soft objects like filter cake which has poor physio-mechanical properties (Amanullah and Tan 2001).

Elkatatny *et al.* (2011) determined the filter cake properties of water base fluid by a new technique. Computed tomography (CT scan) was used to measure the thickness and they concluded that the CT scan is good tool for filter cake properties measurement. The previous tools and models, assume that the filter cake is homogeneous while the CT scan

technique is capable to test homogeneity of the filter cake. Their results revealed that the filter cake has two different layers; each layer had its own thickness. Recently the cake thickness measured by Scanning Electron Microscope (Overveldt *et al.* 2012)

Filter Cake Porosity

Filter cake porosity is one of the six parameters required to characterize the filter cake (Dewan and Chenevert 2001) .They presented a method that was used to measure filter cake porosity. The same method was used by (Dangou and Chandler 2009) to measure the filter cake porosity and they found that the porosity of filter cake is directly dependent on particle size distribution in the cake and indirectly dependent on cake thickness. They used the basic fundamental definition of porosity (e.g. the porosity equal to the pore volume divided by bulk volume $\phi = V_p/V_b$) to determine the porosity of the cake. Where the pore volume is equal to the fluid volume and the bulk volume is equal to the solids volume of the cake.

To get the above values, at the end of the fluid loss the filter cake is immediately removed (formed on the filter paper or disk) from the cell. The wet weight of paper and filter cake combination (as 100% saturated with filtrate) is measured with highly sensitive balance of 0.01 gm resolution balance. The weight of the wet paper is subtracted to get the net wet weight of the filter cake. Then the cake is dried at 200 °F (93 °C) for 24 hours to drive off all water (in water base mud) and its dry weight is measured, and then the weight of the dry filtrate paper is subtracted to give a net dry weight of the filter cake. Denoting the fluid and grain densities by ρ_f and ρ_g respectively, the porosity of the cake ϕ_c can be calculated as:

$$\phi_c = \frac{V_p}{V_b}, \dots\dots\dots (2.3)$$

Where

$$V_b = \frac{\text{net dry weight of the cake}}{\rho_g}, \dots\dots\dots (2.4)$$

$$V_p = \frac{(\text{net wet} - \text{net dry}) \text{ weight of the cake}}{\rho_f}, \dots\dots\dots (2.5)$$

Dewan and Chenevert (2001) rearranged the above equation to give the filter cake porosity as:

$$\phi_c = \frac{\alpha}{\alpha + \frac{\rho_f}{\rho_g}}, \dots\dots\dots (2.6)$$

Where

$$\alpha = \frac{\text{net wet weight of the cake}}{\text{net dry weight of the cake}} - 1, \dots\dots\dots (2.7)$$

The fluid density must be changed in the above equations from the water density to the oil density if an oil base drilling fluid is used.

Elkatatny *et al.* (2011) used CT scan to determine the filter cake porosity of water base drilling fluid as following:

$$\phi_c = \frac{CT_{\text{wet}} - CT_{\text{dry}}}{CT_{\text{water}} - CT_{\text{air}}}, \dots\dots\dots (2.8)$$

Where

CT_{wet} = CT number of the cake in wet conditions

CT_{dry} = CT number of the cake after dried at 250°F for 3 hours.

CT_{water} = CT number of water

CT_{air} = CT number of air

By this method they concluded that the external layer of the cake has zero porosity while the porosity of the internal layer was found to be in the range from 10 to 20%.

Filter Cake Permeability

During drilling a well the permeability of the filter cake, with typical permeabilities ranging from 10^{-5} Darcies to 10^{-7} Darcies (Hanssen *et al.* 1999), controls both static and dynamic filtration. Filter cake permeability is significantly affected by the shear rate due to its effect on cake particle size distribution (Dangou and Chandler 2009). They found that the filter cakes formed at low shear rates consisted of large mean particle sizes and this resulted in higher cake permeability. On the contrary, filter cake formed at high shear rates had low permeability since the mean particle size of the dynamic cake is smaller than the original mean particle size of the drilling fluid.

The cake permeability can be determined from different models. (Burgoyne 1991) used the equation below to calculate the cake permeability under static conditions. It was developed from the relationship between the cumulative filtrate volume and the square root of time;

$$V_f = \sqrt{2k\Delta p \left(\frac{\epsilon_{sav}}{\phi_s} - 1 \right)} A \frac{\sqrt{t}}{\sqrt{\mu}}, \dots\dots\dots (2.9)$$

Where

k = Permeability of the filter cake, darcy

V_f = Filtrate volume, cm^3

Δp = Pressure drop across the mud cake, atm

ϕ_s = Volume fraction of solids in the mud

ϵ_{sav} = Volume fraction of solids in the cake

A = Area of the filter disk, cm^2

t = Time of filtration, sec

μ = Viscosity of the mud filtrate, cp

(Khatib 1994) correlated permeability/porosity data with an average correlation coefficient of 0.95 to obtain the permeability of the filter cake. The empirical relationships for iron sulfide, iron hydroxide, CaCO_3 , CaSO_4 , and silt/clay particles that were free of oil and coated with oil are given in **Table (2.1)** below.

Table 2. 1: Permeability/Porosity Empirical Relationship for Various Filter cakes by (Khatib 1994)

Filter cakes type	Free of oil	Coated with oil
FeS	$K_c = 0.00533(1-\phi_c)^{-2.05}$	$K_c = 0.00625(1-\phi_c)^{-1.7}$
Fe(OH) ₃	$K_c = 0.000163(1-\phi_c)^{-3.03}$	$K_c = 0.003(1-\phi_c)^{-2.16}$
CaCO ₃	$K_c = 112.7e^{-8.8(1-\phi_c)}$	$K_c = 56.4e^{-8.8(1-\phi_c)}$
CaSO ₄	$K_c = 1.419(1-\phi_c)^{-1.741}$	$K_c = 0.778(1-\phi_c)^{-1.6}$
Silt/Clay	$K_c = 0.491(1-\phi_c)^{-1.97}$	$K_c = 92.4e^{-13.4(1-\phi_c)}$

Where: K_c = Permeability of the mud cake, md

ϕ_c = Porosity of the filter cake, fraction

The permeability of the filter cake can be calculated by the method developed by (Mahesh 2000) as:

$$K = Q_w Q_c \frac{\mu}{2 t p A^2}, \dots\dots\dots (2.10)$$

Where

k = Permeability of the filter cake, darcies

Q_w = Filtrate volume in cm^3

Q_c = Volume of the cake in cm^3

μ = Viscosity of the filtrate in cp

t = Time in second

p = Differential pressure in atm

A = Area of the filter cake in cm^2

By using conventional filter press data equation (2.10) becomes

$$K = Q_w Q_c \mu 1.99 \times 10^{-3}, \dots\dots\dots (2.11)$$

k = permeability of the filter cake, md

With fresh water muds μ is approximately one centipoise at 20 °C.

Mahesh (2000) used a new approach to calculate the cake permeability when the accuracy is not so important. To calculate the volume of the cake for water based drilling fluid, initially water loss is taken for 30 minutes and unused mud is decanted off the filter

cell without removing the filter cake. Then the filter cell is washed and rinsed with diesel oil with filter cake intact in its original position and the filtrate is collected again. Initially only water comes and then diesel oil with a little associated water filters out. At the point only diesel oil filters out, the volume of water from the filter cake is recorded. Now oil-water retort kit distillation results for the same fluid are correlated with the results obtained from the above experiment (i. e. water loss and water of the filter cake). In this way the volume of solids associated with filter cake is obtained. Now volume of solids associated with filter cake plus volume of water from filter cake give the volume of filter cake. An

Elkakatny *et al.* (2011) pointed out in their paper (Martinez *et al.* 2000) method to calculate permeability of filter cake

$$\frac{pt}{\mu v} = \left(\frac{1}{2k}\right) L + R_m , \dots\dots\dots (2.12)$$

Where

k = Permeability of the filter cake, m²

v = Volume of filtrate per unit area, m³/m²

L = Filter cake thickness, m

R_m = Resistance of filter medium, 1/m

p = Differential pressure, Pa

t = Time, s

μ = Filtrate viscosity, Pa.s.

The slope of Eq.(12) is equal to $1/(2k)$ as shown in **Figure 2.3**.

Tiller (2002) developed the following equations to calculate the cake permeability.

This method was classified as cake filtration method by (Li *et al.* 2005).

$$c = \phi_s / \left(1 - \frac{\phi_s}{\varepsilon_{sav}}\right), \dots\dots\dots (2.13)$$

$$\frac{pdt}{\mu dv} = \alpha_{av} * cv + R_m, \dots\dots\dots (2.14)$$

$$\alpha_{av} * k * \varepsilon_{sav} = 1, \dots\dots\dots (2.15)$$

Where

k = Permeability of the filter cake, m^2

v = Volume of filtrate per unit area, m

ε_{sav} = Volume fraction of solids in filter cake

R_m = Resistance of filter medium, 1/m

p = Differential pressure, Pa

t = Time, s

μ = Filtrate viscosity, Pa.s.

ϕ_s = Volume fraction of solids in slurry

α_{av} = Average specific cake resistance [$1/m^2$] is obtained from the slope of the line shown in **Figure 2.4**.

Li *et al.* (2005) indicated that the liquid flowing through already formed cake approach method to calculate the cake permeability was not included filter media resistance in calculation, while the filter media resistance was included (Tiller 2002) method but it has a complicated calculation. Li *et al.* (2005) calculated the permeability of filter cake based on Darcy's Law for liquid flow through an already formed cake and a filter media resistance was included. Furthermore, it provided a simple and easy permeability calculation. This method depends on the relationship between the cumulative filtrate volume and time where the slope is equal to the flow rate.

$$R_t = R_c + R_m \text{ ,..... (2.16)}$$

$$\Delta p_t = \Delta p_c + \Delta p_m \text{ ,..... (2.17)}$$

Flow rate q = rate through cake = rate of flow through filter media

$$\text{Flow rate } q = \text{rate through filter cake} = k_c \frac{\Delta P_c}{\mu L_c} \text{ ,..... (2.18)}$$

$$\text{Flow rate } q = \text{rate through filter media} = k_m \frac{\Delta P_m}{\mu L_m} \text{ ,..... (2.19)}$$

Where

R_t = Total resistance

R_c = Resistance of cake

R_m = Resistance of filter media

q = Filtrate rate, $m^3/m^2.s$

k_c = Permeability of the filter cake, m^2

k_m = Permeability of the filter medium, m^2

L_c = Thickness of the filter cake, m

L_m = Thickness of the filter medium, m

Δp_t = Total pressure drop, Pa

Δp_c = Pressure drop across the filter cake, Pa

Δp_m = Pressure drop across the filter medium, Pa

μ = Filtrate viscosity, Pa.s.

The flow rate can be gained from the slope of the straight line region of the filtrate volume vs time curve in **Figure 2.5**, divided by total filtration area. The Media resistance K_m can be determined by a separate clean water flow through filter media only test. Cake thickness L_c and media thickness L_m can be measured. With known K_m , L_m , μ and q , pressure drop across filter media Δp_m can be calculated based on Equation (2.19). With known total pressure p and pressure drop across filter media Δp_m the pressure drop across cake Δp_c can be obtained from Equation (2.17). Finally, the permeability of cake can be determined from Equation (2.18).

Elkatatny *et al.* (2011) concluded that (Li *et al.* 2005) model was a good method to determine filter cake permeability takes into account the change in the filter disk properties and the thickness of the filter cake.

There are also some authors mentioned the methods that were used to determined the permeability of filter cake in their works. (Dewan and Chenevert 2001) applied Darcy's equation for the pressure drop across the filter cake. This type of methods used the cake filtration approach (Li *et al.* 2005)

$$P_{mc} = 14700 \frac{q T_{mc} \mu}{K_{mc}}, \dots\dots\dots (2.20)$$

The above equation can be used to calculate the permeability of filter cake as

$$K_{mc} = 14700 \frac{q T_{mc} \mu}{p_{mc}}, \dots\dots\dots (2.21)$$

Where

K_{mc} = Permeability of the filter cake, md

q = Filtration rate, cm/sec

T_{mc} = Filter cake thickness, cm

μ = Viscosity of the filtrate, cp

p = Pressure across filter cake, psi

Dangou and Chandler (2009) conducted extensive dynamic filtration experiments to test the filter cake parameters at the equilibrium dynamic stage where the filtration flow rate becomes straight line, **Figure 2.6**. They determined the filter cake permeability by applying Darcy's Equation at the equilibrium filtration flow rate.

$$K_{mc} = \frac{q_{eq} T_{mceq} \mu_f}{A_f p_f}, \dots\dots\dots (2.22)$$

Where

q_{eq} = Equilibrium filtration rate, $m.sec^{-1}$

K_{mc} = Permeability of the filter cake, m^2

T_{mceq} = Equilibrium cake thickness, m

μ_f = Filtration viscosity, Pa.sec

p_f = Filtration pressure, Pa

Filter Cake Structure Analysis

Most investigators attribute to obtain a better understanding of the microscopic structure of filter cakes. Such information could lead to improved filtration control additives that minimize formations damage and selection of an effective recipe for removing the filter cake without exposure of the well to fluid loss through completion operations. For that Purpose several devices were used to study the structure of filter cake such as scanning electron microscopy (SEM), X-ray diffraction (XRD) and X-Ray Fluorescence (XRF) (Kenneth 1980; Peden *et al.* 1982; Hartmann *et al.* 1988; Chenevert and Huycke 1991; H.A. Nasr-EL-Din *et al.* 2007; A.S. Al-Yami *et al.* 2008; M.B. Al Otaibi *et al.* 2008; S.M. Elkatatny *et al.* 2011). The objective of this part is to identify the uses in detail the uses of each device and the preparation method of cake sample.

SEM technique is a kind of electron microscope used to determine the crystal structure and grain orientation of crystal on the surface of prepared specimen. One of the

most promising advances in the development of SEM is the capability to provide high resolution picture of the samples and determine qualitatively or semi-quantitatively chemical compositions (Goldstein *et al.* 1981). Field Emission Scanning Electron Microscope (FE-SEM) approach was addressed by (Kenneth 1980) to understand the structure and concepts behind the design of drilling fluids. Peden *et al.* (1982) employed SEM to qualitatively identify particulate plugging of the invaded zone near well bore and they recommended it as a good tool to identify the nature of damage. The microscopic structure of drilling fluid filter cakes formed under both static and dynamic conditions were studied using SEM for different water/oil base drilling fluid composition (Borst and Shell 1971; Kenneth 1980; Hartmann *et al.* 1988; Plank and Gossen 1989; Chenevert and Huycke 1991; M.B. Al Otaibi *et al.* 2008; Elkatatny *et al.* 2011).

Considering to (Kenneth 1980) study, the preparation method of filter cake sample for SEM analysis must be evaluated to determine what are the acceptable methods to prevent the sample distortion due to very high vacuum operation conditions in SEM equipment. Thus, (Kenneth 1980) prepared the filter cake sample with dry, freeze drying techniques that presented by (Borst and Shell 1971) as new technique for studying the fabric of clay muds to try to retain the clay structure. To study structure of the filter cake formed by the water base drilling fluid using SEM, the samples must be derided before examination because it contains about 70% water (Hartmann *et al.* 1988). They carried out *Shock-freezing* and *Freeze-drying* techniques to prepare filter cake samples for SEM analysis. Using these techniques allow SEM to examine the variation of the cake structure versus position in the filter cake and to investigate the effect of the different mud additives and have been (Chenevert and Huycke 1991).

Freeze-drying is removal of water from the frozen filter cake. Once the filter cake has been formed and removed from the filtration cell, the freeze-drying of the filter cake sample began. Immediately after the filter cake removed from the filtration cell, a razor blade was used to cut tiny pieces (2-5 mm wide, 15-20 mm lengths) of the filter cake attached to filter paper. Then, the small pieces are cooling down to 133°K [-220°F, -140°C] rapidly as possible within a few milliseconds to avoid large ice crystal growth damage. This process is calling Shock-freezing process. After Shock-freezing, the samples were broken again to have undisturbed surface for SEM Study. In the next step, the frozen water in the filter cake is removed by transition from solid to gaseous stage by sublimation without passing through the liquid stage. Sublimation prevents the reordering of the clay platelets that takes place during evaporation of water from a filter cake .It usually carried out at about 200°K [- 100°F, -73°C] and pressure 20 to 100 MPa. Finally the freeze-dried filter cake samples were coated with an electrical ducting and study with SEM (Kenneth 1980; Hartmann *et al.* 1988; Chenevert and Huycke 1991).

The Environmental Scanning Electron Microscope (ESEM) was developed to break the barrier to imaging the specimens in their "native" states in (SEM). It has the ability to image and analyze the specimens in their natural wet or dry state without drying, freezing, or coating such as core flooding, matrix acidizing and clay and cement hydration illustrate (Mehta 1991; Gauchet *et al.* 1993; Simanjuntake and Haynes 1994).

Robin *et al.* (1999) confirmed that the advances in scanning electron microscopy allow the observation the samples either under a frozen state in the case of Cryo-SEM (Cryo Scanning Electron Microscopy) or directly with ESEM (Environmental Scanning

Electron Microscopy). Both techniques enhanced the knowledge of the different interactions within the porous media.

ESEM allows visualization of fluid capillary rise in rock samples. It allows the observation of dynamic experiments, for example wetting fluid imbibition in presence of a non-wetting fluid (Robin *et al.* 1999) and test the effect of field water on core flooding included a determinations of scale optional (Raju *et al.* 2005).

Cryo-SEM and SEM used to study size and distribution of minerals on physico-chemical behavior of the sample towards fluids (Robin *et al.* 1999) and to provide the morphology of the filter cake (Elkatatny *et al.* 2011). The microstructure of the filter cake for oil base drilling fluid and penetration of particles into the core were further examined by SEM and ESEM (Overveldt *et al.* 2012).

As mentioned pervious, SEM deals with a tiny piece of filter cake. Hence the data generated from SEM is collected over a small selected area of the surface of the filter cake sample. Therefore, two or three different points are tested for each filter cake sample to make sure that representative area of filter cake sample has been covered in determining the chemical compositions or visualizing the particles distribution. Such method will ensure that the cake structure analysis was performed in a complementary manner.

Recently development in technology enhanced our understating of elements and crystal structure of filter cake and rock samples by using X-ray diffraction (XRD) along with SEM. XRD provides the phase identification of filter cake fabric and determines modal amounts of minerals (quantitative analysis). It has the capability to cover the entire

sample in one run as well as determine quantitatively and analyze chemical composition of elements with an accuracy and precision approaching 1% (Goldstein *et al.* 1981). To prepare the filter cake sample for XRD analysis, it must be dry and powder sample.

Nasr-EL-Din *et al.* (2007) in their study of removing the filter cake determined the filter cake mineralogy using XRD. At the end of the HPHT fluid loss test, the filter cake was separated and dried for XRD test. Al Otaibi *et al.* (2008) studied the filter cake of formed by formate-based drilling mud characteristics and how to remove it. They also used XRD to examine the solids after dried in an oven. Al Moajil and Nasr-El-Din (2011) determined the drawbacks of employing different acids and cleaning means to dissolve Mn_3O_4 -based filter cake. They also used XRD to analyze solids remaining after the reaction of selected organic acids and chelating agents with Mn_3O_4 particles.

Other properties of Filter Cake

Cerasi *et al.* (2001) described experimental techniques aimed at directly probing the mechanical properties of filter cakes. The use of these techniques allowed them to assess yield stress of filter cakes and other properties such as the dynamical elastic and viscous moduli, the plastic and elastic compressibility coefficients entering the Cam Clay model and the cake/substrate adhesion. The three methods are complementary as the rheometer measurements were done on filter paper grown cakes, the scraping apparatus probed cakes grown on a rock core and the one-dimensional consolidation experiment was done on an initial small volume of drilling mud.

Berntsen *et al.* (2010) presented the main method to assess filter cake mechanical properties using different oil-based mud formulations. The mechanical properties were

studied by scratch tester which measure the strength of the filter using a flexible cutting blade, with a strain gauge attached, in place of the rigid cutter.

The particle size distributions (PSD) of solids in the filter cake were determined using a conventional laser light scattering instrument (Pitoni *et al.* 1999) and using a laser diffraction method (Zulkeffeli *et al.* 2000) .Also it was measured by a Leica microscope (Elkatatny et al. 2011)

Pitoni et al. (1999) evaluated the filter cake properties on a texture analysis instrument. This instrument determines some of physical properties of materials by measuring their responses to applied loads and deformations. For testing the filter cakes a flat 6 mm diameter probe was pushed into the cake at a constant speed of 10 mm/min and the resulting load was measured. This test was particularly useful for determining the physical characteristics of a filter cake.

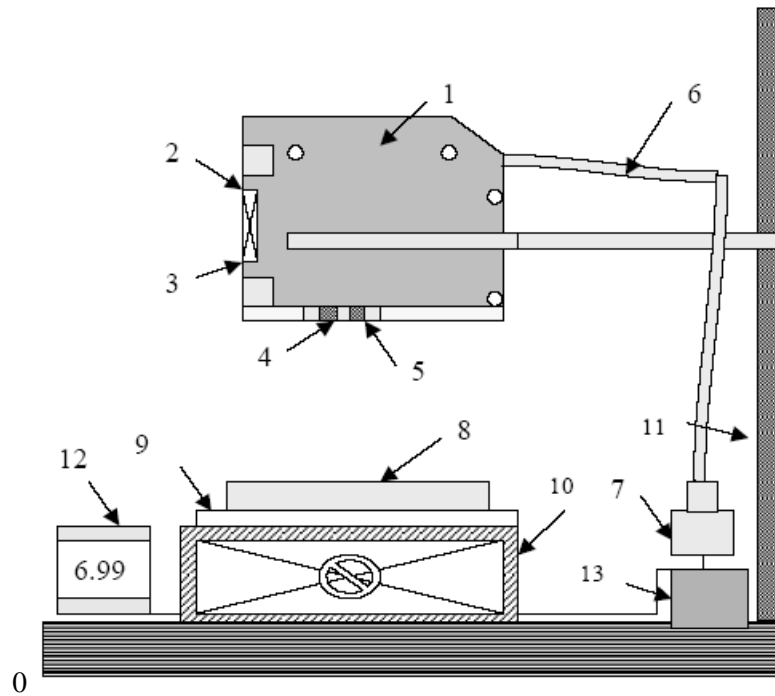


Figure 2. 1: Laser Apparatus for Filter Cake Thickness Measurement (M.d. Amanullah and C.P. Tan, 2001).

- | | | | |
|---|---------------------------|----|---------------------|
| 1 | <i>Laser Head</i> | 8 | <i>Filter Cake</i> |
| 2 | <i>Far Indicator</i> | 9 | <i>Filter Paper</i> |
| 3 | <i>Near Indicator</i> | 10 | <i>Lab Jack</i> |
| 4 | <i>Emitter</i> | 11 | <i>Stand</i> |
| 5 | <i>Receiver</i> | 12 | <i>Multi-meter</i> |
| 6 | <i>Connector</i> | 13 | <i>Power Supply</i> |
| 7 | <i>Signal Conditioner</i> | | |

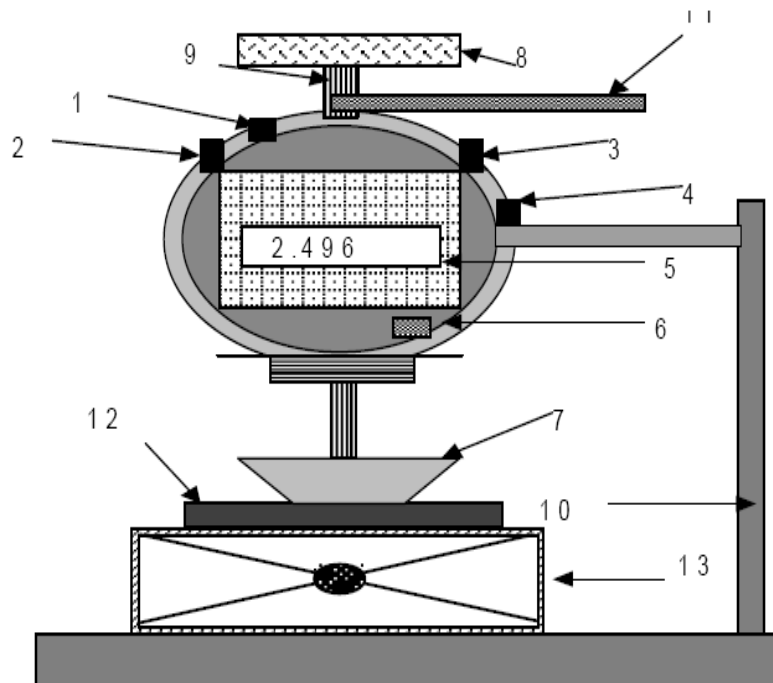


Figure 2. 2: Dial Gauge for Filter Cake Thickness Measurement (M.d. Amanullah and C.P. Tan 2001).

- | | | | |
|---|-----------------------------|----|-----------------|
| 1 | Power Supply | 8 | Load Platform |
| 2 | On/Off Switch | 9 | Transducer Stem |
| 3 | Inch/mm Changeover Switch | 10 | Stand |
| 4 | Direction Changeover Switch | 11 | Lifting Lever |
| 5 | Digital Display | 12 | Filter Cake |
| 6 | Reset Button | 13 | Lab Jack |
| 7 | Disk | | |

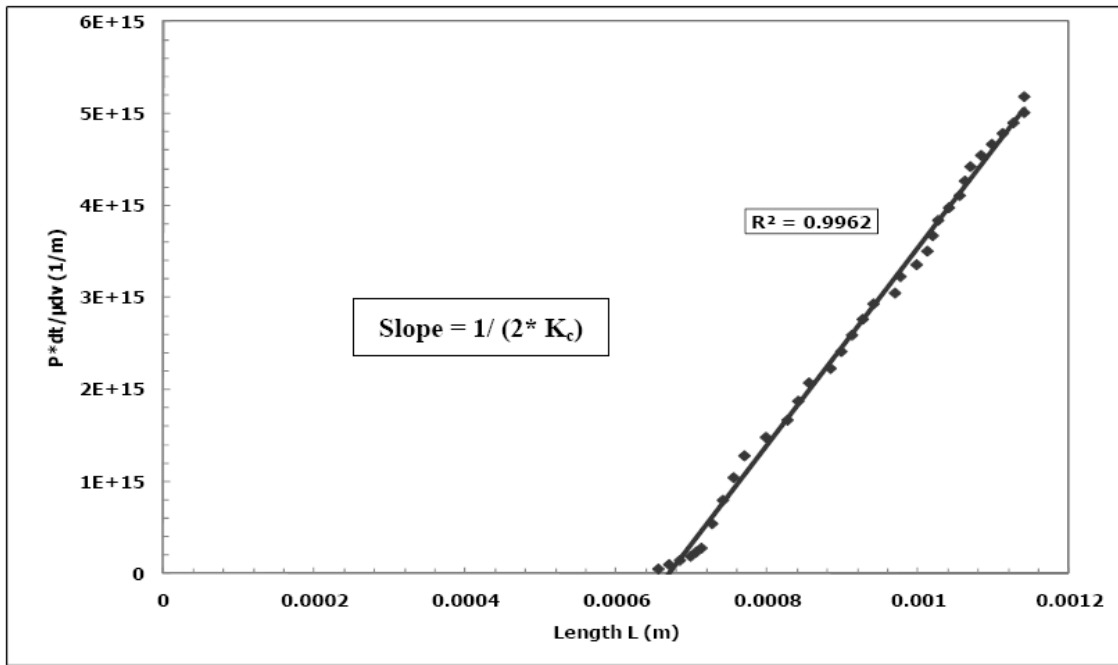


Figure 2. 3: Martinez et al. (2000) Method to Determine the Permeability of Filter Cake

Presented by (Elkatatny *et al.* 2011)

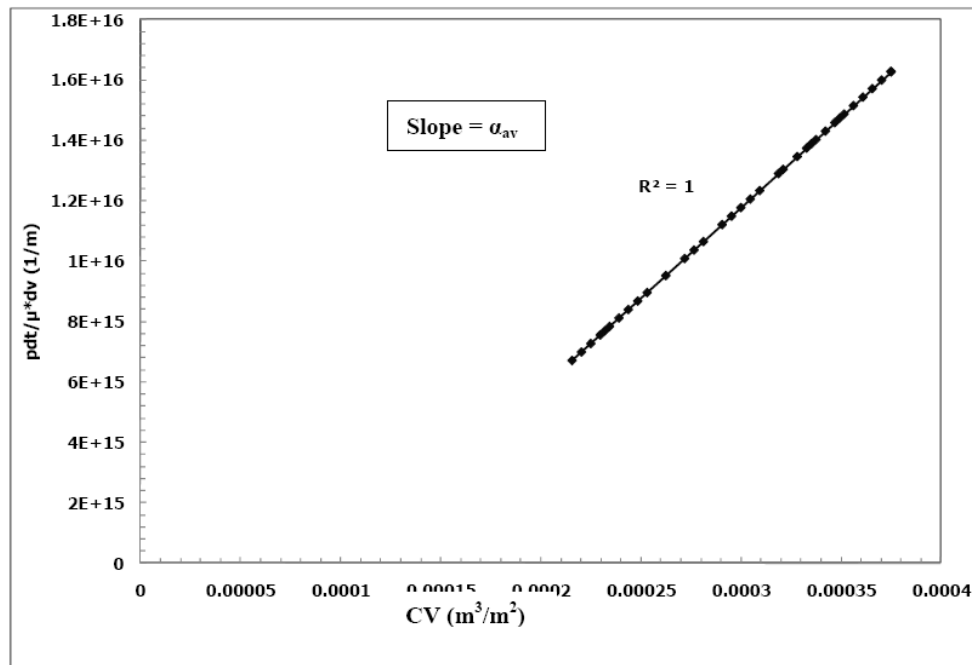


Figure 2. 4: Tiller (2002) Method to Determine the Permeability of Filter Cake

Presented by (Elkatatny *et al.* 2011)

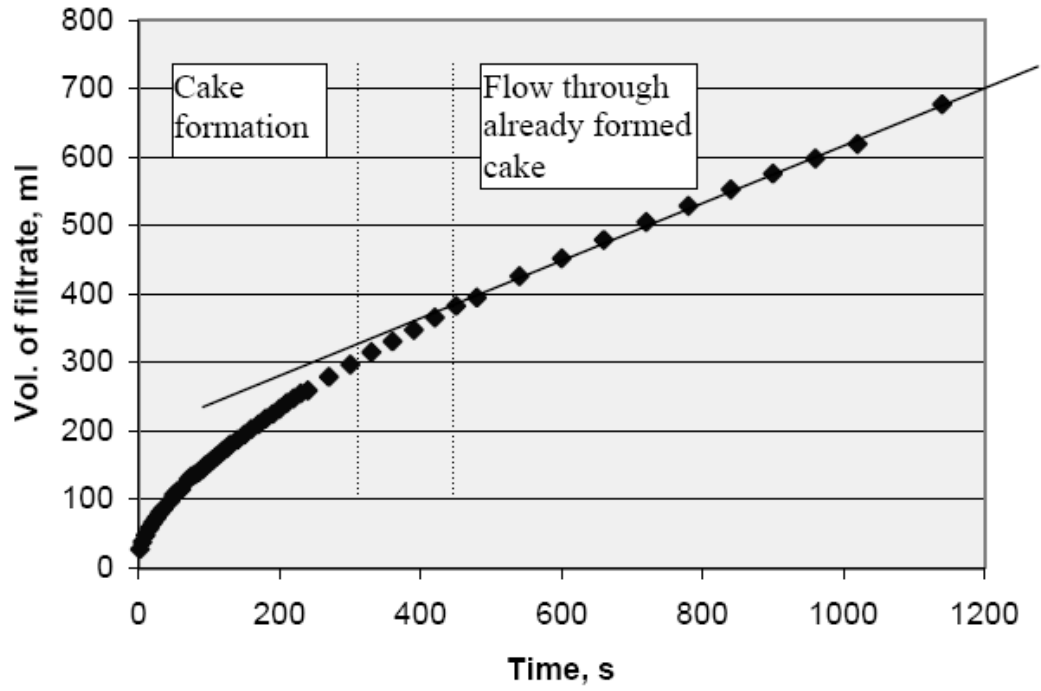


Figure 2. 5: Li *et al.* (2005) Method to Determine the Permeability, Typical Volume of Filtrate vs Time Curve

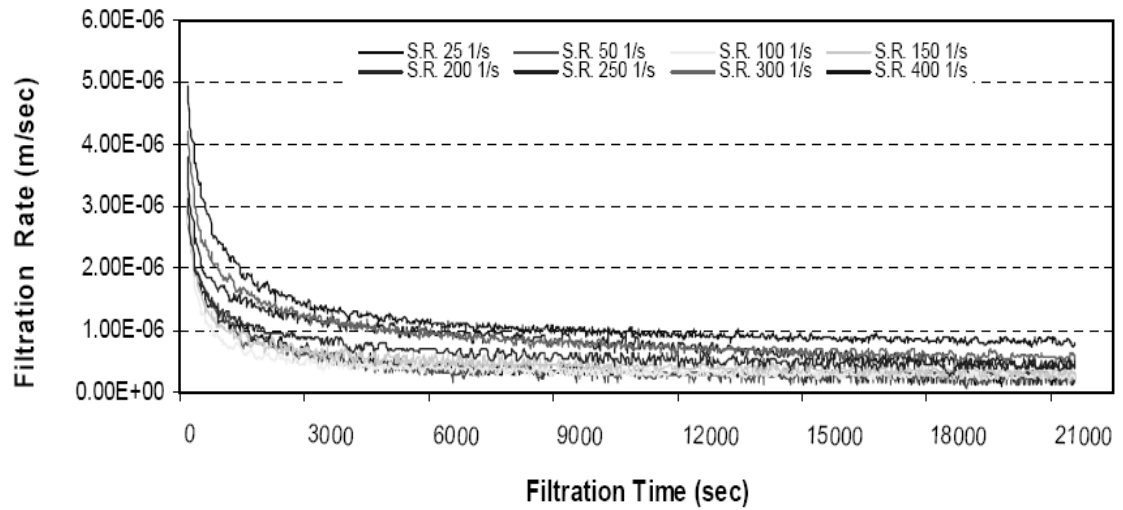


Figure 2. 6: Dangou and Chandler (2009) Change in the Dynamic Filtration Flow Rate with the Shear Rate and Filtration

CHAPTER 3

3.1 STATEMENT OF THE PROBLEM

Filter cake or mud cake occurs intentionally during the drilling operations to prevent fluid losses to the formation and to allow good circulation for drilling fluids to the surface. Formation of an effective filter cake is known to depend on a very well designed drilling mud fluids and additives. The drilling mud is normally designed to allow for minimum filtration and solid invasions to the formation. On our hand, the filter cake must withstand high differential overbalance pressures as well. On the other hand, reduced oil and gas production can result from reservoir damage when a poor filter cake allows deep filtrate invasion. It is very well known that penetration rates and bit life decrease and hole problems increase with a high concentration of drill solids.

The design of drilling mud usually includes several additives that are compatible with reservoir fluids and a spectrum of accurately sized solids that can prevent filtration but still provide a thin cake. In a horizontal wellbore, this process is detrimental because fluid losses can be more severe.

The drilling mud program involves comprehensive testing procedures to determine filtration rate and filtercake properties. However, current cake properties do not go

beyond being tested for cake thickness, toughness, slickness and permeability. Thickness is important because cake that forms on permeable zones in the wellbore can cause stuck pipe.

The two primary sources of solids are drilling mud chemical additives and formation cuttings. Formation cuttings are usually removed using sand solid control equipment because their presence will degrade the performance of the drilling fluid. These cuttings are ground into smaller particles if not properly removed. All current solid separation methods are either based on size exclusion or gravity. They ignore the chemical composition of the solids. For long horizontal wellbores penetrating clastic formations, the chemical composition and the physical properties of the mud play a significant role. Ground clastic fragments and debris are mixed with drilling mud during mud circulation. As so, these materials become an integral part of fabric of the filter cake.

The effect of introducing sand particles to the structure of the filter cake is significant from the filter cake removal point of view. The sand percentage might reach to 40% by volume of the mud solids making it prohibitively difficult to be removed with regular acids. Filter cake removers are designed to remove acid soluble particles such as calcium carbonate. The intrusion of sand to the fabric of the filter cake renders these treatments ineffective.

The objective of this research work is to investigate the chemical composition of the filter cake in horizontal wells. It is of the main goals of this study to quantify the sand content along the horizontal section of long reach horizontal well.

3.2 OBJECTIVE & APPROACH

Evaluate the characteristics of the filter cake in horizontal wells in terms of sand content, using real drilling fluid samples from the field.

APPROACH

To achieve the above objective the following will be conducted:

- a) Select a candidate well and design mud sampling program.
- b) Analyze the drilling fluid properties used to drill the horizontal wells.
- c) Perform filtration press experiments on **ceramic disk** under a recommended pressure drop and time to form a filter cake using the different drilling fluid samples from the different locations along the horizontal section.
- d) Use the X-ray Diffraction (XRD) and scanning electron microscopy (SEM) techniques to determine the mineralogy of the filter cake.
- e) Evaluate the results to find out if the filter cake characteristics are constant in terms of sand content along the lateral section.

CHAPTER 4

EXPERIMENTAL SETUP & PROCEDURE

In this chapter the materials, apparatus and experimental procedures employed in this study are described.

4.1 Drilling Fluid Properties

Drilling fluid samples used in this study were collected from horizontal well in an oil field. By the time the bit entered the horizontal section, the drilling fluid samples were collected along a specified length. For a 3175 feet horizontal section length, one drilling fluid sample was collected with 200 feet of sandstone formation drilled. The drilling fluid samples were collected at the surface while they return back from the well during drilling operation, **Figure 4.1**.

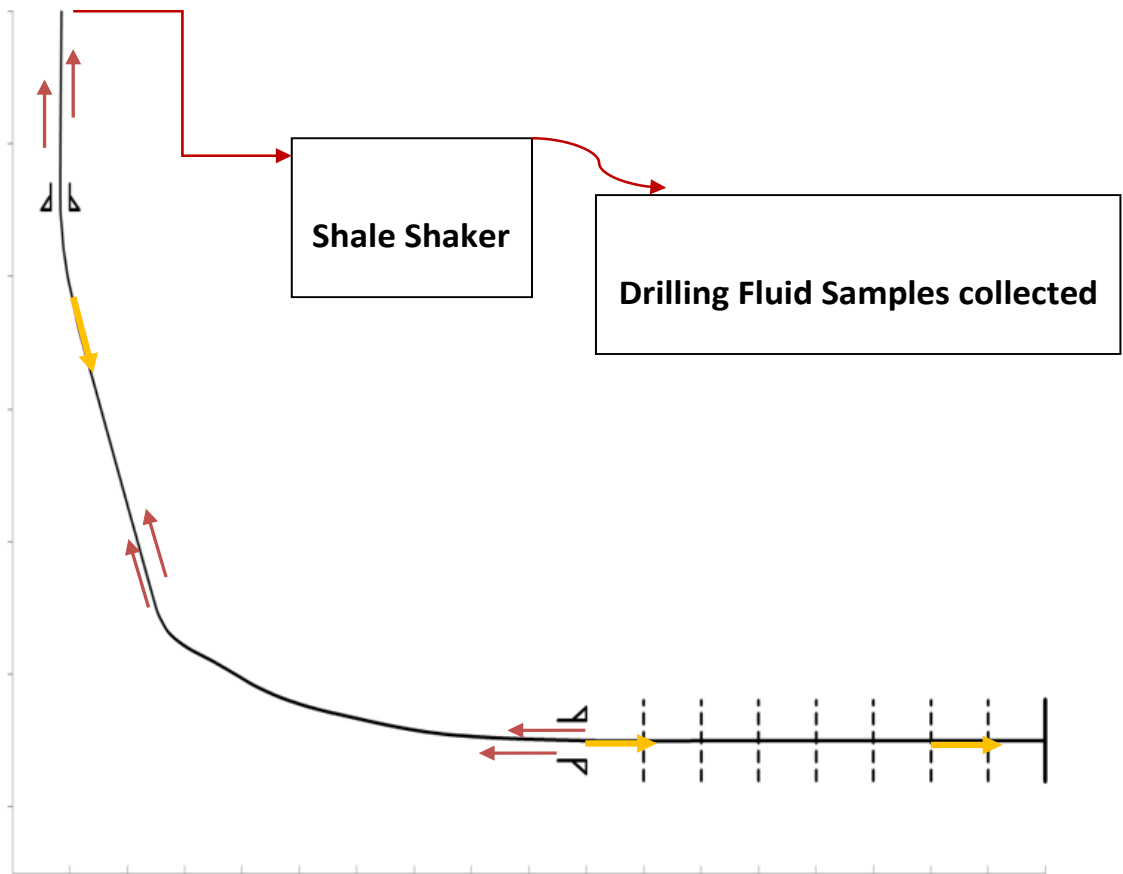


Figure 4. 1: A Schematic of Horizontal Well Shows the Collection Point of Drilling Fluid Samples

4.1.1 Drilling Fluid Density

Density of drilling fluid samples is commonly measured by mud balance, **Figure 4.2**. The density of the drilling fluid is expressed in pounds per gallon (lb/gal) and pounds per cubic foot (lb/ft³). The mud balance can be calibrated with fresh water. The density of fresh water is 8.33 lb/gal at (21°C).



Figure 4. 2: Balance Arm for Determining the Drilling Fluid Density, (Ib/gal), (Darley and Gray 1988)

4.1.2 Drilling Fluid Rheological Characteristics

The rheological properties were studied with a rotational viscometer which is used to measure shear rate/shear stress of a drilling fluid. The essential elements are shown in **Figure 4.3**. The apparent viscosity (μ_a), the plastic viscosity and the yield point (YP) are calculated as following:

$$\mu_a = \frac{300 \theta_N}{N}, \dots\dots\dots (4.1)$$

So that apparent viscosity can equal to $\mu_a = \frac{\theta_{600}}{2}, \dots\dots\dots (4.2)$

$$PV = \theta_{600} - \theta_{300}, \dots\dots\dots (4.3)$$

$$YP = \theta_{300} - \mu_p, \dots\dots\dots (6.4)$$

Where:

μ_a = apparent viscosity, cp

PV = plastic viscosity, cp

YP = yield point, Ib/100ft²,

$\theta_N, \theta_{600}, \theta_{300}$ = the dial reading, Ib/100ft² and

N = the rotor speed, rpm.

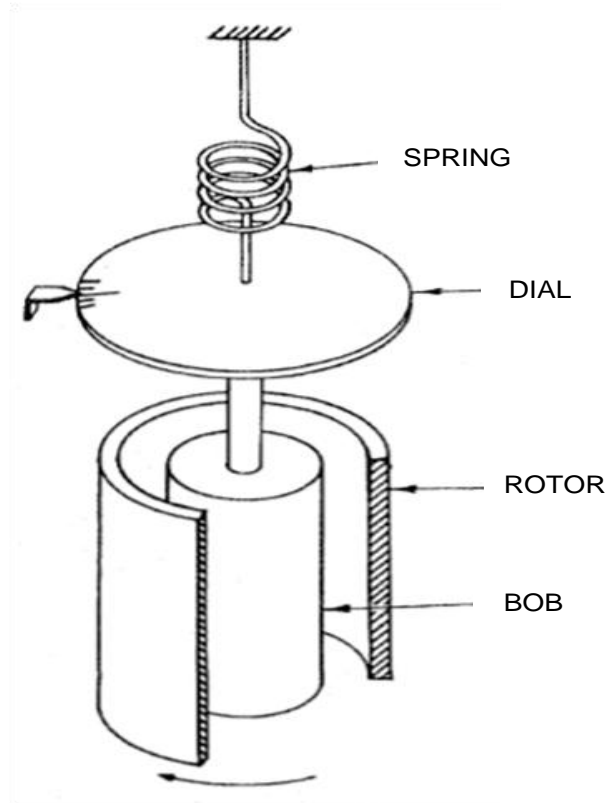


Figure 4. 3: Schematic Diagram of the Viscometer (Darley and Gray 1988)

A bob suspending from a spring hangs concentrically in an outer cylinder. The assembly is lowered to a prescribed mark in a cup of mud, and the outer cylinder rotated at a constant speed. The viscous drag of the mud turns the bob until balanced by the torque in the spring.

4.2 Static Filtration Tests

Two types of filtration are considered static and dynamic. Static filtration occurs when the fluid is not in motion in the hole. Dynamic filtration occurs when the drilling fluid is being circulated.

Dynamic filtration differs from static filtration in that drilling fluid velocity tends to erode the wall cake even as it is being deposited on permeable formations. As the rate of erosion equals the rate of buildup of the wall cake, equilibrium is established. In static filtration, the wall cake will continue to be deposited on the borehole.

Static filtration tests are used to indicate filter cake quality and filtration volume loss for a drilling mud under specific testing conditions. Based on the test conditions, there are two types of tests: API low-pressure filter press (Pressure is applied to the top of the cell at 100 psi) and high temperature/high pressure (HTHP) (test is run at a temperature greater than ambient and a differential pressure of 500 psi).

As the objective of this work is to study the filter cake mineralogy, thus we operate static loss test under high pressure of 500 psi. The tests were performed using 500 ml HPHT cell, **Figure 4.4**. The ceramic disks (35 micron) were used as filtration medium in the test to match the properties of the formation. The disk diameter is 2.5 inch and the thickness is 0.25 inch.

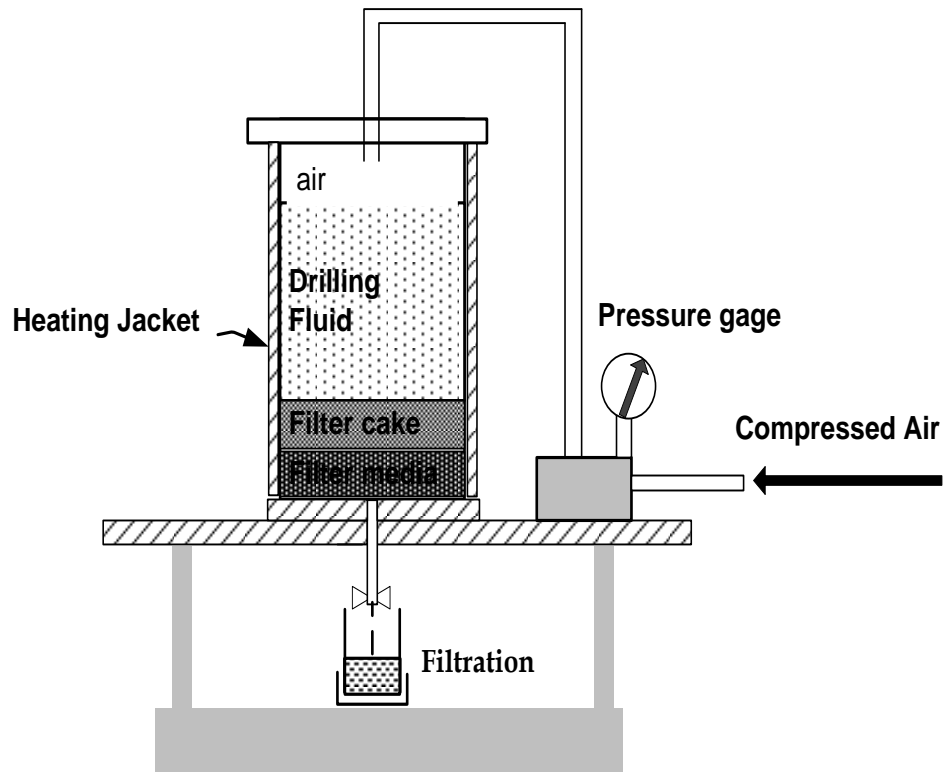


Figure 4. 4: Assembled High Pressure High Temperature Cell

4.3 Filter Cake Properties

The properties of the filter cake obtained from fluid loss test were analyzed to evaluate these properties at the horizontal section of sandstone formation.

4.3.1 Filter Cake Thickness

After fluid loss test was performed, the ceramic disk was removed from the fluid loss cell carefully so as not to disturb the filter cake which was set on top of the ceramic disk. Excess mud was gently washed from the filter cake with a small stream of oil. Subsequently the total thickness of filter cake with ceramic disk was measured with vernier caliper and the filter cake thickness was calculated by subtracting the ceramic disk thickness from the total thickness.

4.3.2 Filter Cake Minerology

The mineralogy of the external filter cake was studied using Scanning Electron Microscopy (SEM) and X-Ray Diffraction (XRD).

A) Scanning Electron Microscopy (SEM)

Scanning Electron Microscopy is generally used to examine the surface morphology of samples and identify the elemental constitution of a material. This is accomplished by generating high-resolution images of the areas of interest within the sample and detects changes in its chemical composition at microstructural level. In our study, Field Emission Scanning Electron Microscope (FE-SEM Model FEI Nova Nano SEM 230) was used to undertake analysis of as-received uncoated samples. An accelerating voltage of 20 kV was used during analysis and imaging was performed using secondary electron imaging mode. Microchemical analysis of samples was carried out using energy dispersive x-ray (EDS) detector coupled with INCA EDS software (Detector Model: Oxford INCA Penta FETx3 with 30 mm² detectable area). The Si(Li) EDS detector was equipped with an atmospheric thin window capable of detecting elements down to Be.

B) X-Ray Diffraction (XRD)

X-ray diffraction is used to identify different phases present within a crystalline material. In our study, an x-ray diffractometer (Model: Rigaku Ultima IV MPD) equipped with a solid state ultra D/teX detector and a monochromator was employed to study the

phase constitution of filter cake samples. The diffraction spectra were generated using CuK_α radiation ($\lambda=1.54184 \text{ \AA}$) source operating at 40 kV and 40 mA. Bragg-Brentano (BB) configuration with $2\theta/\theta$ continuous scan control axis was employed during analysis. The samples were scanned at a rate of 2 degree per minute for diffraction angles (2θ) of 4-80 degrees. Divergence slit and divergence height limiting slit were fixed at $2/3$ degrees and 10 mm respectively while scattering and receiving slits were kept open during data acquisition. Peaks in XRD spectrum were indexed using Rigaku PDXL software while concentrations of phases were quantified using Rietveld analysis.

Preparation of filter cake samples for SEM and XRD test passes through the following procedures:

A) Drying

After filter cake thickness measurements, the ceramic disk with the filter cake is housed inside an oven where the wet filter cake obtained from fluid loss test can be dried from water. The filter cake is dried at about 100°C (220°F) for 3 to 6 hours (Elkatatny *et al.* 2011; Dewan and Chenevert 2001).

B) Washing

The drilling fluid samples used in fluid loss tests were oil-based drilling fluid. Thus the filter cake was washed by using any solvent such as Toluene ($\text{C}_6\text{H}_5\text{-CH}_3$) to remove oil from the particles deposited in the filter cake.

C) Filtration

To remove the solids from the solvent (Toluene), a simple filtration process was conducted using filter paper to have the solids on filter paper.

D) Re-Drying

Again the filter paper with the washing solids was placed in an oven at 100°C for about 3 hours to dry the solids.

E) Graining

The collected solids were grained gently to have a nice and smooth powder ready for XRD and SEM analysis. Some equipment can be used for this purpose but as the filter cake solids amount are too small, this operation was done manually to avoid losing solid samples.

4.4 Internal Filter Cake Evaluation

To evaluate the internal invasion depth, CT scanner for the ceramic disks was applied. CT scanner divided ceramic disk to five layers (each layer has 1mm thickness) to visualize the depth of invasion in these layers. Although CT scanner cannot provide the exact depth of invasion, it gives us useful information to compare the effect of increasing the sand content on an internal invasion by examining the photos of each sample and comparing the CT number of invaded layers with CT number of the non-invaded layer (new ceramic disk).



Figure 4. 5: Scanning Electron Microscope (SEM)

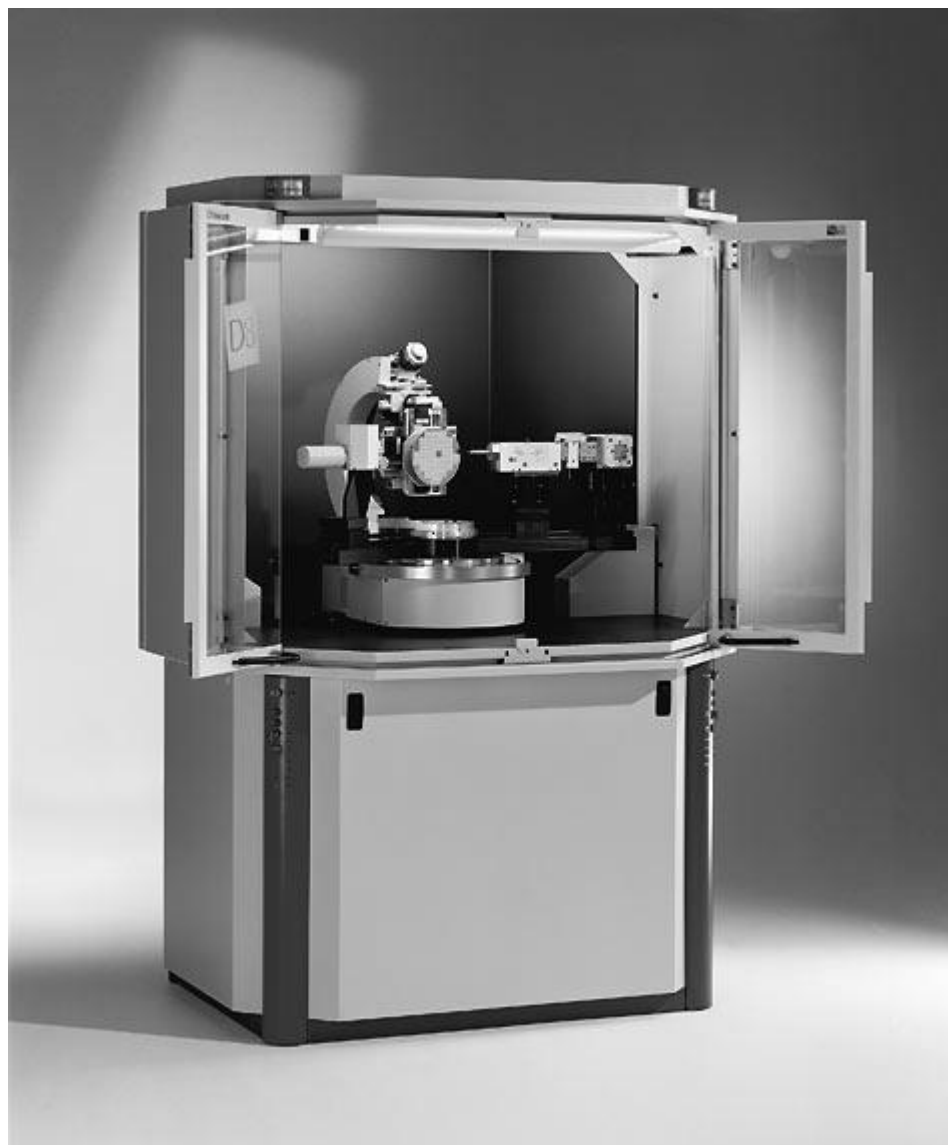


Figure 4. 6: X-ray Diffraction (XRD)



Figure 4. 7: CT scanner

CHAPTER 5

RESULTS AND DISCUSSION

5.1 Drilling Fluid Properties

Filter cake is strongly dependent on drilling fluid properties such as density, apparent viscosity, plastic viscosity and yield point. These properties were analyzed and evaluated at the horizontal section of the well.

5.1.1 Drilling Fluid Density

Drilling fluid density depends on the percentage of component in the drilling fluids. Therefore, any change in the drilling fluid density will give an indication of a change in the drilling fluid composition.

The density of the selected drilling fluid samples during drilling the horizontal section is tested to show if there is a change in the density with more feet of formation drilled. The results show that there is a slight increase in the drilling fluid density with more feet of horizontal section drilled, as shown in **Figure 5.1**. Along the 3175 ft of the

horizontal section, the density increased only about 0.22 ppg (1.67 pcf) as **Figure 5.2** shows.

Table 5. 1: Drilling Fluid Density

Sample no.	Measured Depth ft	Density ppg
1	6700	10.7
2	6900	10.57
3	7100	10.8
4	7300	10.65
5	7500	11
6	7700	10.7
7	7900	10.78
8	8100	10.78
9	8300	10.8
10	8500	10.8
11	8700	10.78
12	8900	11
13	9100	10.9
14	9300	10.83
15	9500	10.78
16	9675	10.85

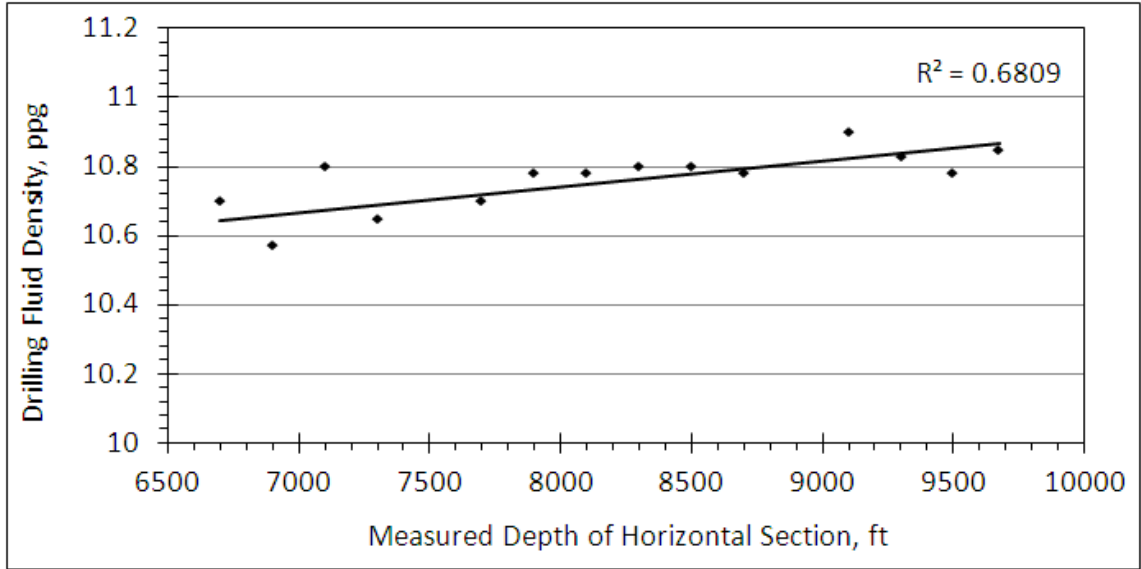


Figure 5. 1: Changes of Drilling Fluid Density with Horizontal Measured Depth

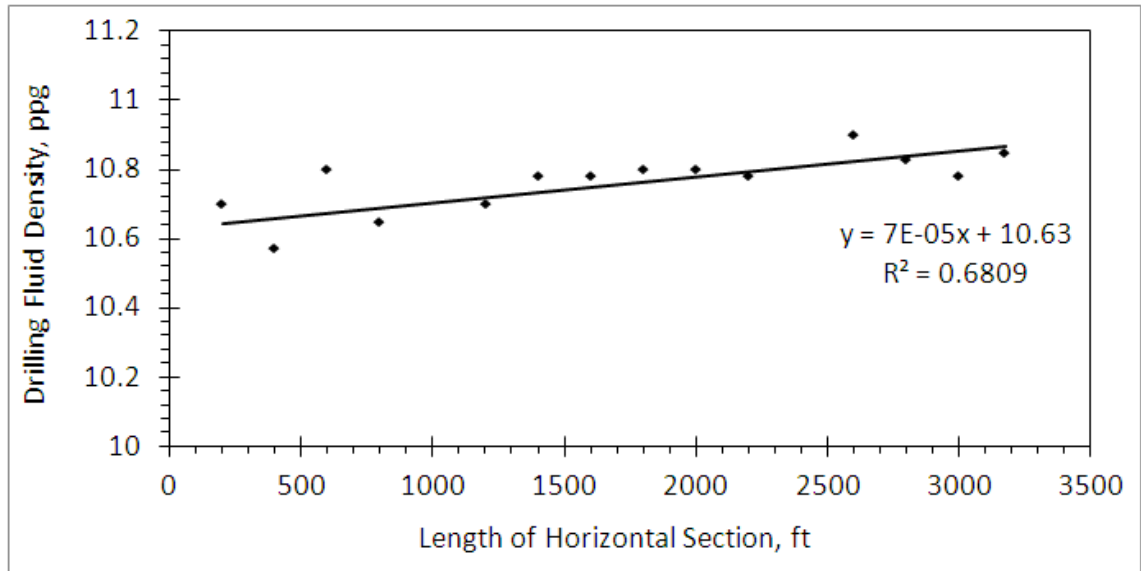


Figure 5. 2: Changes of Drilling Fluid Density with Horizontal Length

5.1.2 Drilling Fluid Rheological characteristics

The drilling fluid rheological characteristics are mainly represented by apparent viscosity (μ_a), plastic viscosity (μ_p), yield point (YP), and gel strength (Gel). It is basically controlled by solid particles added to the drilling fluid. **Table 5.2** shows the value of (μ_a), (μ_p), (YP) and (Gel) which reveals that the rheological properties continuously change in the horizontal section due to mixing of small cutting particles with the drilling fluid which were not properly removed during the separation process. The cuttings are mixed with drilling fluids during mud circulation and become an integral part of it. The experimental results show that the drilling fluids become more viscous with an increase in length of the horizontal section, **Figure 5.3 and Figure 5.5**.

Figure 5.4 shows that the apparent viscosity and plastic viscosity increase about (20%; 18%) respectively, along the entire section. The yield point and gel strength are more sensitive functions of the length of the distance drilled. The results indicated that the yield point increased from (15 to 21 lb/100ftsq) which is about an increase of 40%, as shown in **Figures 5.4 & 5.6**. The gel strength (10 minute and 10 second) increased 32.5% and 42.5% respectively as **Figure 5.6** shows.

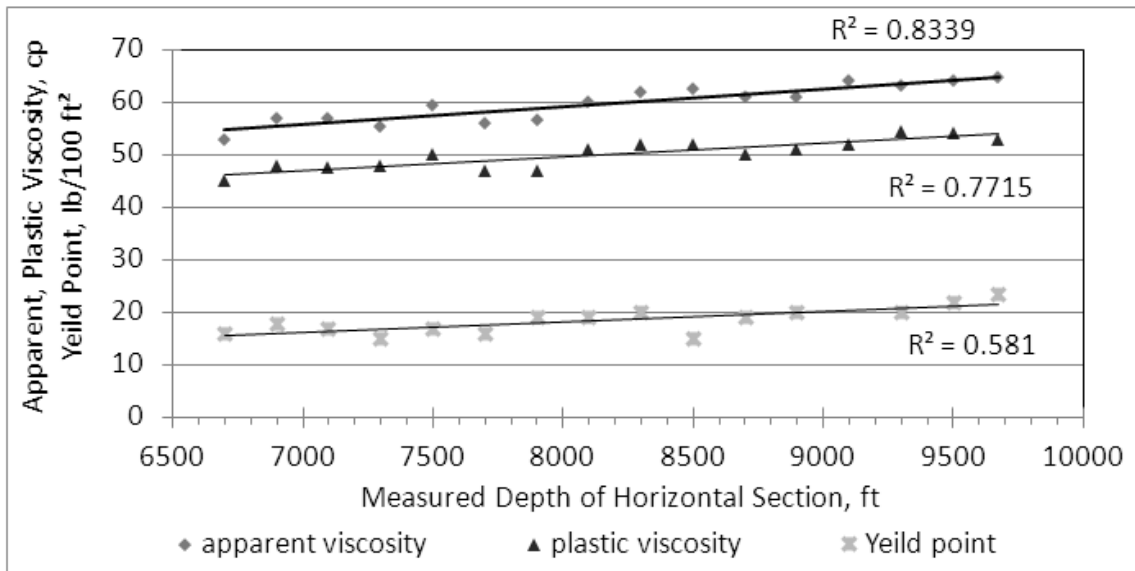


Figure 5. 3: Changes in Drilling Fluid Apparent Viscosity, Plastic Viscosity, and Yield Point with Horizontal Measured Depth

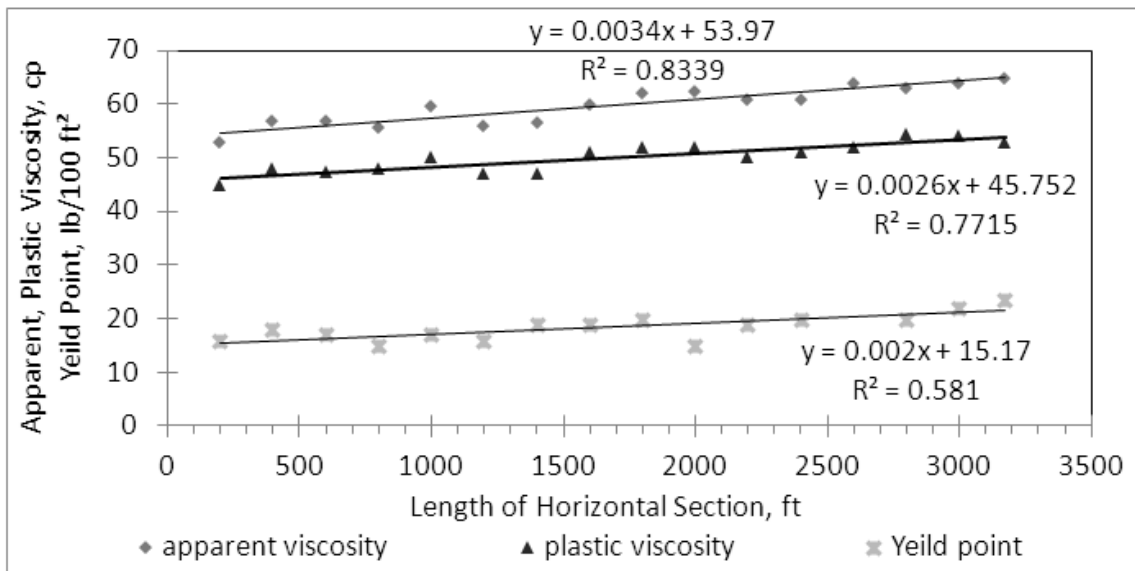


Figure 5. 4: Changes in Drilling Fluid Apparent Viscosity, Plastic Viscosity, and Yield Point with Horizontal Length

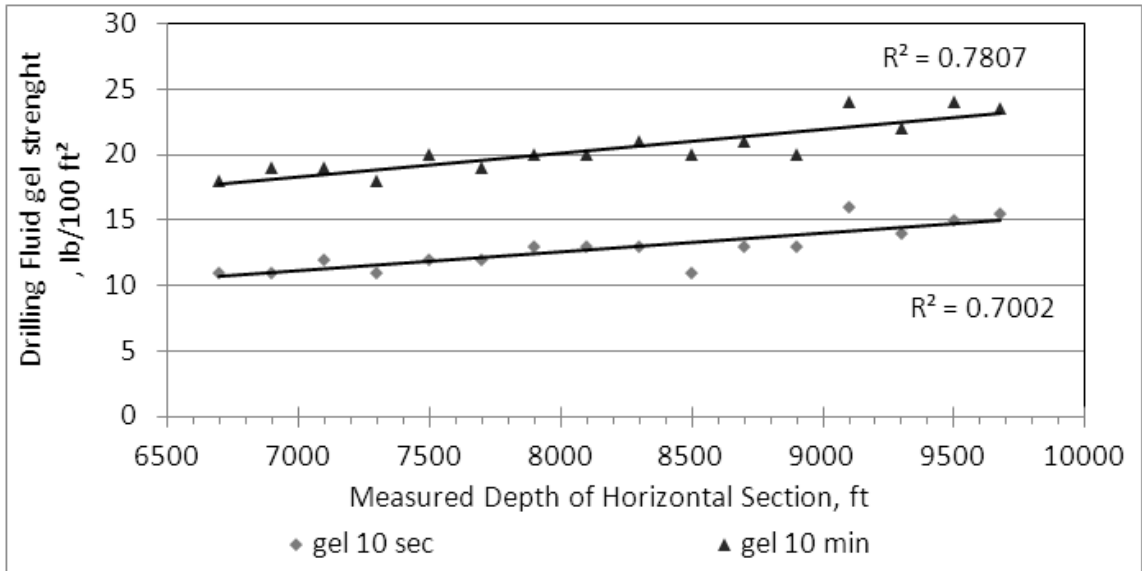


Figure 5. 5: Changes in Drilling Fluid Gel Strength (10 Minutes / 10 Seconds) with Measured Depth of Horizontal Section

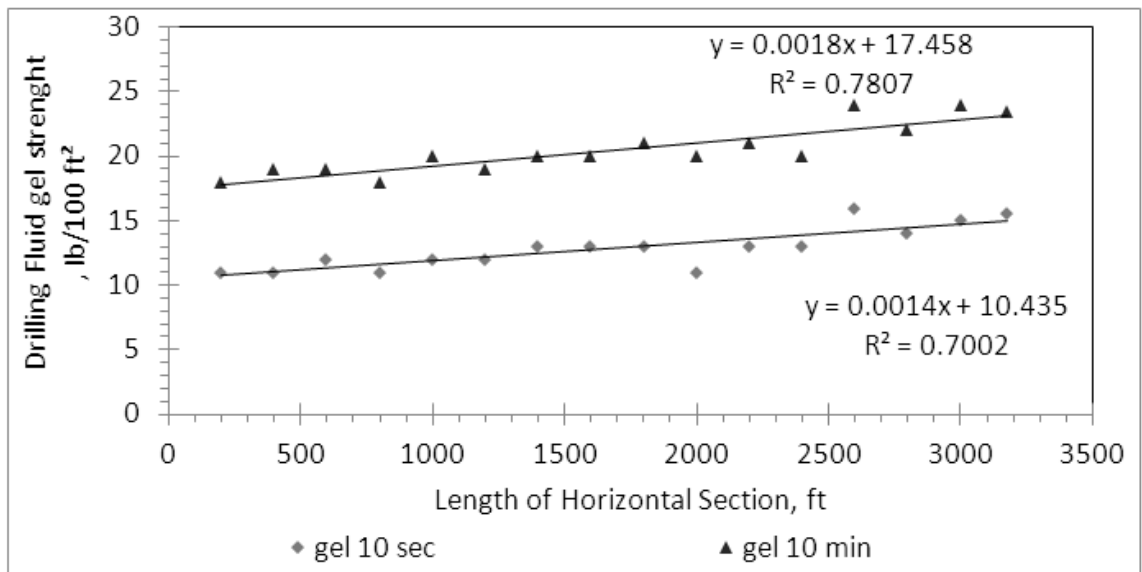


Figure 5. 6: Changes in Drilling Fluid Gel Strength (10 Minutes / 10 Seconds) with Horizontal Length

Table 5. 2: Drilling Fluid Rheological Characteristics

L ft	Depth ft	Apparent viscosity μ_a (cp)	Plastic viscosity μ_p (cp)	Yield point Ib/100 ft ²	Gel 10 sec Ib/100 ft ²	Gel 10 min Ib/100 ft ²
200	6700	53	45	16	11	18
400	6900	57	48	18	11	19
600	7100	57	47.5	17	12	19
800	7300	55.5	48	15	11	18
1000	7500	59.5	50	17	12	20
1200	7700	56	47	16	12	19
1400	7900	56.5	47	19	13	20
1600	8100	60	51	19	13	20
1800	8300	62	52	20	13	21
2000	8500	62.5	52	15	11	20
2200	8700	61	50	19	13	21
2400	8900	61	51	20	13	20
2600	9100	64	52	29	16	24
2800	9300	63	54.5	20	14	22
3000	9500	64	54	22	15	24
3175	9675	64.75	53	23.5	15.5	23.5

5.2 External Filter Cake Properties

Fluid loss (static-high pressure) tests of drilling fluid samples were conducted to analyze and evaluate the properties of the filter cake generated by the samples selected, **Figure 5.7** shows a filter cake sample obtained from fluid loss tests.

5.2.1 Filter Cake Thickness

The thickness of solids deposited on the permeable ceramic disk was measured to have a preliminary estimate about filter cake properties. It is clear that for the same test conditions, there is a linear relationship between the lengths of horizontal section drilled and cake thickness, as **Figure 5.8** shown.

The increase of filter cake thickness with the lateral length of this well can be seen in **Figure 5.9** as follows:

The filter cake thickness increased 12% per 1000 ft length drilled of the horizontal sandstone section. Along the entire section it increased by about 36%. This increase in the cake thickness coincides with increasing of the drilling fluid apparent viscosity, plastic viscosity, yield point, gel strength 10 second and gel strength 10 minute by 20%, 18%, 40%, 42.5% and 32.5% respectively while the increase of the density can be neglected. Therefore, filter cake thickness can be described as a sensitive function of drilling fluid rheological characteristics, which can cause stuck pipe.

Modeling the filter cake thickness with the length drilled in the horizontal section of this well gives a straight line relationship, as can be seen in Eq. 5.1.

$$h_c = 2 \times 10^{-5} L + 0.1767, \dots \dots \dots (5.1)$$

Where:

L = the lateral length, ft

hc = the cake thickens, inch

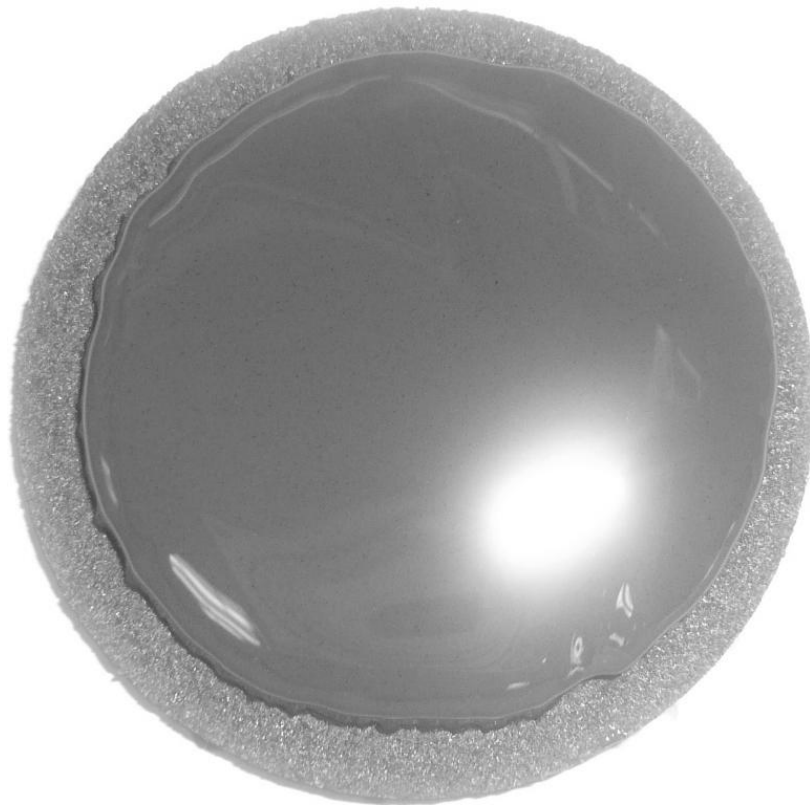


Figure 5. 7: Filter Cake Sample Obtained from Fluid Loss Tests

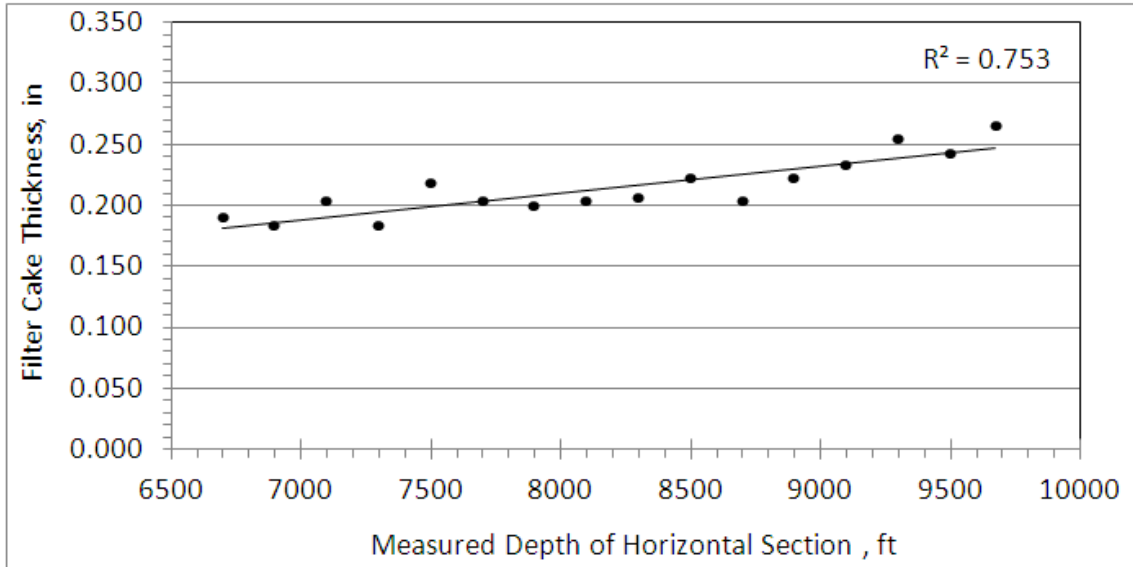


Figure 5. 8: Changes in Filter Cake Thickness with Horizontal Measured Depth

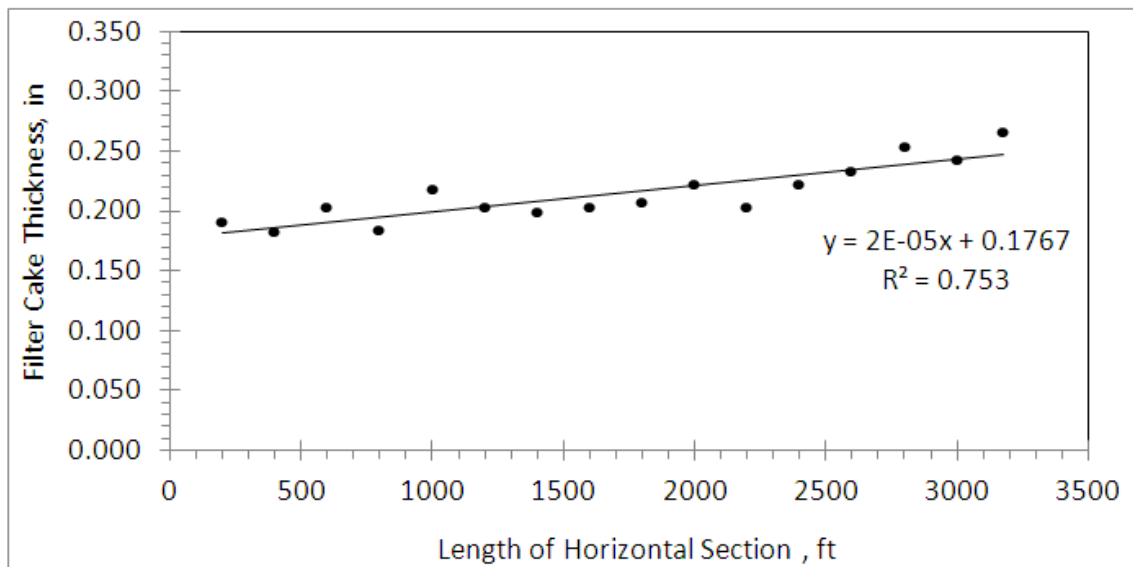


Figure 5. 9: Changes in Filter Cake Thickness with Horizontal Length

5.2.2 Filter Cake Characterization

The mineralogy of the external filter cake formed by fluid loss test is described in detail using both Scanning Electron Microscopy (SEM) and X-Ray Diffraction (XRD). Utilizing both of the SEM tests and the XRD tests will ensure that the cake structure analysis was performed in a complementary manner. The qualitative analysis by SEM guarantees that there are no components in small proportions have been ignored by XRD. Due to the inability to analyze the elements with less than two percent of the weight is one of the disadvantages of XRD.

A) Scanning Electron Microscopy (SEM) Analysis

The chemical compositions of the dried powder filter cake are determined by SEM which is able to qualitatively or semi-quantitatively determine chemical compositions. Data generated from SEM is collected over a small selected area of the surface of the filter cake powder sample. Therefore, two or three different points are tested for each filter cake sample to make sure that representative area of filter cake sample has been covered in determining the chemical compositions.

Figure 5.6 shows the average quantitative chemical compositions of the first filter cake (sample 6) using Scanning Electron Microscopy (SEM). The two different locations (spectrum 1&2) of this sample are shown in **Figure 5.7** respectively.

The test indicates that the filter cake contains three main elements, Silicon (Si), Calcium (Ca) and Chlorine (Cl). These results revealed that the presence of Si in filter

cake is expected since Si is the main component of sandstone rock. Also it highlights the potential distribution of these elements in conjunction with oxygen and/or with each other to form the main phases of the filter cake. The quantitative elemental analysis using SEM leads to better understanding of the results that are obtained from XRD.

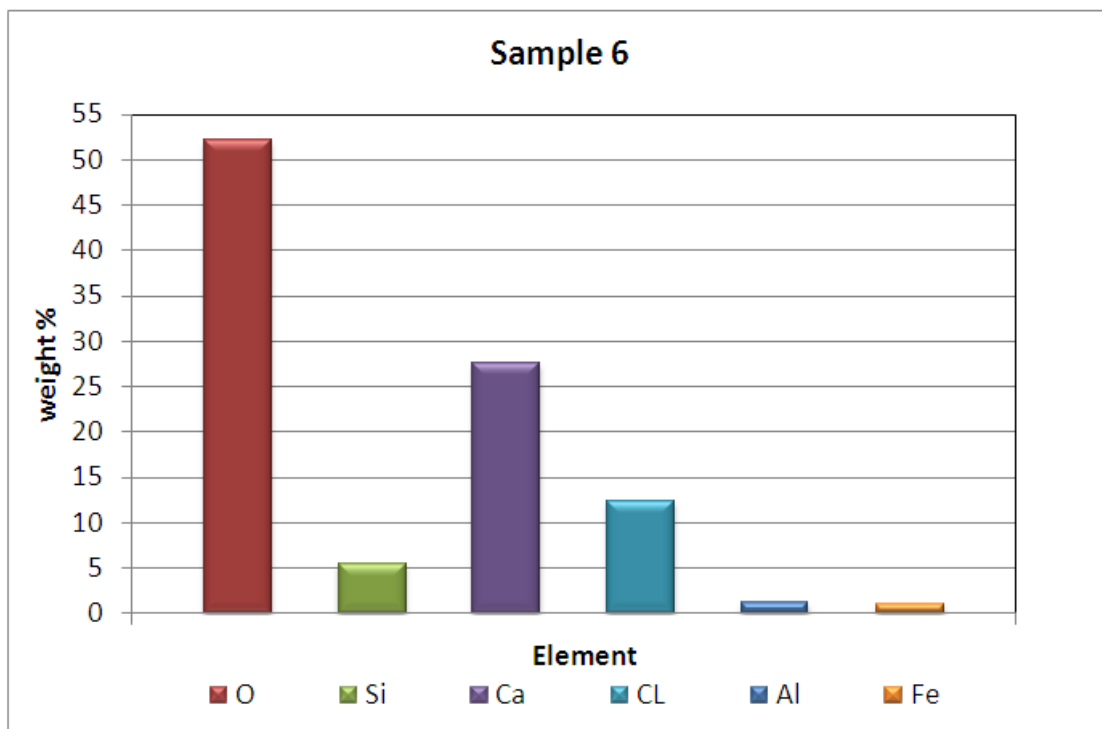
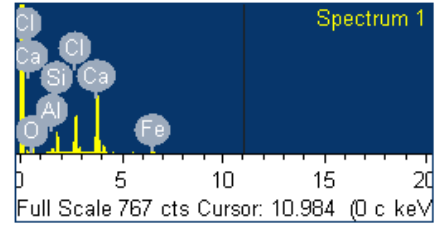
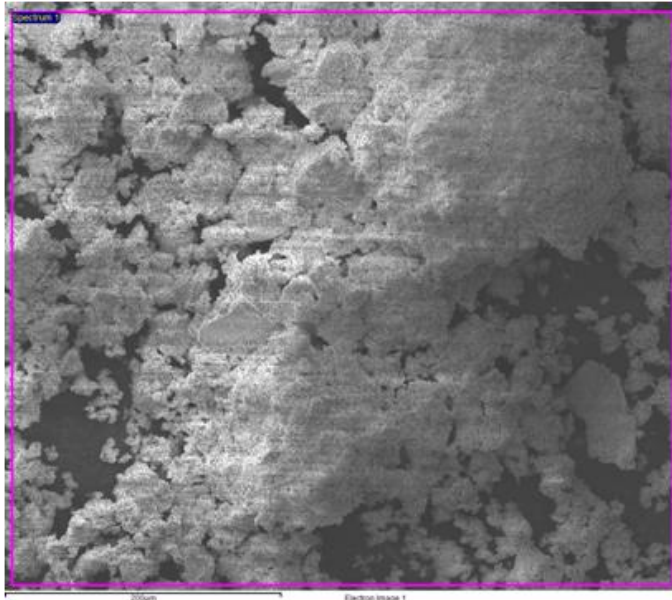
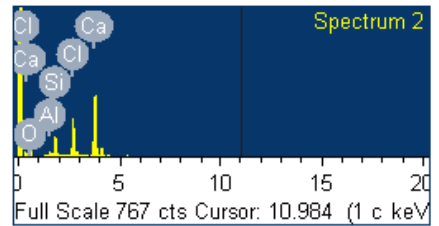
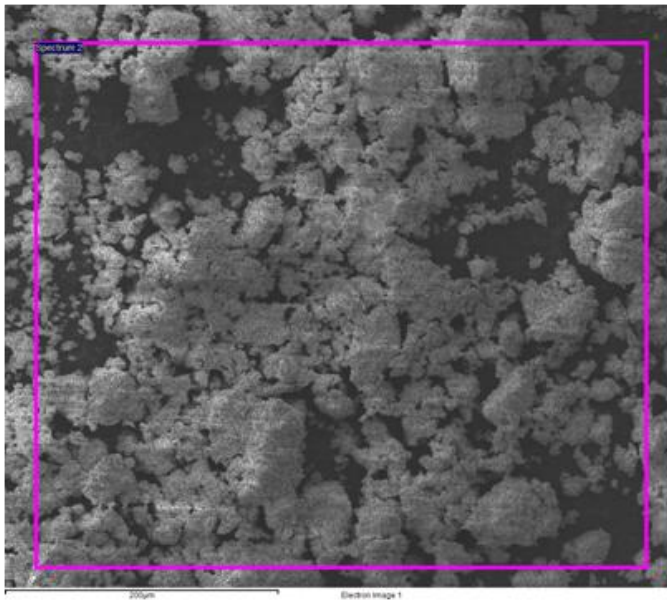


Figure 5. 10: The Chemical Compositions of the Filter Cake (Sample 6) Using (SEM)



Spectrum	In stats.	O	Al	Si	Cl	Ca	Fe	Total
Spectrum 1	Yes	50.54	1.01	5.81	13.56	26.98	2.10	100.00



Spectrum	In stats.	O	Al	Si	Cl	Ca	Total
Spectrum 2	Yes	53.75	1.42	5.27	11.31	28.24	100.00

Figure 5. 11: Two Different Locations (Spectrum 1&2) of Filter Cake (Sample 6) Using (SEM)

Similarly to sample 6 of the filter cake, the other fifteen samples were characterized by SEM using the same method.

It has been pointed out previously that to determine the chemical compositions using SEM two or three different areas are tested for each filter cake sample to make sure that representative filter cake area has been covered. SEM results of each sample were averaged and the summary of the whole sample results are shown in **Table 5.3**. Quantitatively, the results of all samples show that the filter cake contains Silicon (Si) because of sandstone formation. The percentage of Si might change to reflect its concentration at particular locations, not in the entire filter cake. This is also true for other elements. **Figure 5.8** shows the main four elements of whole filter cake samples using SEM.

Table 5. 3: The Summary of SEM Results of Whole Filter Cake Samples

sample no.	MD ft	Elements weight %										
		O	Si	Ca	Cl	Al	Fe	Mg	Na	Ba	S	Ti
1	6700	44.48	7.21	24.94	11.45	0.78				9.27	1.86	
2	6900	46.96	3.43	32.13	16.1	0.95			0.43			
3	7100	50.16	6.925	27.92	13.36	1.225	0.415					
4	7300	52.20	4.99	28.43	12.49	1.153	0.3266	0.1766	0.223			
5	7500	49.81	6.76	27.13	14.51	1.185	0.6					
6	7700	52.14	5.54	27.61	12.435	1.215	1.05					
7	7900	50.06	6.16	28.92	13.6	1.255						
8	8100	54.65	7.01	26.26	10.86	1.215						
9	8300	52.22	6.58	26.19	13.70	1.295						
10	8500	55.16	10.445	21.46	10.97	1.505	0.45					
11	8700	51.74	8.62	28.6	8.6	1.79		0.645				
12	8900	54.27	7.44	27.52	9.45	1.325						
13	9100	54.19	21.8	15.97	7.235	0.795						
14	9300	52.82	10.24	25.46	9.22	1.255	0.995					
15	9500	57.92	8.46	23.35	8.18	1.465	0.625					
16	9675	52.33	19.77	18.15	7.87	1.505						0.365

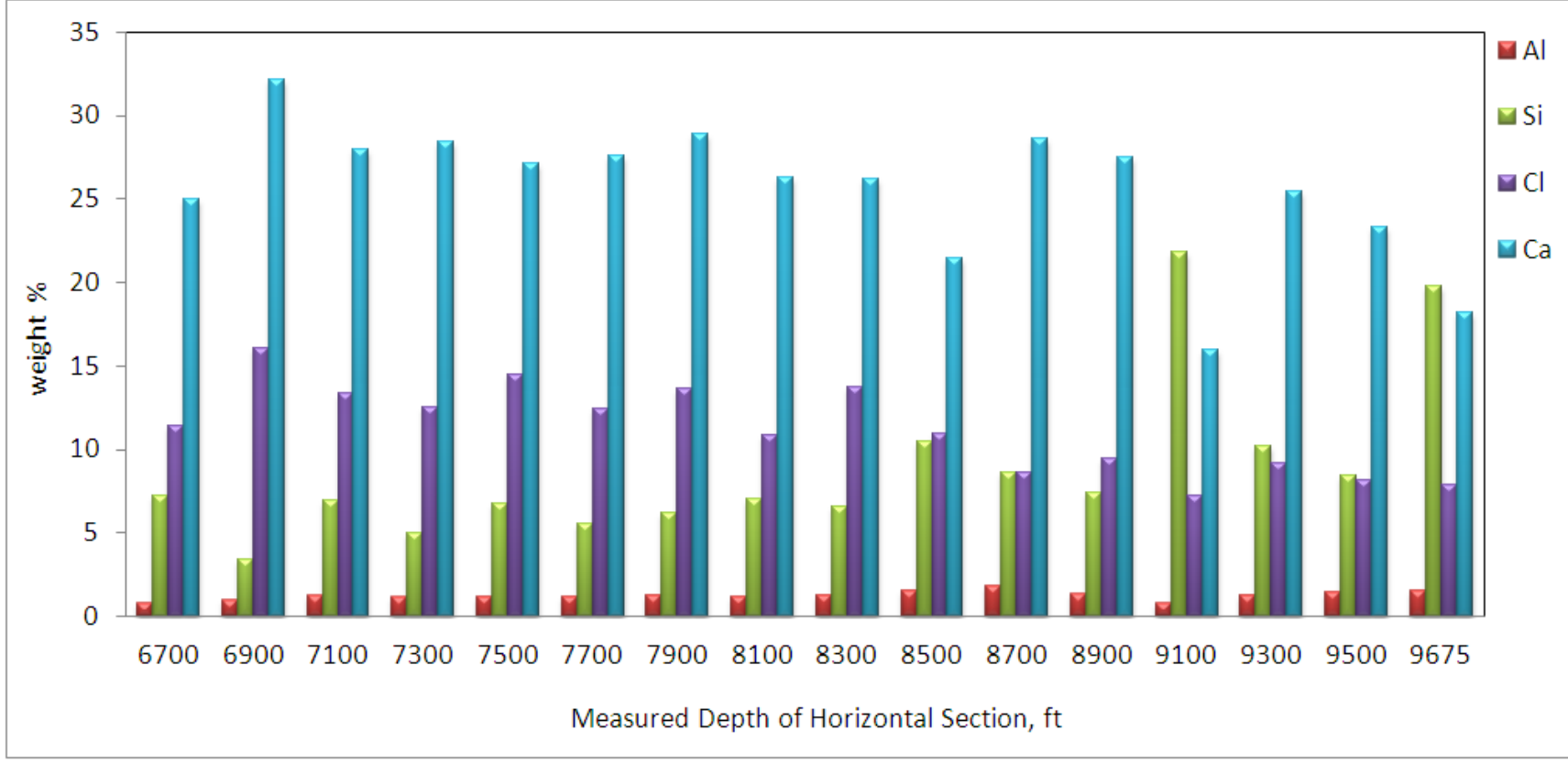


Figure 5. 12: The Summary of SEM Results of the Main Four Elements

B) X-Ray Diffraction (XRD) Analysis

In addition to SEM analysis, XRD provides the phase identification (minerals) of filter cake fabric and determines modal amounts of minerals (quantitative analysis).

Figure 5.9 shows that the main phase peaks of filter cake (sample 6) are Quartz and Calcite. In addition, quantitative analysis results show percentage of each constituent in the filter cake mineralogy using XRD, **Table 5.4**. These phases are produced due to conjunction of the elements Si and Ca with the oxygen with certain chemical formulas.

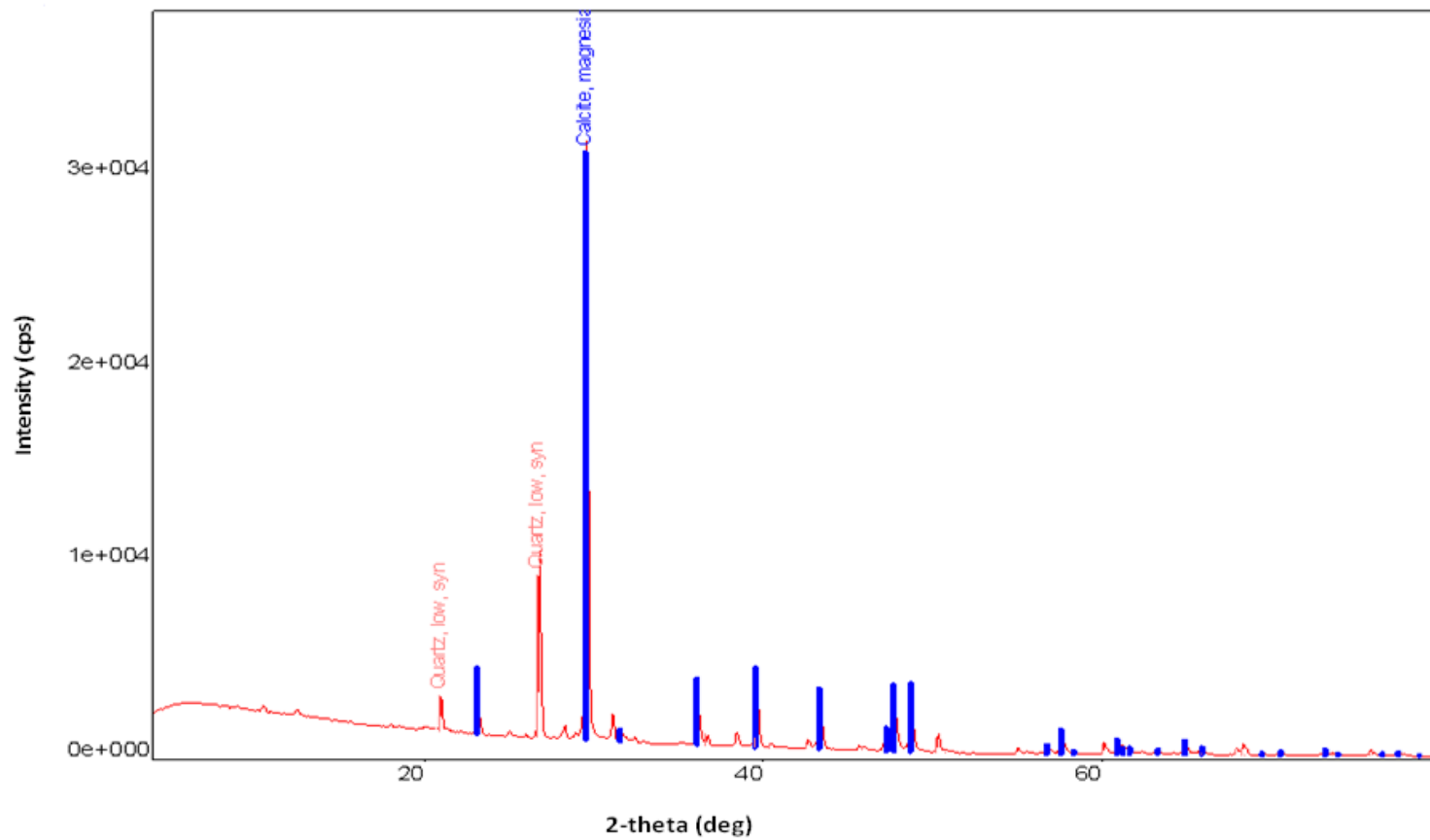


Figure 5. 13: The Phases Identification of the Filter Cake (Sample 6) Using (XRD)

Table 5. 4: Quantitative Analysis of the Filter Cake (Sample 6) Using (XRD)

Quantitative analysis results (WPPF)

Phase name	Content (%)
Calcite, magnesian	81
Quartz, low, syn	19

Similarly the other fifteen samples were tested using XRD to determine the changes in phase constitution through the horizontal sandstone formation section of the well.

XRD results suggest that the concentration of sand increases with an increase in the length of sandstone formation drilled. XRD investigation reveals that for long horizontal wellbores penetrating clastic formations, the drilling cuttings are mixed with drilling mud during mud circulation and are not removed completely by surface separation equipment. Due to this reason, these materials become an integral part of the fabric of the filter cake. The sand percentage might reach up to 40% by volume of the mud solids making it prohibitively difficult to be removed with regular acids.

Figure 5.10 shows XRD results of whole filter cake samples. It can be seen that there are three regions based on the sand content in filter cake, **Figure 5.11**. The first region is characterized by the low sand level (22%) in the first part of the horizontal section from 6700 ft to 7700 ft. The second region is characterized by the Medium sand level (33%) from 7900 ft to 8900 ft and the last part of the horizontal section is the high sand percentage region where the average of sand percentage reaches higher than 40%. **Figure 5.12** shows that the relationship between the lengths of horizontal section drilled and sand percentage in filter cake. The sand percentage increases as the length of horizontal section increases.

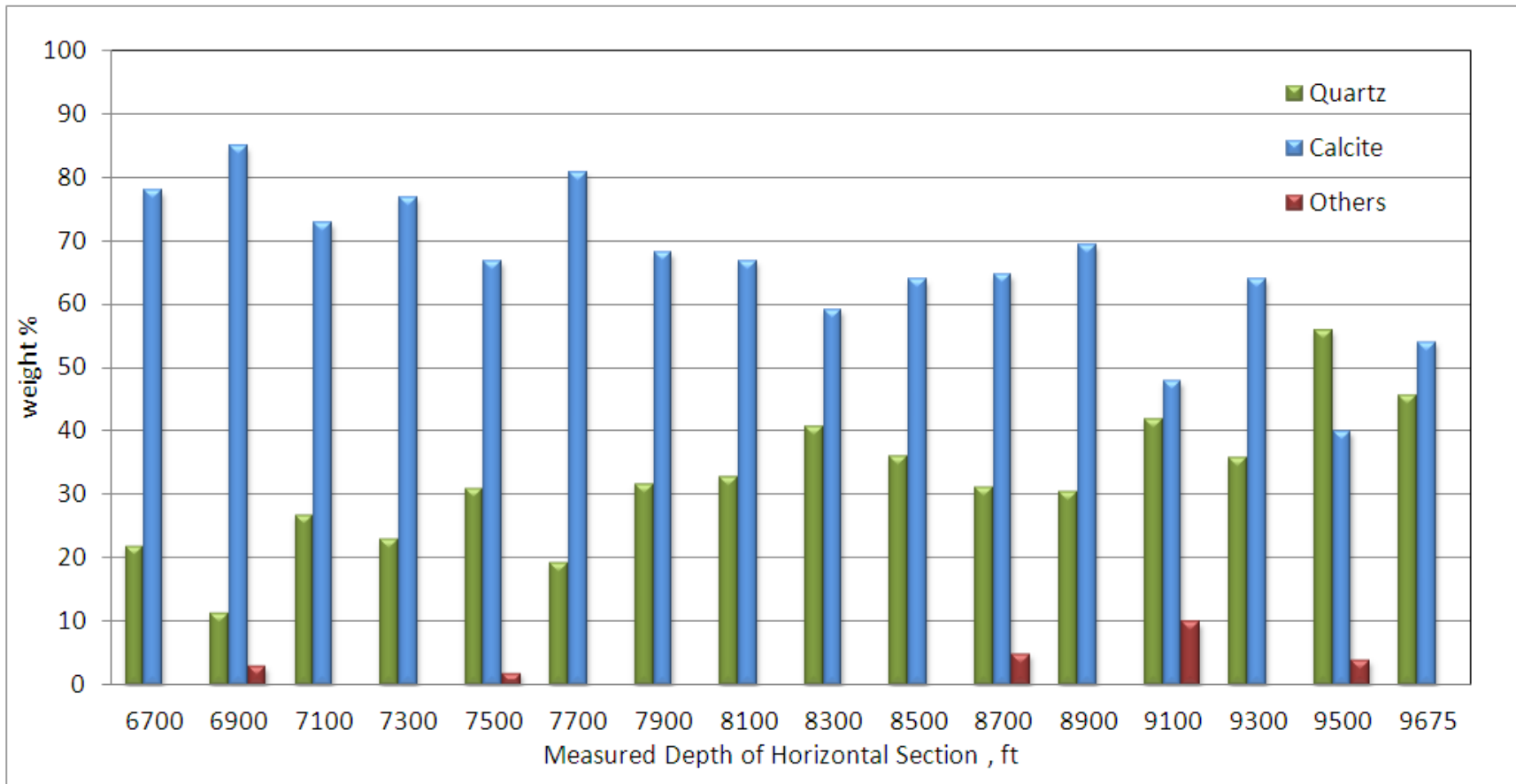


Figure 5. 14: The Minerlogy of Filter Cake Using XRD

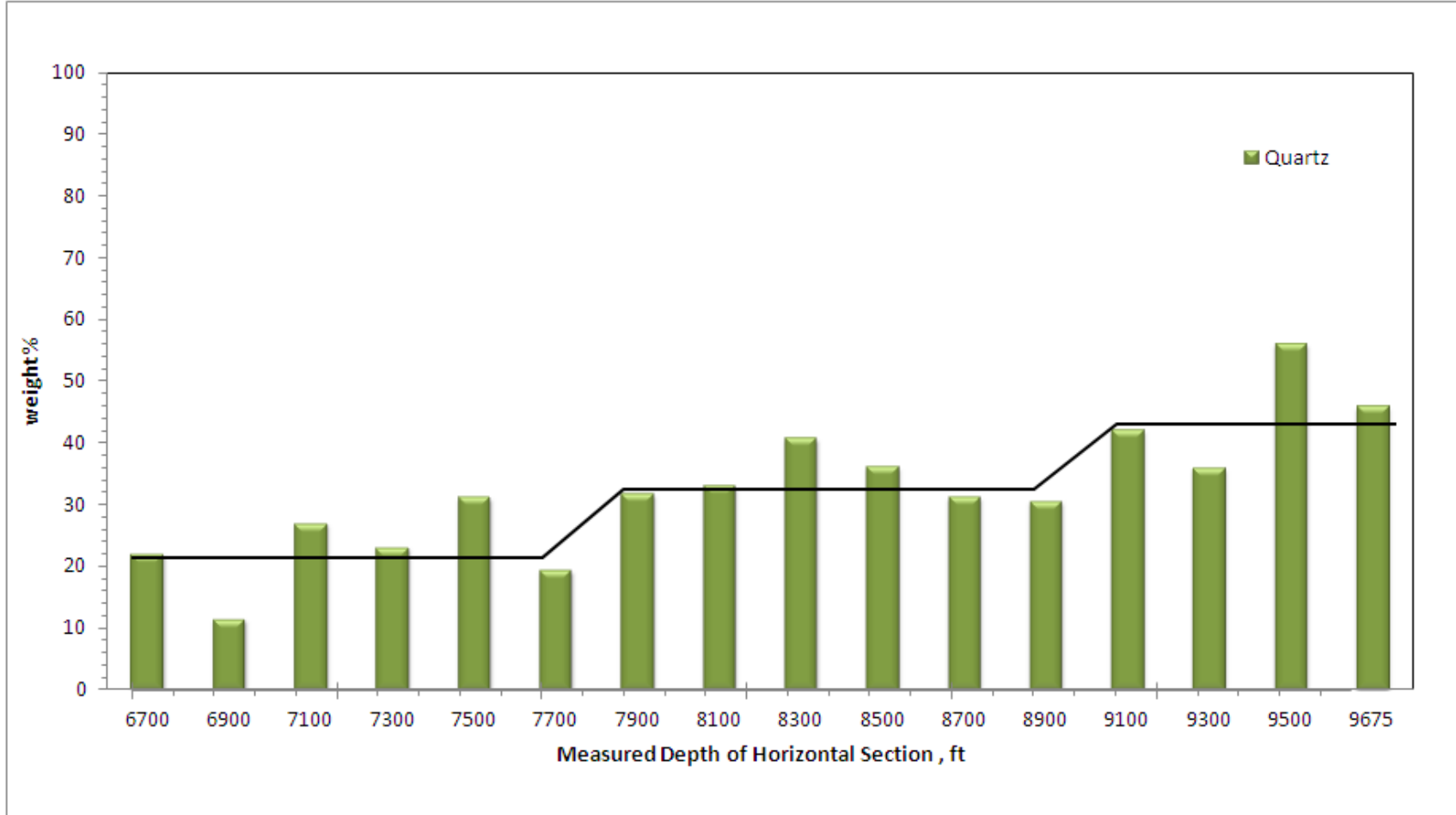


Figure 5. 15: Shows the Three Regions Based on the Sand Content in Filter Cake

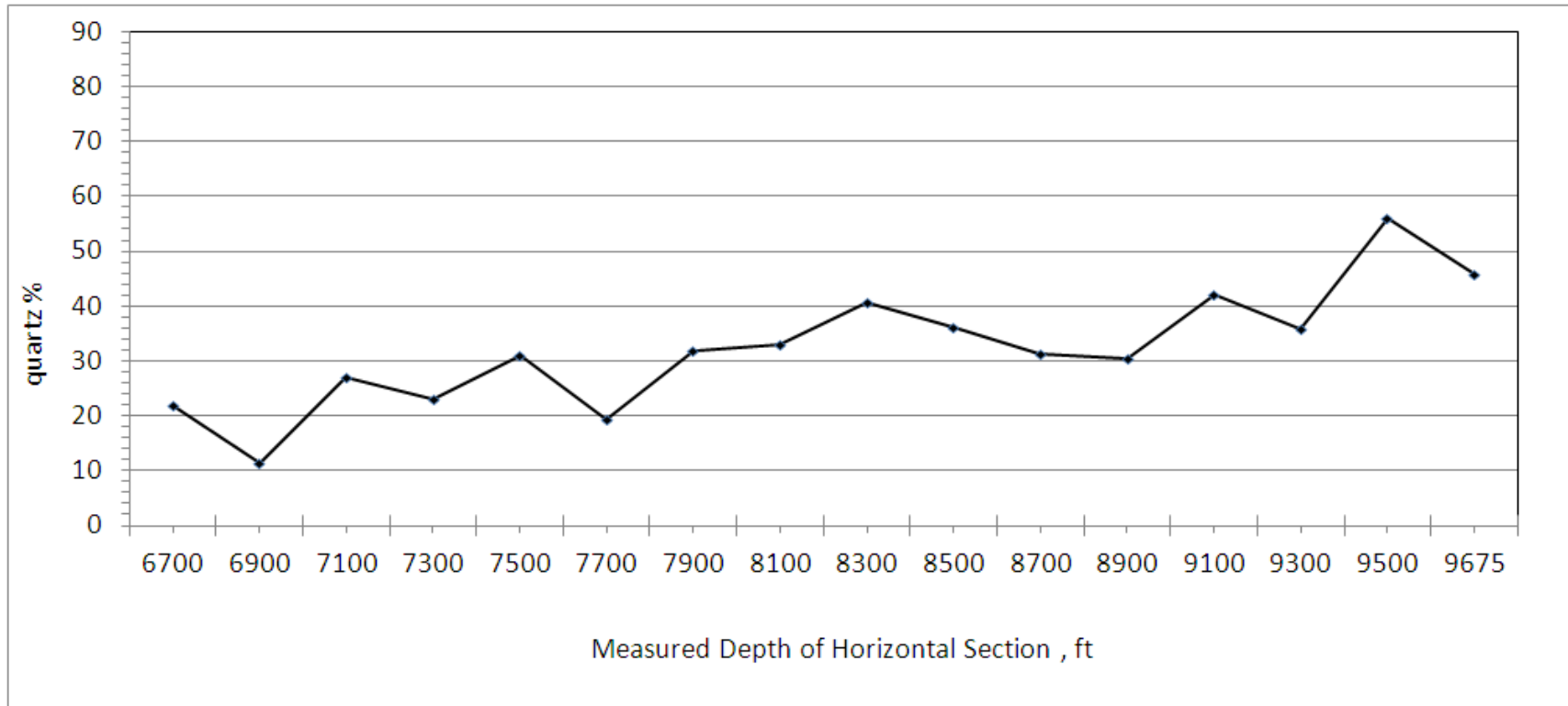


Figure 5. 16: The Relationship between the Lengths of Horizontal Section Drilled and Sand Percentage in Filter Cake

Table 5. 5: The Summary of XRD Results of Whole Filter Cake Samples

Sample no.	MD ft	Quartz%	Calcite%	Others %
1	6700	22	78	
2	6900	11.4	85	3 Kyanite
3	7100	26.9	73	
4	7300	23	77	
5	7500	31.1	66.9	2 Calcium Chloride Hydroxide
6	7700	19	81	
7	7900	31.7	68.3	
8	8100	33	67	
9	8300	40.7	59.3	
10	8500	36.1	63.9	
11	8700	31.2	64.8	5 Calcium Chloride Hydroxide
12	8900	30.5	69.5	
13	9100	42	48	10 Fluorite
14	9300	35.9	64.1	
15	9500	56	40.1	4 Titanium Oxide
16	9675	45.8	54.2	

5.3 Internal Filter Cake Evaluation Using CT Scan

The solids invasion into the ceramic disks is evaluated by using the CT scanner technique. The CT scanner divides the ceramic disk to small layers (each layer has 1mm thickness) to visualize the depth of invasion in the disks. Although, The CT scanner cannot provide the exact depth of invasion; it can compare the solids invasion during horizontal section of sandstone formation by taking images of each sample and comparing the CT number of invaded layers with CT number of the non invaded layer (new ceramic disk).

For the same sample, qualitatively the CT pictures show that the solids invasion concentrate on the first three layers while the last two layers have almost the same shape as that of the uninvaded ceramic, **Figure 5.13**. Moreover, statistically the CT number reaches to the highest value in the first layer and then begins to decrease slightly until it reaches a value closer to the value of the new ceramic disk (before using it in the fluid loss test).

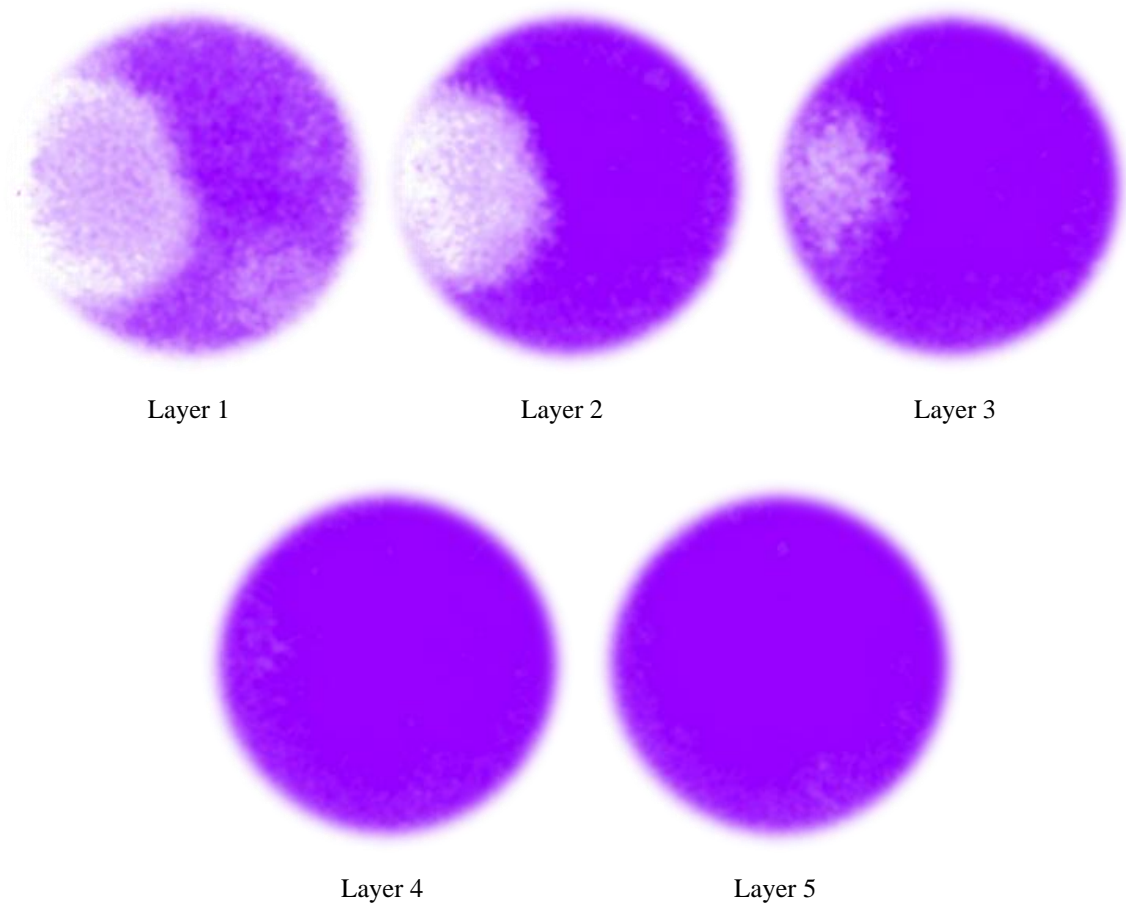


Figure 5. 17: The Internal Solid Invasions Using CT scan

Since the CT number represents the presence of solids, an increase in the CT number represents an increase of the solids invasion in the ceramic disk .It was also clear that by comparing the CT number of the different samples, as more feet of the sandstone formation in the horizontal section is drilled, the average CT number of the disk increases; meaning that the internal damage increases as well, **Figure 5.14**. For the first and the middle part of the horizontal section the solids invasion exists in the first two layers but it becomes significant in the last section because it reaches deeper layers. This indicates poor insulation properties of the filter cake in that part.

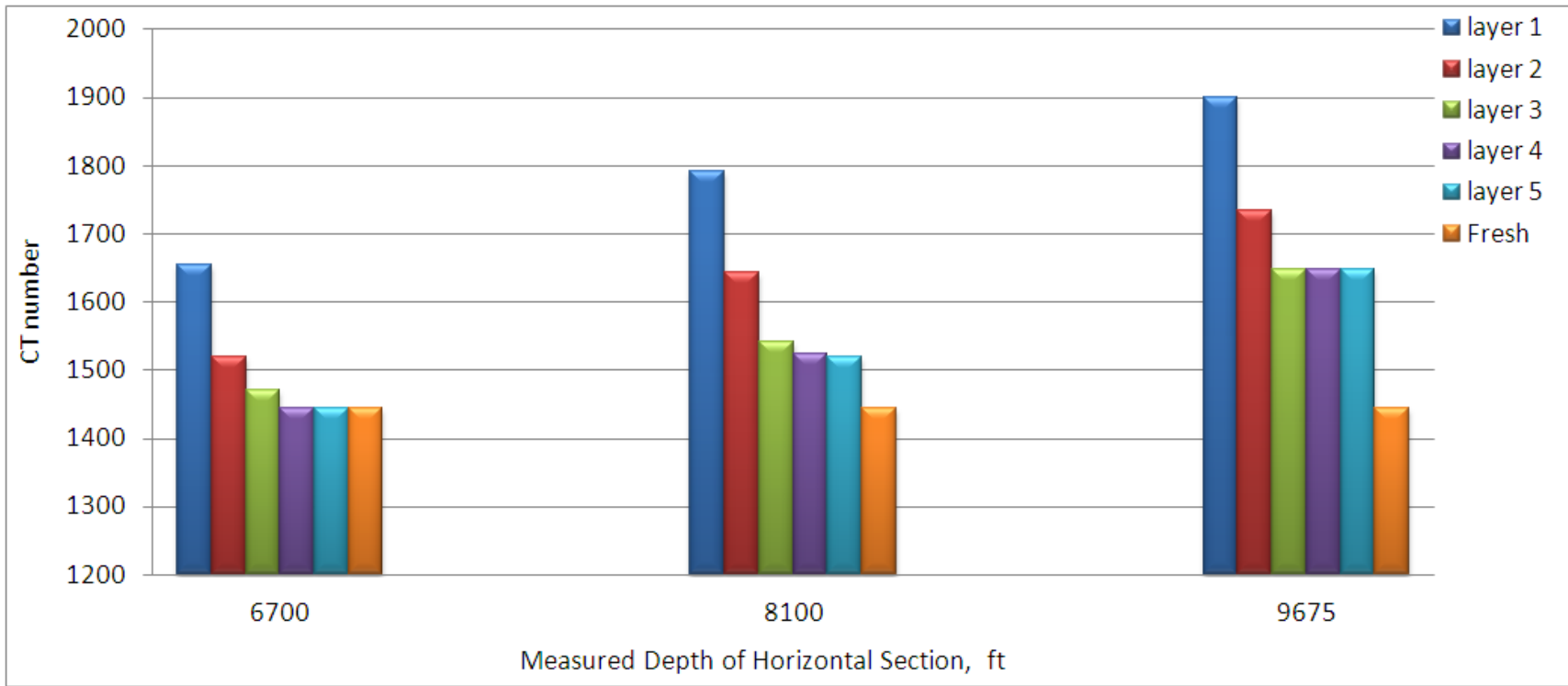


Figure 5. 18: CT scan Number Result.

CHAPTER 6

IMPACT OF SAND

The results in the previous chapter confirmed that the sand percentage increases with more feet of sandstone formation drilled. In this chapter the impact of sand particles mixing with the drilling fluid during the fluid circulation on drilling fluid and filter cake properties will be discussed.

6.1 Impact of Sand on Drilling Fluid Properties

The two primary sources of solids are drilling mud chemical additives and formation cuttings. For long horizontal wellbores penetrating clastic formations, the small sand particles in the drilling cutting are mixed with drilling mud during mud circulation and are not removed completely by surface separation equipment. As so, these materials will degrade the performance of the drilling fluid and become an integral part of the fabric of the filter cake as shown in previous results.

6.1.1 Drilling Fluid Density

Drilling fluid density has to be controlled carefully during drilling operations to maintain it at the designed level. The solids type and their concentrations influence the density thus the drilling fluids require special attention and equipment to control the levels and types of solids. This study is concentrated on studying the impact of one drilling solids type (e.g., sand particles). The impact of introducing sand particles to drilling fluid during drilling long sandstone horizontal section produces denser drilling fluid, **Figure 6.1**.

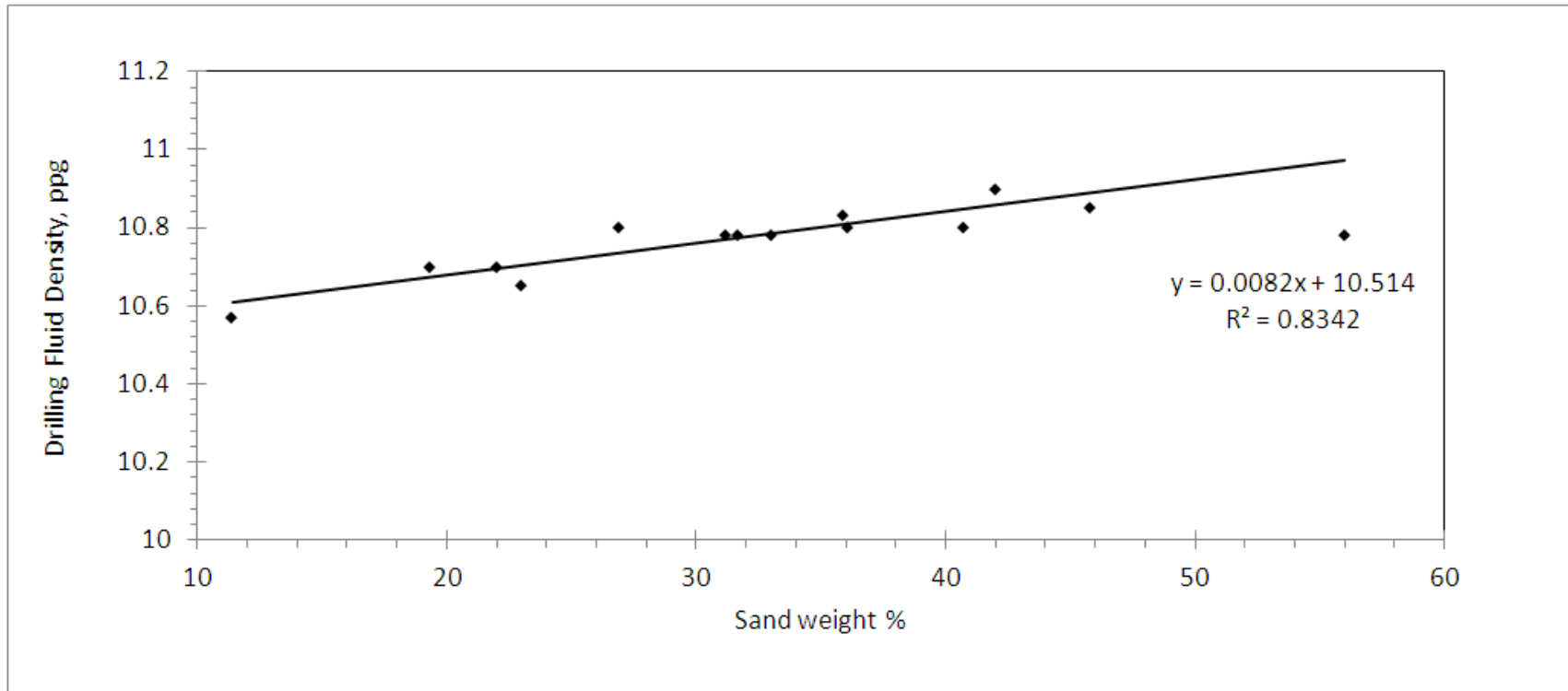


Figure 6. 1: Changes in Drilling Fluid Density with Sand Weight %

6.1.2 Drilling Fluid Rheological Characteristics

The viscosity of a drilling fluid must be maintained within certain limits to optimize the efficiency of a drilling operation and it has to be high enough to transport cuttings out of the hole efficiently, and as low as possible to remove cuttings from beneath the bit. As the sand particles concentration increases in the drilling fluid, the drilling fluid viscosity increases. The results show that the apparent viscosity, plastic viscosity, yield point, 10 second gel strength and 10 minute gel strength increase as the percentage of sand particles increases, **Figure 6.2 and 6.3.**

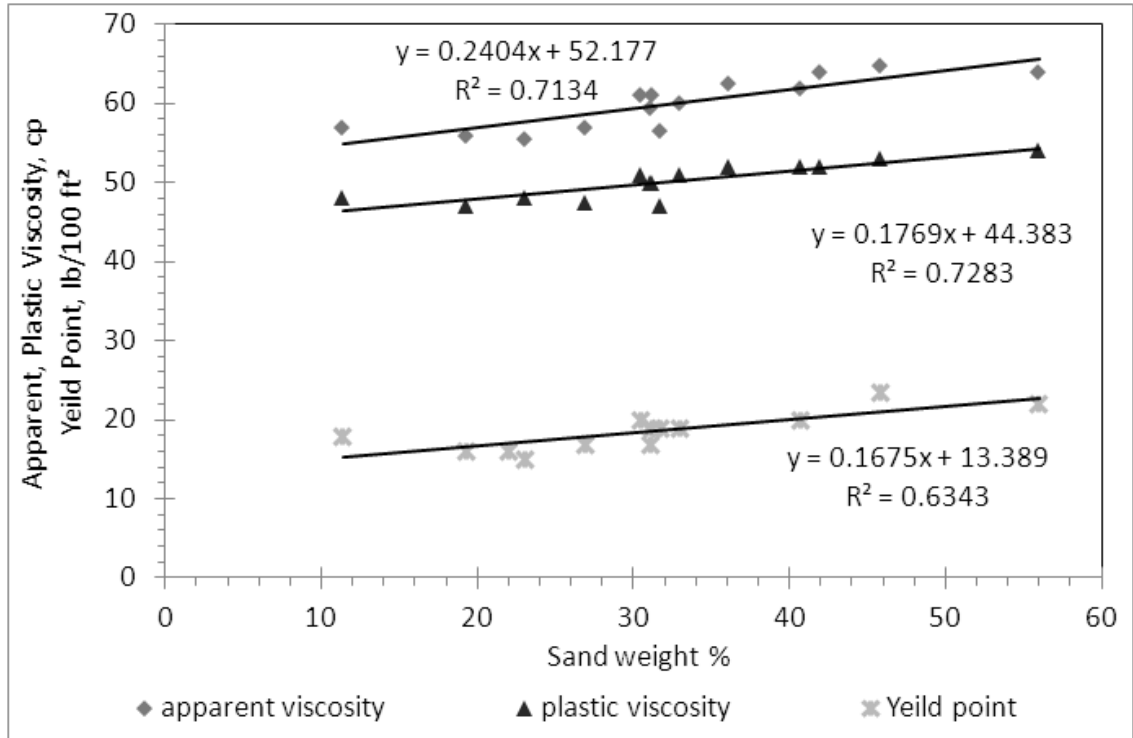


Figure 6. 2: Changes in Drilling Fluid Apparent Viscosity, Plastic Viscosity, and Yield Point with Sand Weight %

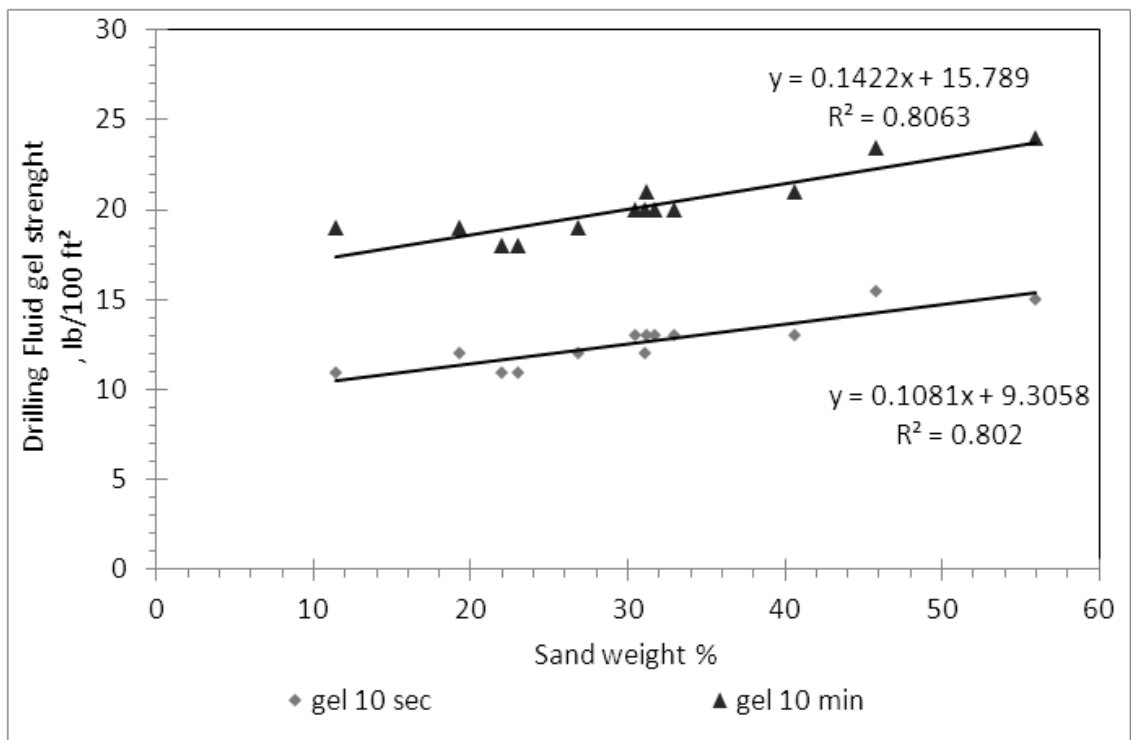


Figure 6. 3: Changes in Drilling Fluid Gel Strength (10 Minutes / 10 Seconds) with Sand Weight %

6.2 Impact of Sand on External Filter Cake & Solids Invasion

Correct fluid composition, bridging material selection, and good maintenance of the drilling fluid system are the keys to success for an effective filter cake (e.g., impermeable and thin filter cake). An effective filter cake that allows a better flow profile along the entire wellbore by forming impermeable filter cake reduces the risks of stuck pipe during the drilling operation. The rationale behind this selection is to study the effect of sand content on the thickness and the sealing properties of the filter cake.

There is a linear relationship between the sand percentage and filter cake thickness, **Figure 6.4**. This investigation reveals that for long horizontal wellbores penetrating clastic formations, the sand particles are not removed completely by surface separation equipment. As so, these materials become an integral part of the fabric and structure of the filter cake. It increases the cake thickness which can cause stuck pipe.

To study the impact of sand content on the internal solids invasion, the CT scan analysis was conducted for three of the ceramic disks. These disks were used in the fluid loss test using three drilling fluid sand levels (level-1 22%, level-2 33% and level-3 45.6%).

The CT scan results of the ceramic disks show that the internal invasion is directly affected by the changes of sand contents in the drilling fluids. Therefore, the invasion depth along the horizontal section will not be constant since the percentage of sand in the drilling fluid increases along the section.

This internal invasion becomes critical when the sand percentage reaches higher than 40% of the filter cake composition. This is indicated by the high CT scan number values

compared to the non-invaded CT scan number values (fresh). This is a result of the degrade in the sealing properties of the filter cake. **Figure 6.5** shows that the invasion of the internal solids is deeper as the CT scan number increases.

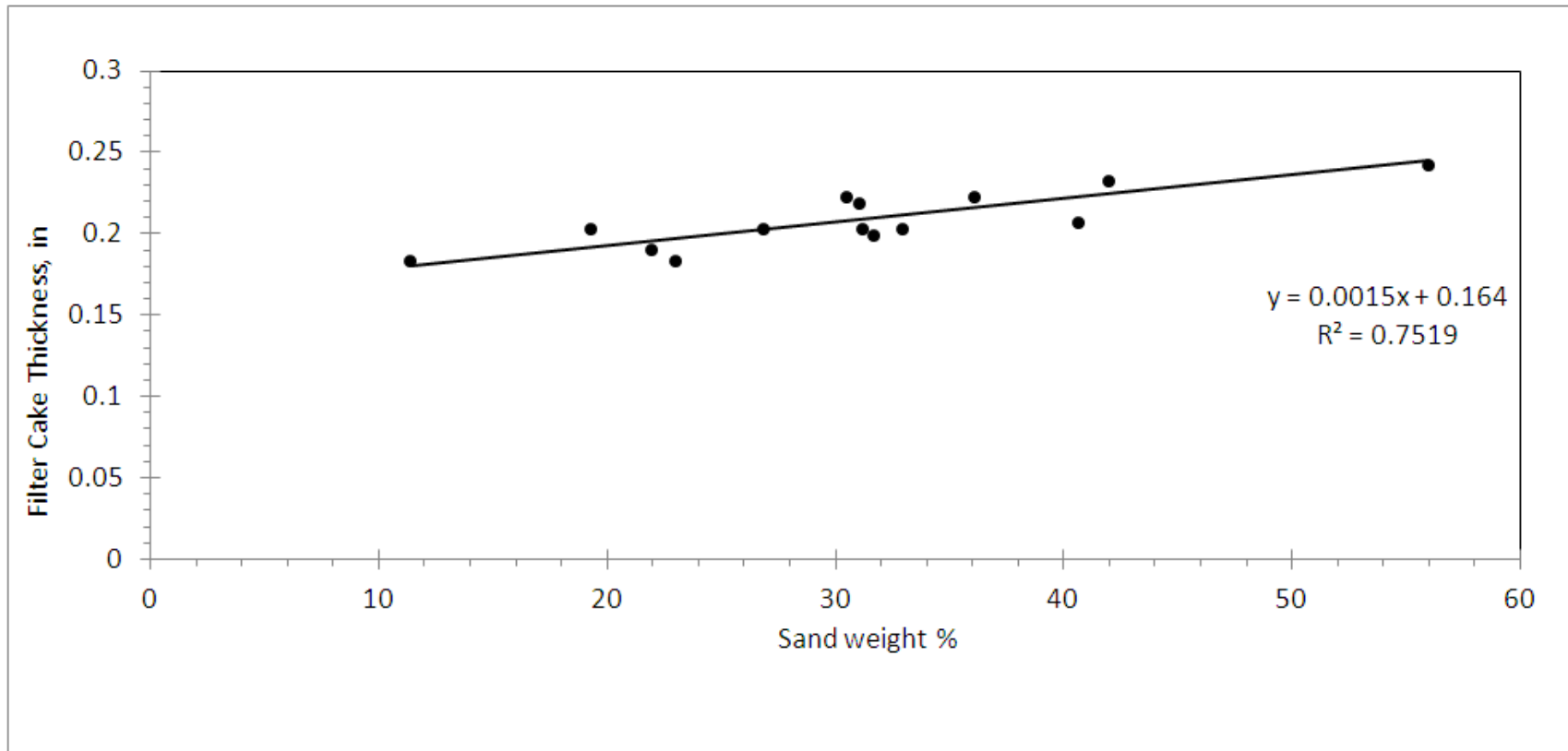


Figure 6. 4: Changes in Filter Cake Thickness with Sand Weight %

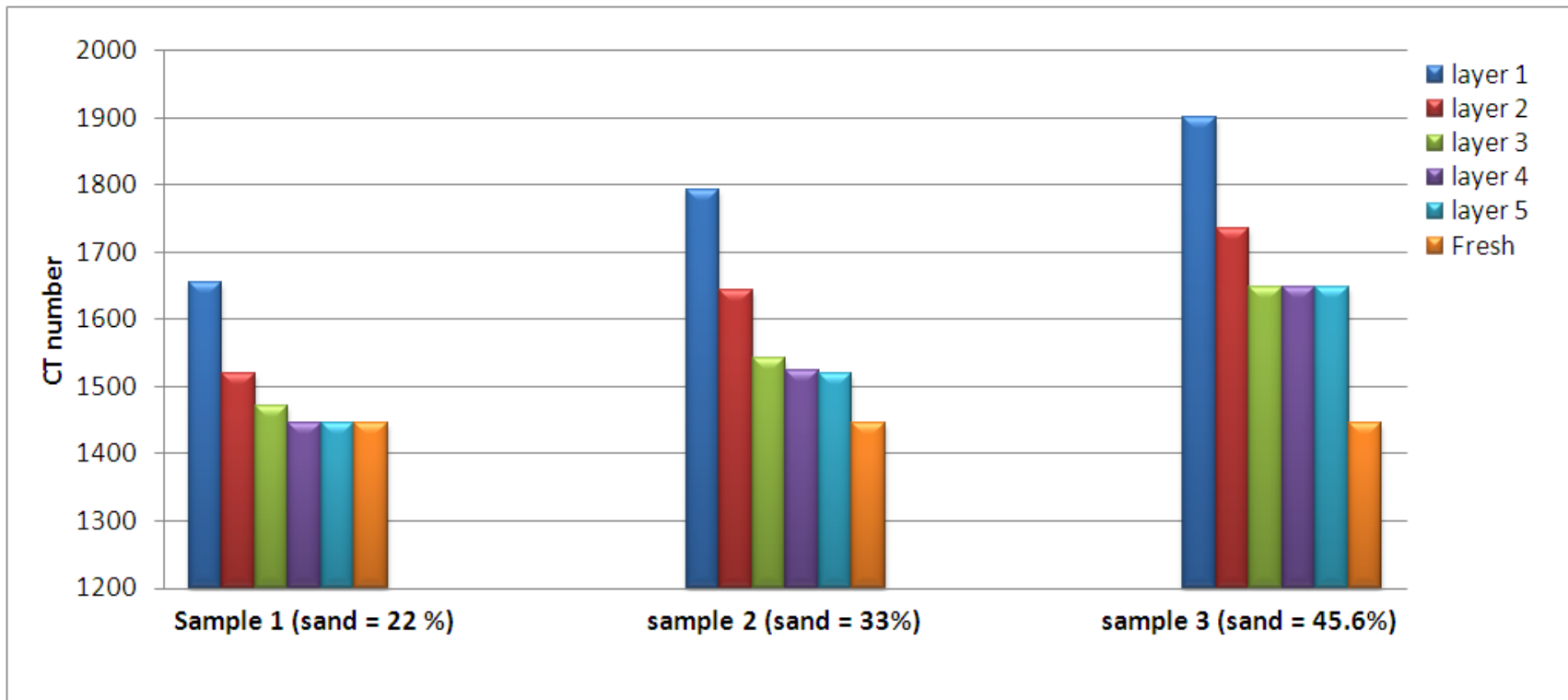


Figure 6. 5: Impact of Sand Particles Percentages on Internal Invasion Using CT scan

6.3 A Model to Predict Filter Cake Sand Content

From the obtained results, there is a linear relationship between the drilling fluid density and the length of horizontal section, **Figure 6.6**. This relationship can be described by linear equations

$$D = C_1 L + D_i , \dots\dots\dots (6.1)$$

Equation (6.1) can be written as

$$(D - D_i) = \Delta D = C_1 L , \dots\dots\dots (6.2)$$

The increment in the drilling fluid density can be given also from the relationship between the density of the drilling fluid and sand content **Figure 6.7**.

$$D = C_2 S_i + D_i , \dots\dots\dots (6.3)$$

$$(D - D_i) = \Delta D = C_2 S_i , \dots\dots\dots (6.4)$$

Where

D = drilling fluid density at certain horizontal length, ppg

D_i = initial drilling fluid density, intercept of y axis, ppg

ΔD = increment in the drilling fluid density with horizontal length , ppg

L = horizontal length, ft

S_i = sand content percentage

C_1 = the slope of **Figure 6.6**, $=7 \times 10^{-5}$ ppg/ft

C_2 = the slope of **Figure 6.7**, =0.0082 ppg/sand wt%

By adding equations (6.2) and (6.4) the sand percentage can be given as

$$\Delta D + \Delta D = C_1 L + C_2 Si, \dots\dots\dots (6.5)$$

$$Si = \frac{2\Delta D - C_1 L}{C_2}, \dots\dots\dots (6.6)$$

Following the same procedure, from the linear relationship between the drilling fluid viscosity and the length of horizontal section as well as the linear relationship between the drilling fluid viscosity and the sand content percentage, **Figure 6.8 & 6.9**, the sand percentage can be given as

$$(\mu - \mu_i) = \Delta\mu = C_3 L, \dots\dots\dots (6.7)$$

$$(\mu - \mu_i) = \Delta\mu = C_4 Si, \dots\dots\dots (6.8)$$

$$Si = \frac{2\Delta\mu - C_3 L}{C_4}, \dots\dots\dots (6.9)$$

Where

μ = drilling fluid viscosity at certain horizontal length, cp

μ_i = initial drilling fluid viscosity, intercept of y axis, cp

$\Delta\mu$ = increment in the drilling fluid viscosity with horizontal length , cp

C_3 = the slope of **Figure 6.8**, =0.0034 cp/ft

C_4 = the slope of **Figure 6.9**, =0.240 cp/sand wt%

Note: for drilling fluid viscosity we can use any of the drilling fluid rheological characteristics for instance apparent viscosity (μ_a), plastic viscosity (μ_p), yield point (YP), and gel strength (Gel 10 sec, Gel 10 min).

Equations (6.6) and (6.9) can be combined together to get one equation for prediction the filter cake sand content as:

$$2Si = \frac{2\Delta D - C_1 L}{C_2} + \frac{2\Delta\mu - C_3 L}{C_4}, \dots\dots\dots (6.10)$$

$$2Si = \frac{C_4(2\Delta D - C_1 L) + C_2(2\Delta\mu - C_3 L)}{C_2 C_4}, \dots\dots\dots (6.11)$$

$$Si = \frac{(2C_4\Delta D + 2C_2\Delta\mu) - (C_1 C_4 + C_2 C_3)L}{2C_2 C_4}, \dots\dots\dots (6.12)$$

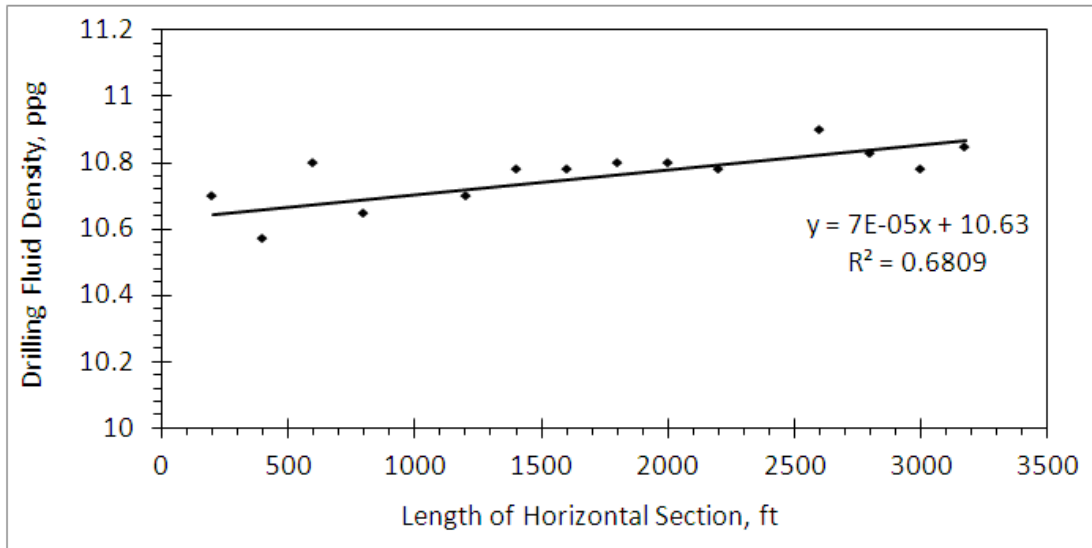


Figure 6. 6: Drilling Fluid Density and the Length of Horizontal Section Relationship

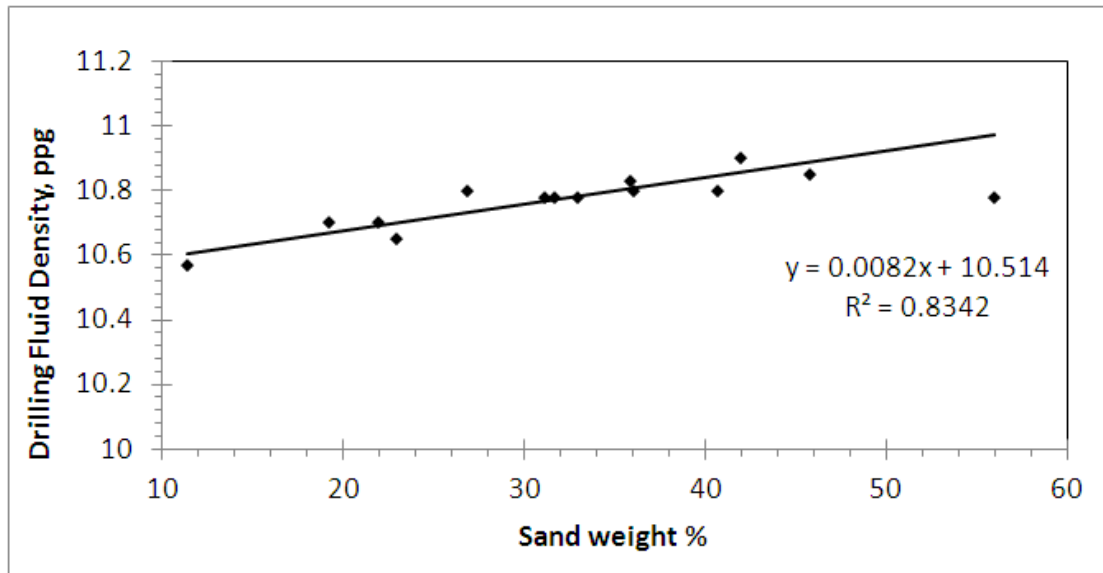


Figure 6. 7: Drilling Fluid Density and Sand Content Relationship

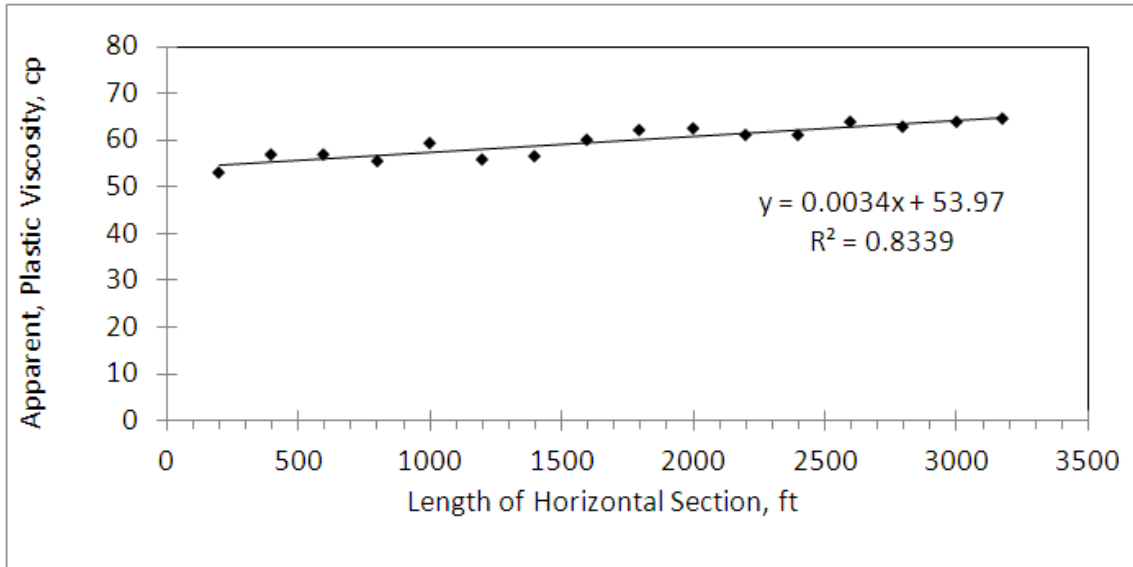


Figure 6. 8: Drilling Fluid Apparent Viscosity and the Length of Horizontal Section

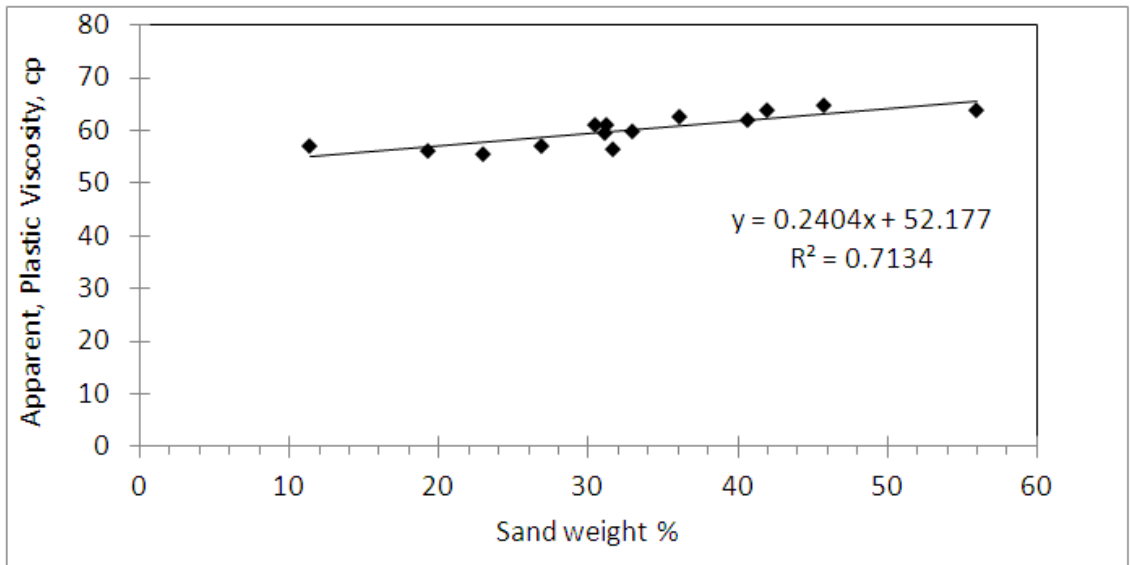


Figure 6. 9: Drilling Fluid Apparent Viscosity and Sand Content Relationship

Procedure to Predict Sand Content in the Filter Cake

The following steps should be followed to predict sand content in filter cake using equation (6.2)

1. By the time the horizontal section open drilling fluid samples must be collected every certain length.
2. Determine the drilling fluid density and plot the relationship between the density and horizontal length to calculate C_1 value.
3. Determine the drilling fluid viscosity and plot the relationship between the viscosity and horizontal length to calculate C_3 value.
4. Determine the filter cake sand content of these drilling fluid samples and plot the relationship between the sand content and drilling fluid density and viscosity to calculated C_2 and C_4 .
5. Three drilling fluid samples are enough to determine the value of C_1 , C_2 , C_3 and C_4 . Then as more samples collected these values can be corrected if the trends of the first few samples are not good.
6. Finally, this model helps to predict the sand content in the filter cake through the horizontal section and gives a good estimate to see if the sand content will reach to high value or no.
7. Based on this model results we can avoid reaching high value sand content either by treat the current drilling fluid or by replacing the current drilling fluid with new fluid in term of high sand content which will degrade the performance of the fluid and making it prohibitively difficult to remove the filter cake with regular acids.

6.4 A Model to Predict Filter Cake Thickness

Based on the linear relationship that was obtained between the filter cake thickness and the horizontal section length **Figure 6.10**, the filter cake thickness at any length can be given as

$$h_c = C_5 L + h_{ci} , \dots\dots\dots (6.13)$$

The filter cake thickness can be obtained from the linear relationship between the thickness and the sand content **Figure 6.11** as

$$h_c = C_6 Si + h_{ci} , \dots\dots\dots (6.14)$$

The predicted sand content value using equation (6.12) give can be using to predict the filter cake thickness.

h_c = filter cake thickness at certain horizontal length, inch

h_{ci} = initial filter cake thickness, intercept of y axis, inch

C_5 = the slope of **Figure 6.10**, $=2 \times 10^{-5}$ inch/ft

C_6 = the slope of **Figure 6.11**, $=0.0015$ inch/sand wt%

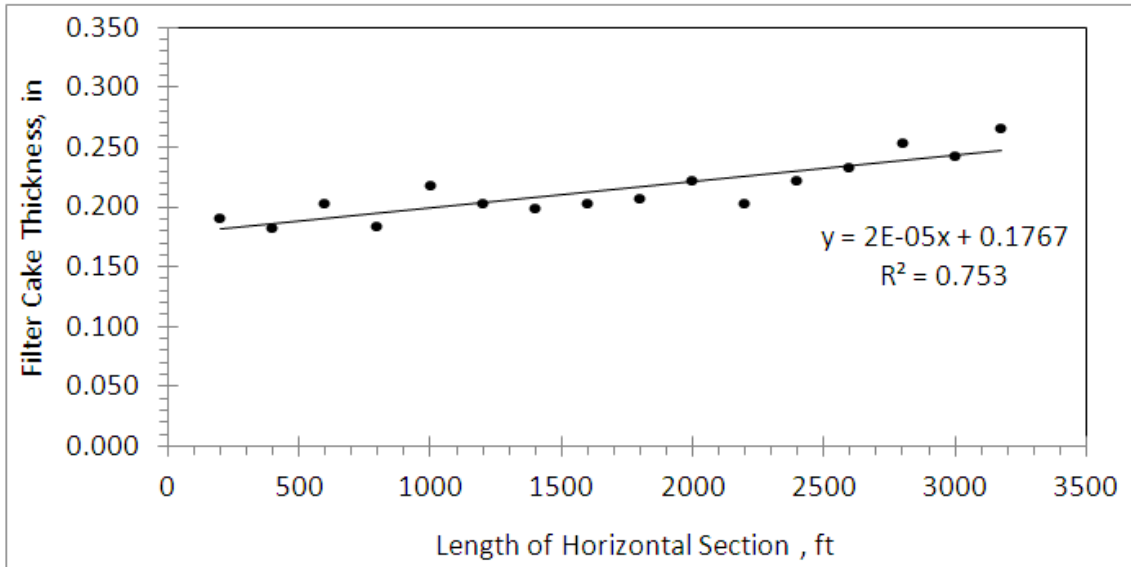


Figure 6. 10: Filter Cake Thickness and the Horizontal Section Length Relationship

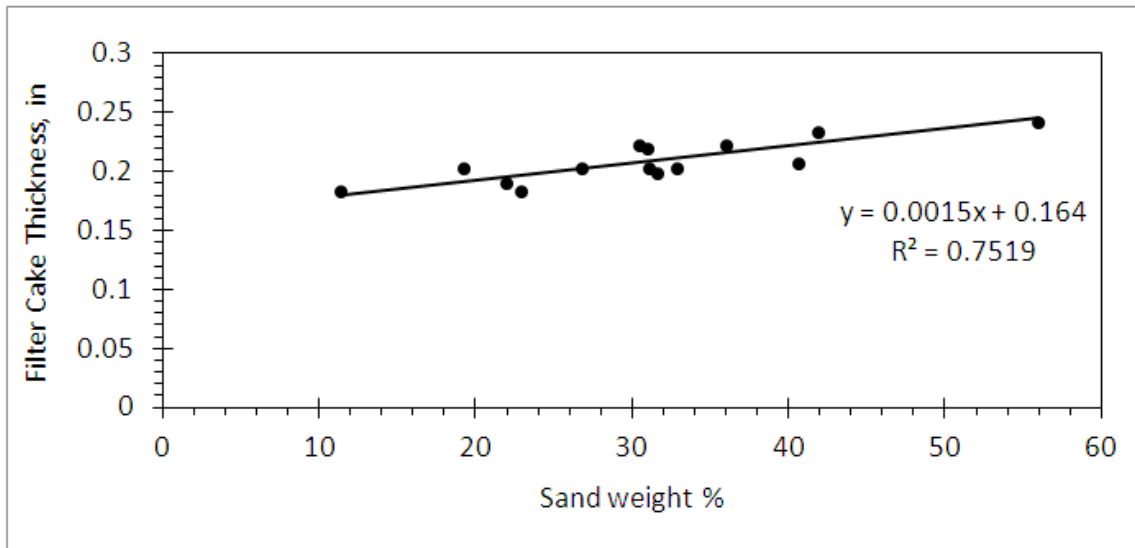


Figure 6. 11: Filter Cake Thickness and the Sand Content Relationship

CHAPTER 7

7.1 CONCLUSIONS

Drilling fluid samples from the field were examined in this study. These samples contained drilled solids from a horizontal sandstone section. The objective was to evaluate the filter cake mineralogy along the horizontal section. Based on the results obtained the following conclusions can be drawn:

- The study found that the mineralogy of the filter cake is varying over the 3175 ft. of the horizontal sandstone section, the concentration of the sand content increases in the filter cake as more feet of horizontal section is drilled. It reaches more than 40% by weight of the filter cake solids at the last part of the horizontal section. XRD results show that there are three regions based on the sand content of the filter cake, low sand level (22%), medium sand level (33%) and high sand level (higher than 40%). Stimulation treatments to clean the filter cake can be designed based on this result.

- Qualitatively, SEM results show that the chemical composition (minerology) of the filter cake is not constant from its toe to heel. This is due to the presence of drilling solids which become an integral part of filter cake structure. The Si element is present in whole filter cake samples because it is the main component of sandstone formation. In addition, there are some elements appearing only in one and/or two samples due to the heterogeneity of the formation.

- For long horizontal wellbores penetrating sandstone formations, the ground clastic fragments are not completely removed by the surface separation equipment. Hence, these solids are mixed with the drilling fluid during the fluid circulation and become an integral part of the drilling fluid and the filter cake fabric. As a result , the following changes in the drilling fluid properties arise:
 - There is a negligible increase in the drilling fluid density with more feet of sandstone horizontal section drilled. Within 3175 ft horizontal section, the density of the drilling fluid increases approximately (0.223 lb/gal, 1.67 lb/ft³).
 - The rheological characteristics of the drilling fluid degrade due to the increase of the sand content, which leads to producing to a more viscous fluid. The apparent viscosity and plastic viscosity increase about (20%; 18%) respectively along the section. The yield point and gel strengths are more sensitive functions of the drilled solids in sandstone reservoir. The results obtained reveals that the yield point increases from (15 to 21 lb/100 ft²) which is a 40% increment from its initial value, and the gel strength (10 second and 10 minute) increases 46% and 42% respectively.

- The filter cake thickness increases by 36% over the 3175 ft. length of the horizontal section. This increase in the cake thickness coincides with increase in the drilling fluid apparent viscosity, plastic viscosity, yield point, gel strength (10 second) and gel strength (10 minute) by 20%, 18%, 40%, 42.5% and 32.5% respectively. Therefore, it can be observed that the filter cake thickness is a sensitive function of the levels of sand content in the drilling fluid.

- The CT scan results of the ceramic disks show that the internal invasion is directly affected by the changes of sand contents in the drilling fluids. The depth of invasion increases as the sand content increases. Therefore, the invasion depth along the horizontal section will not be constant since the percentage of sand in the drilling fluid increases along the section. This internal invasion becomes critical when the sand percentage reaches higher than 40%.

7.2 RECOMMENDATION

For long horizontal sections of sandstone formations, our results generally show an increase of sand percentage as more feet of sandstone formation is drilled. The intrusion of high sand percentage into the drilling fluid and filter cake fabric degrades their qualities and performance. Therefore, it is important to minimize the sand percentage in drilling fluids during drilling of horizontal sections.

In this study, the following suggestions for future work in the same area are recommended:

- Evaluate the effectiveness of drill cuttings removing equipment in order to control sand content in the drilling fluids.
- In order to study the real solids invasion, real core samples should be used instead of ceramic disks.

NOMENCLATURE

(Hassen 1980)

V = filtration volume, ml

t =time, hr

C =static/dynamic filtrate volume constant

u_f = filtrate velocity, ml/cm².hr

t =time, hr

γ =shear rate at the well, s⁻¹

(Burgoyne 1991)

k = Permeability of the filter cake, Darcy

V_f = Filtrate volume, cm³

Δp = Pressure drop across the mud cake, atm

ϕ_s = Volume fraction of solids in the mud

ε_{sav} = Volume fraction of solids in the cake

A = Area of the filter disk, cm²

t = Time of filtration, sec

μ = Viscosity of the mud filtrate, cp

(Khatib 1994)

K_c = Permeability of the mud cake, md

ϕ_c = Porosity of the filter cake, volume fraction

(Martinez et al. 2000)

μ = Filtrate viscosity, Pa.s.

k = Permeability of the filter cake, m^2

v = Volume of filtrate per unit area, m^3/m^2

L = Filter cake thickness, m

R_m = Resistance of filter medium, 1/m

p = Differential pressure, Pa

t = Time, s

(Dewan and Chenevert 2001)

\emptyset_c =filter cake porosity

V_b =bulk volume of solid in filter cake, cm^3

V_f =fluid volume of solid in filter cake, cm^3

ρ_g =solid density, gm/cm^3

ρ_f =fluid density, gm/cm^3

(Tiller 2002)

k = Permeability of the filter cake, m^2

v = Volume of filtrate per unit area, m

ϵ_{sav} = Volume fraction of solids in filter cake

R_m = Resistance of filter medium, 1/m

p = Differential pressure, Pa

t = Time, s

μ = Filtrate viscosity, Pa.s.

ϕ_s = Volume fraction of solids in slurry

α_{av} = Average specific cake resistance

(Dangou and Chandler 2009)

q_{eq} = Equilibrium filtration rate, $m \cdot sec^{-1}$

K_{mc} = Permeability of the filter cake, m^2

T_{mceq} = Equilibrium cake thickness, m

μ_f = Filtration viscosity, Pa.sec

p_f = Filtration pressure, Pa

(Li *et al.* 2005)

K_{mc} = Permeability of the filter cake, md

q = Filtration rate, cm/sec

T_{mc} = Filter cake thickness, cm

μ = Viscosity of the filtrate, cp

p = Pressure across filter cake, psi

(Elkatatny *et al.* 2011)

CT_{wet} = CT number of the cake in wet conditions

CT_{dry} = CT number of the cake after dried at 250°F for 3 hours.

CT_{water} = CT number of water

CT_{air} = CT number of air

μ_a = apparent viscosity, cp

PV = plastic viscosity, cp

YP = yield point, lb/100ft²

$\theta_N, \theta_{600}, \theta_{300}$ = the dial reading in lb/100ft² and N is the rotor speed in rpm.

D = drilling fluid density at certain horizontal length, ppg

D_i = initial drilling fluid density, intercept of y axis, ppg

ΔD = increment in the drilling fluid density with horizontal length , ppg

μ_i = initial drilling fluid viscosity, intercept of y axis, cp

$\Delta\mu$ = increment in the drilling fluid viscosity with horizontal length , cp

L = the lateral length, ft

hc = the cake thickens, inch

SEM= Scanning Electron Microscope

XRD= X-ray Diffraction

REFERENCE

1. Cook E.L., 1954: "Filter Cake Thickness Gauge", United States Patent 2,691,298, Patented Oct. 12, 1954
2. Outmans, H. D., 1963: "Mechanics of Static and Dynamic Filtration in the Borehole", SPE Journal (Sept. 1963), pp. 236-244.
3. Borst, R.L., Shell, F.J., 1971,: "The Effect of Thinners on the Fabric Of Clay Muds and Gels", SPE journal paper (October 1971) Volume 23, 1193-1201
4. Abrams, W., 1977: "Mud Design to Minimize Rock Impairment Due to Particle Invasion," Paper SPE 5713 presented at the SPE-AIME Second Symposium of Formation Damage Controls, held in Houston, Feb. 1977.
5. Kenneth, P. E., 1980: "A Basic Scanning Electron Microscope Study of Drilling Fluids" Paper SPE 8790, presented at SPE Formation Damage Symposium, 28-29 January 1980, Bakersfield, California
6. Hassen, B. R., 1980: "New Technique Estimates Drilling Filtrate Invasion," Paper SPE 8791, presented at SPE Formation Damage Symposium, 28-29 January 1980, Bakersfield, California
7. Ershaghi, I. and Mehdi A., 1980: "Modeling of Filter Cake Buildup under Dynamic-Static Conditions," Paper SPE 8902, presented at the 50th Annual California regional meeting of the society of petroleum Engineering of AIME held in Los Angeles California, April 1980.
8. Goldstein et al.: "Scanning Electron Microscopy and X-Ray Microanalysis", Third Edition, New York City (1981)

9. Peden, Margarita, R., Avalos, and Arthur, K. G.,1982: "The Analysis of the Dynamic Filtration and Permeability Impairment Characteristics of Inherited Water Based Muds," Paper SPE 10655, presented at SPE Formation Damage Control Symposium, held in Lafayette, LA, March 24-25, 1982.
10. Peden, J.M., Arthur, K.G. and Avalos, M.R.,1984: "The Analysis of Filtration Under Dynamic and Static Conditions" Paper SPE 12503, presented at the 1984 Formation Damage Control Symposium, Bakersfield, CA., Feb. 13-14, 1984.
11. Darley, H.C.H. and Gray, G.R.: "Composition and Properties of Drilling and Completion Fluids", Fifth Edition, Gulf Publishing Company, Houston (1988).
12. Hartmann, A., Cherler, M., Marx, C., and Neumann, H.I., 1988: "Analysis of Mud Cake Structures Formed under Simulated Borehole Conditions", SPE Drilling Engineering, Dec. 1988.
13. Arthur, K.G., E.P.D.S. Ltd, and Peden, J.M., 1988 : "The Evaluation of Drilling Fluid Filter Cake Properties and Their Influence on Fluid Loss," Paper SPE 17617, presented at SPE Int'l Meeting on Petroleum Engineering, held in Tianjin, China, November 1-4, 1988
14. Plank, J.P. and Gossen, EA., 1989: "Visualization of Fluid Loss Polymers in Drilling Mud Filter Cakes", Paper SPE 19534, presented at the SPE Annual Technical Conference, San Antonio, Texas, October 8-11, 1989.
15. Mehta,S.,1991: "Imaging of Wet Specimens in Their Natural State Using Environmental Scanning Electron Microscope (ESEM) : Some Examples of Importance to Petroleum Technology", Paper SPE 22864, presented at the 66th SPE Annual Technical Conference and Exhibition, Dallas, TX, Oct. 6-9, 1991.

16. Bourgoyne Adam T. Jr., Millheim Keith K., Chenevert Martin E., and Young F. S. Jr.: "Applied Drilling Engineering" .(Richardson, Texas: Society of Petroleum Engineers, 1991)
17. Chenevert, M.E., Huycke, J., 1991,: "Filter Cake Structure Analysis Using the Scanning Electron Microscope," Paper SPE 022208
18. Jiao, Di. and Sharma, M.M., 1992: "Formation Damage Due to Static and Dynamic Filtration of Water-Based Muds" Paper SPE 23823, presented at the SPE Intl. Symposium on Formation Damage Control, Lafayette, LA, Feb. 26-27, 1992.
19. Jiao, Di Sharma, M.M., 1993, "Investigation of Dynamic Mud Cake Formation: The Concept of Minimum Overbalance Pressure," Paper SPE 26323, presented at SPE Annual Technical Conference and Exhibition, 3-6 October 1993, Houston, Texas
20. Gauchet R.,P. Cheneviere, and Tricart ,J. P., 1993: "Visualization of Rock Samples in Their Natural State Using Environmental Scanning Electron Microscope" Paper SPE 26620, presented at SPE Annual Technical Conference and Exhibition, 3-6 October 1993, Houston, Texas
21. Michael J. Economides, A. Daniel Hill, and Christine Ehlig- Economides: "Petroleum Production Systems" Prentice Hall, 1994.
22. Khatib Z.I., 1994: "Prediction of Formation Damage Due to Suspended Solids: Modeling Approach of Filter Cake Buildup in Injectors," Paper SPE 28488, presented at the Annual Technical Conference and Exhibition, New Orleans, Louisiana, 25-28 September.
23. Simanjuntak, A.B.M. and Haynes, L.L., 1994,:" ESEM Observations Coupled With Coreflood Tests Improve Matrix Acidizing Designs," Paper SPE 27405, presented for

- SPE Formation Damage Control Symposium, 7-10 February 1994, Lafayette, Louisiana
24. Yidan Li, Peden, Elisabeth Rosenbreg, and Arguillier, J.F., 1995: "Correlation between Filter Cake Structure and Filtration Properties of Model Drilling fluid" Paper SPE 28961, presented for the SPE Int'l Symposium on oilfield chemistry, held in San Antonio, TX, U.S.A, February 14-17, 1995.
 25. Burnett, D.B. and Hodge, R.M., 1996: "Laboratory and Field Evaluation of Role of Drilling Solids in Formation Damage and Reduced Horizontal Well Productivity" SPE 37125, presented at SPE Int'l Conference on Horizontal Well Technology, held in Calgary, Canada, November 18-20, 1996.
 26. Amanullah, Md., 1997: "Dynamic Filtration of Water-Based Muds", Annual Report, Drilling Research Program, Center for Petroleum and Geo-systems Engineering, The University of Texas at Austin 1997.
 27. Pitoni, E., Ballard, D.A., Kelly, R.M., 1999, "Changes in Solids Composition of Reservoir Drill in Fluids During Drilling and the Impact on Filter Cake Properties," Paper SPE 54753, presented at SPE European Formation Damage Conference, The Hague, Netherlands, 31 May-1 June 1999
 28. Isambourg, P. and Marti, J.: "Down-hole simulation cell for measurement of lubricity and differential pressure sticking", Paper SPE/IADC 52816 presented at Drilling Conference, Amsterdam, Holland, SPE/IADC 1999
 29. Hanssen, J.E., Jian, P., Pedersen, H.H. and Jorgensen, J.F., 1999: "New Enzyme Process for downhole Cleanup of Reservoir Drilling Filtercake," Paper SPE 50709,

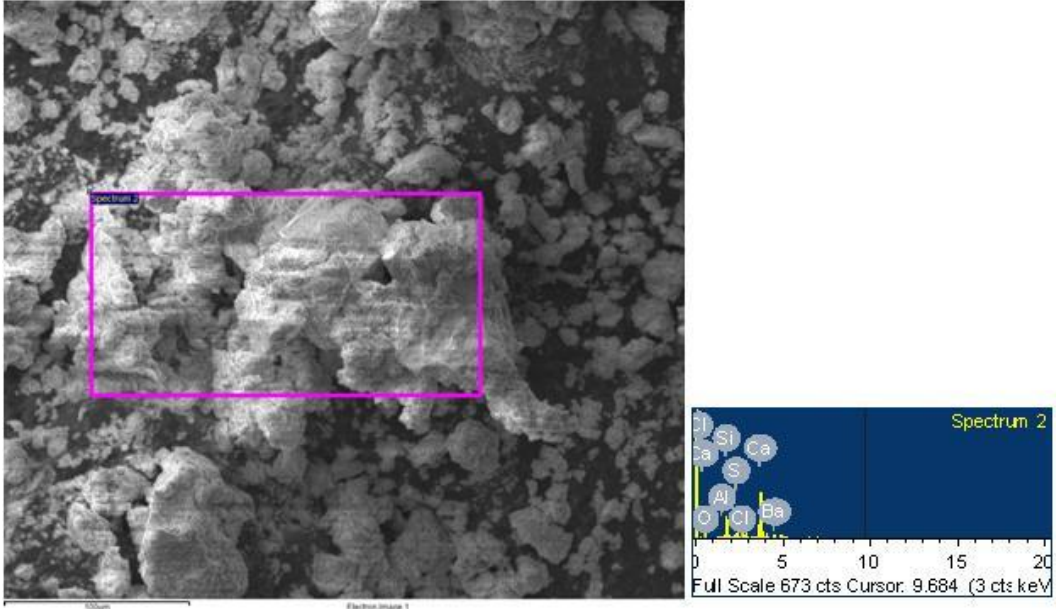
- presented at the SPE International Symposium on Oilfield Chemistry, Houston, Texas, 16-19 February 1999.
30. Robin, M., Combes, R., Rosenberg, E., 1999,: ” Cryo-SEM and ESEM: New techniques to Investigate Phase Interactions within Reservoir Rocks,” Paper SPE 56829, presented at SPE Annual Technical Conference and Exhibition, 3-6 October 1999, Houston, Texas
 31. Zulkeffeli, M. Z., Ajay, S., Sharma, M. M., 2000: “ Mechanisms of Mud Cake Removal During Flowback,” Paper SPE 58797, presented at SPE International Symposium on Formation Damage Control, 23-24 February 2000, Lafayette, Louisiana
 32. Mahesh, S. Rautela, 2000: A Method for Determination of the Permeability of the Filter Cake at Wellsite,” Paper SPE 50692.
 33. Cerasi, P., Ladva, H.K., Bradbury, A.J., Soga, K., 2001,” Measurement of the Mechanical Properties of Filter cakes,” Paper SPE 68948, presented at SPE European Formation Damage Conference , 21-22 May 2001, The Hague, Netherlands
 34. Dewan, J. T., and Chenevert, M. E., 2001, “A model for filtration of water-base mud during drilling” determination of mud cake parameters: *Petrophysics*, vol. 42, no. 3, p. 237–250.
 35. Amanullah, Md. and Tan, C.P., 2000: “A Non-Destructive Method of Cake Thickness Measurement”, Paper SPE 64517, presented at Asia Pacific Oil and Gas Conference and Exhibition, Brisbane, Australia, 16-18 October, (2000)
 36. Tiller, F. M. and W. Li.: ” Theory and Particle of Solid/Liquid Separation” Fourth edition, 2002, university of Houston.

37. Raju, K.U., Nasr-El-Din, H.A., Hilab, V., Siddiqui, S., and Mehta, S., 2005: "Injection of Aquifer Water and Gas/Oil Separation Plant Disposal Water in Tight Carbonate Reservoirs," SPE Journal (December 2005) 374-384
38. Wenping Li, C.K., Quintin Richard 2005: "Development of a Filter Cake permeability Test Methodology," the American Filtration & Separation Society 2005 International Externalical Conference & Exposition, September 19-22, Ann Arbor Michigan 5.
39. Nasr-El-Din, H.A., Al-Otaibi, M.B., Al-Qahtani, A.A., 2007: "An Effective Fluid Formulation to Remove Drilling-Fluid Mud cake in Horizontal and Multilateral Wells," SPE Journal Paper (March 2007) Volume 22, 26-32
40. A.S. Al-Yami and H.A. Nasr-El-Din, 2008,;" Impact of Water-Based Drill-In Fluids on Solids Invasion and Damage Characteristics" Paper SPE 117162, presented at SPE Eastern Regional/AAPG Eastern Section Joint Meeting, 11-15 October 2008, Pittsburgh, Pennsylvania, USA
41. M.B.AL Otaibi, H.A.Nasr-El-Din, and A.D.Hill, 2008,; "Characteristics and Removal of Filter Cake Formed by Formate- Based Drilling Mud," Paper SPE 112427 presented at SPE International Symposium and Exhibition on Formation Damage, Louisiana. Feb. 13-15, 2008.
42. Dangou, M. and Chandler, H., 2009: "Potential Increase of Formation Damage at Horizontal Wells as a Result of Changing Dynamic Filter Cake Parameters with the Shear Rate" Paper SPE 120867, presented at 8th European Formation Damage Conference, 27-29 May 2009, Scheveningen, The Netherlands

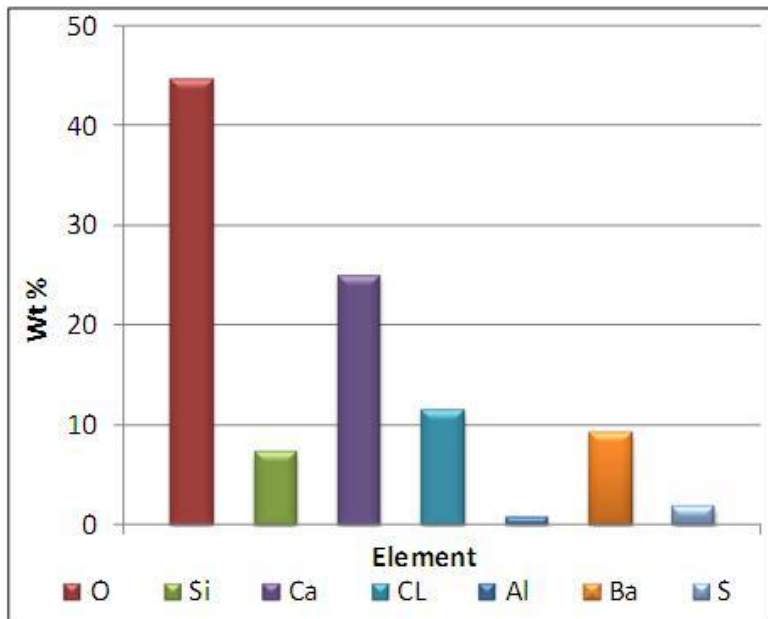
43. Berntsen, A.N., Robbes, A. S., Cerasi, P.R., Zwaag, C.H., 2010,: “Laboratory Investigation of Brine Diffusion Through Oil-Based Mud Filter Cakes,” Paper SPE128027 presented at SPE International Symposium and Exhibiton on Formation Damage Control, Lafayette, Louisiana, USA, 10-12 February 2010
44. Al Moajil, A.M., and H. A. Nasr-El-Din, 2011,:” Formation Damage Caused by Improper Mn3O4-based Filter Cake Cleanup Treatments,” Paper SPE 144179, SPE European Formation Damage Conference, 7-10 June 2011, Noordwijk, The Netherlands
45. Elkattatny, S.M., M.A. Mahmoud, and Nasr-El-Din, H.A., 2011: “A New Approach to Determine Filter Cake Properties of Water-Based Drilling Fluids,” Paper SPE 149041 presented for DGS Saudi Arabia Section Technical Symposium and Exhibition held in Al-Khobar, Saudi Arabia, 15–18 May 2011
46. Overveldt,A. S., Bedrikovetsky,P., Zitha, P. L.J., 2012: “A CT Scan Study of the Leakoff of Oil-Based Drilling Fluids,” Paper SPE 151856, presented for SPE International Symposium and Exhibition on Formation Damage Control, 15-17 February 2012, Lafayette, Louisiana, USA

APPENDIX-A (SEM RESULTS)

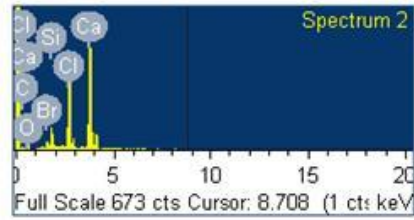
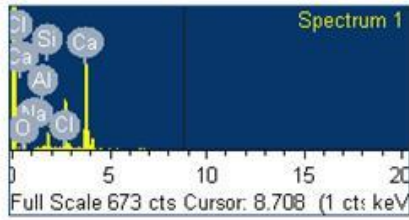
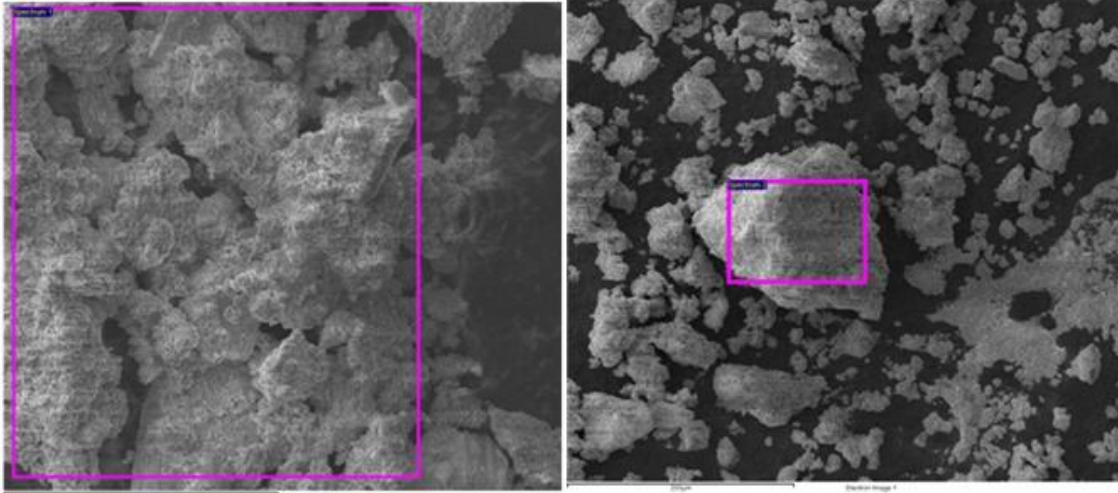
Sample 1 (6700 ft)



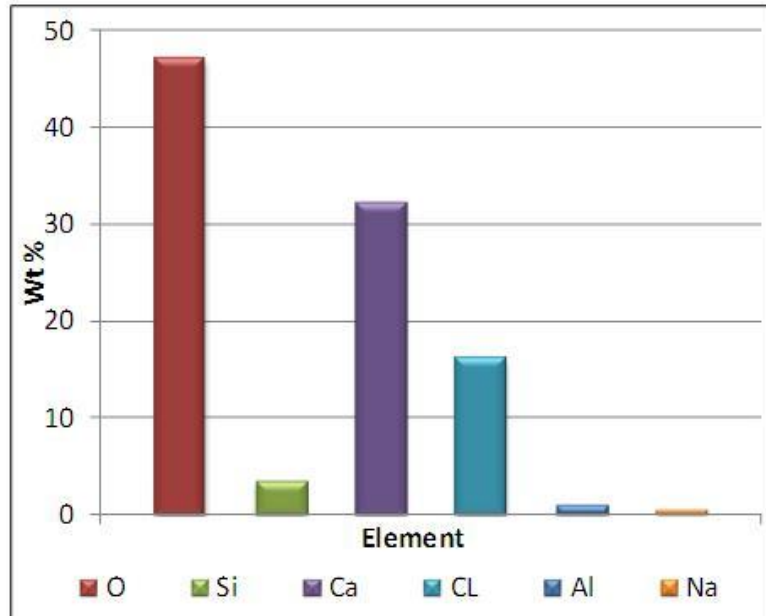
Spectrum	In stats.	O	Al	Si	S	Cl	Ca	Ba	Total
Spectrum 2	Yes	44.48	0.78	7.21	1.86	11.45	24.94	9.27	100.00



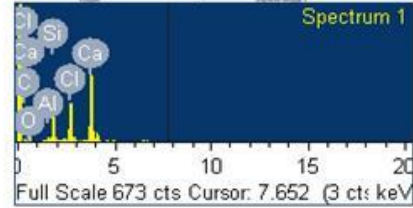
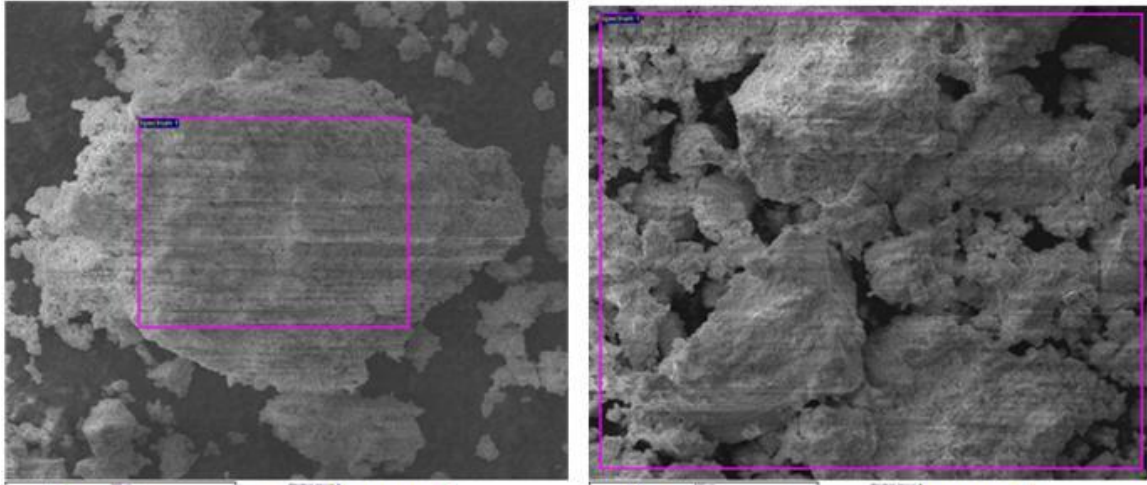
Sample 2 (6900 ft)



Spectrum	In stats.	O	Na	Al	Si	Cl	Ca	Total
Spectrum 1	Yes	43.83	0.86	0.73	3.53	15.95	35.11	100.00
Spectrum	In stats.	O	Al	Si	Cl	Ca	Total	
Spectrum 2	Yes	50.10	1.17	3.33	16.25	29.16	100.00	

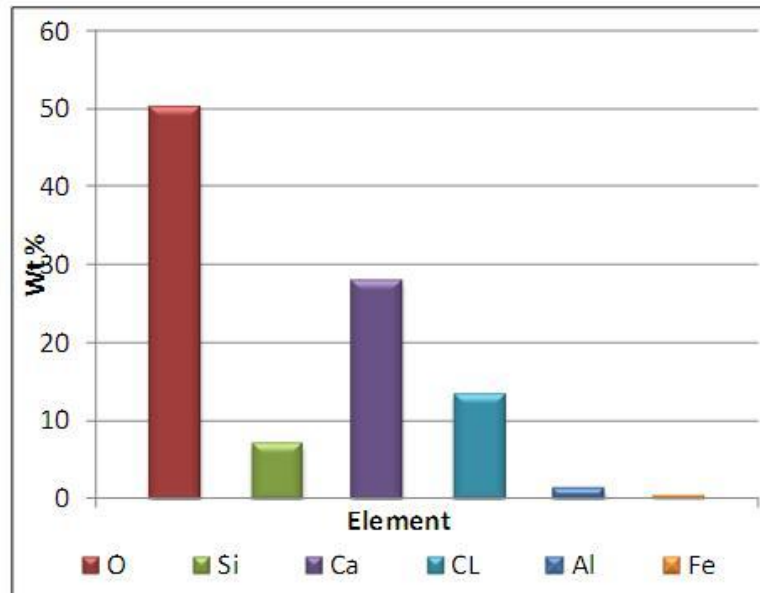


Sample 3 (7100 ft)

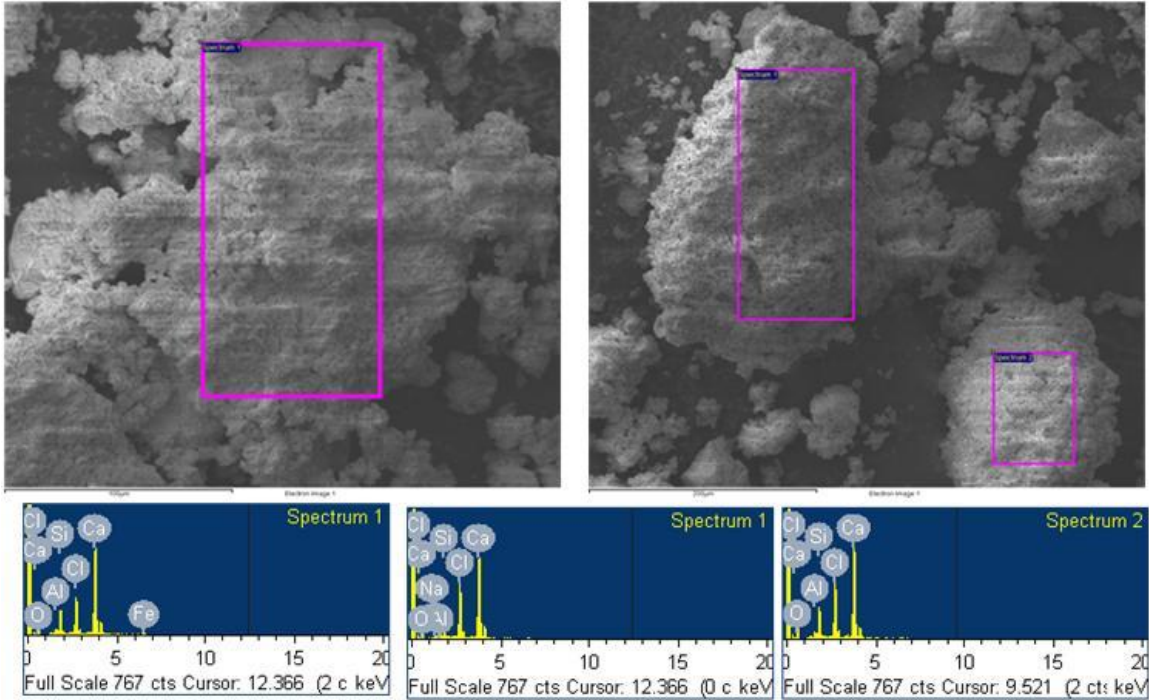


Spectrum	In stats.	O	Al	Si	Cl	Ca	Fe	Total
Spectrum 1	Yes	49.46	1.37	4.93	14.55	28.87	0.83	100.00

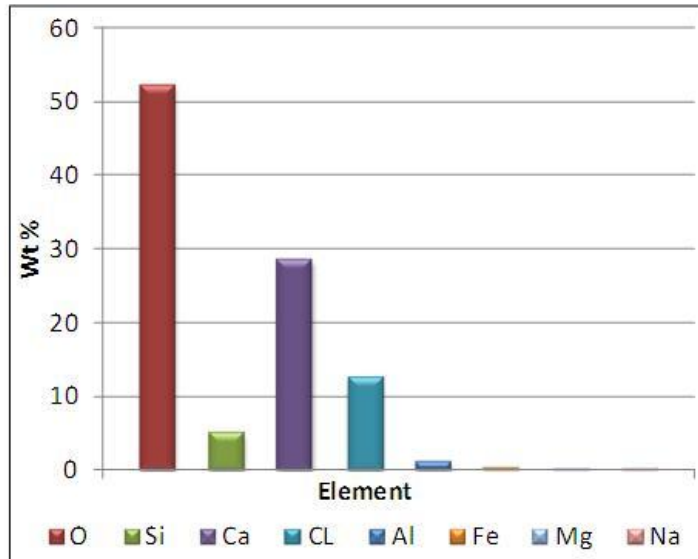
Spectrum	In stats.	O	Al	Si	Cl	Ca	Total
Spectrum 1	Yes	50.86	1.08	8.92	12.17	26.97	100.00



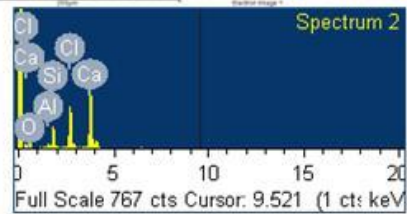
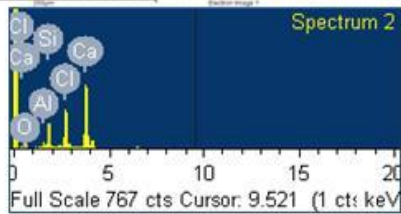
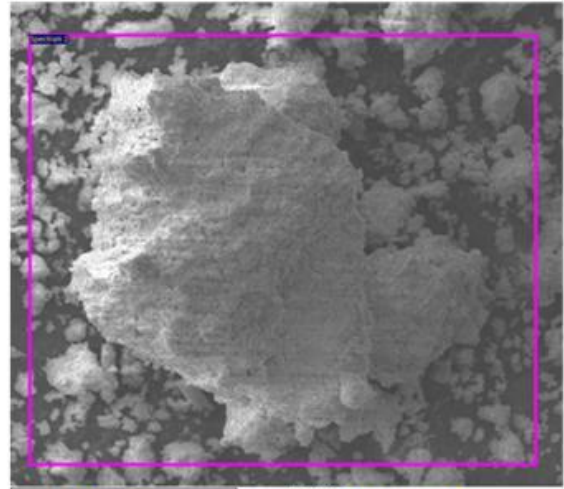
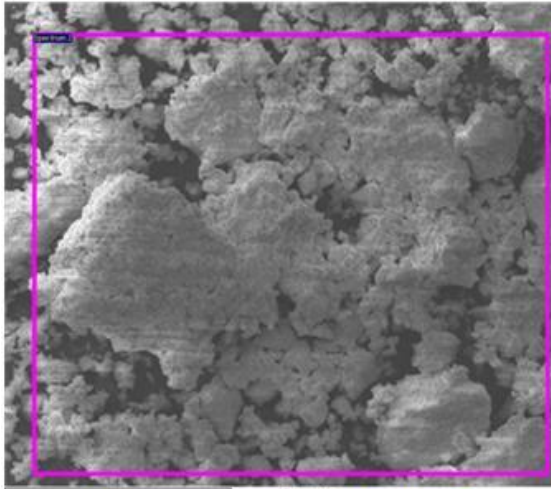
Sample 4 (7300 ft)



Spectrum	In stats.	O	Al	Si	Cl	Ca	Fe	Total	
Spectrum 1	Yes	53.68	1.05	4.96	9.65	29.68	0.98	100.00	
Spectrum	In stats.	O	Na	Mg	Al	Si	Cl	Ca	Total
Spectrum 1	Yes	51.94	0.67	0.53	1.10	4.59	13.92	27.24	100.00
Spectrum 2	Yes	51.00	--	--	1.31	5.42	13.90	28.37	100.00

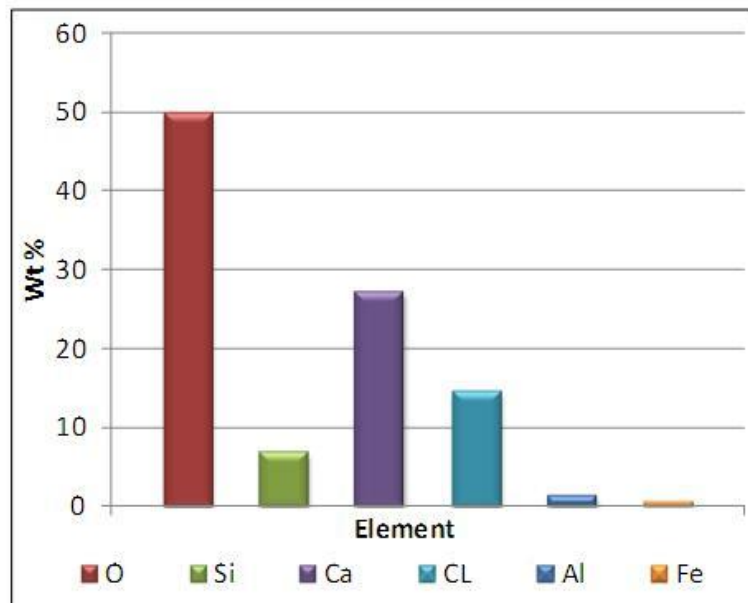


Sample 5 (7500 ft)

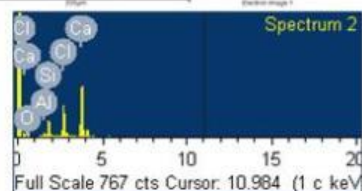
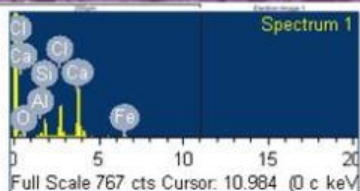
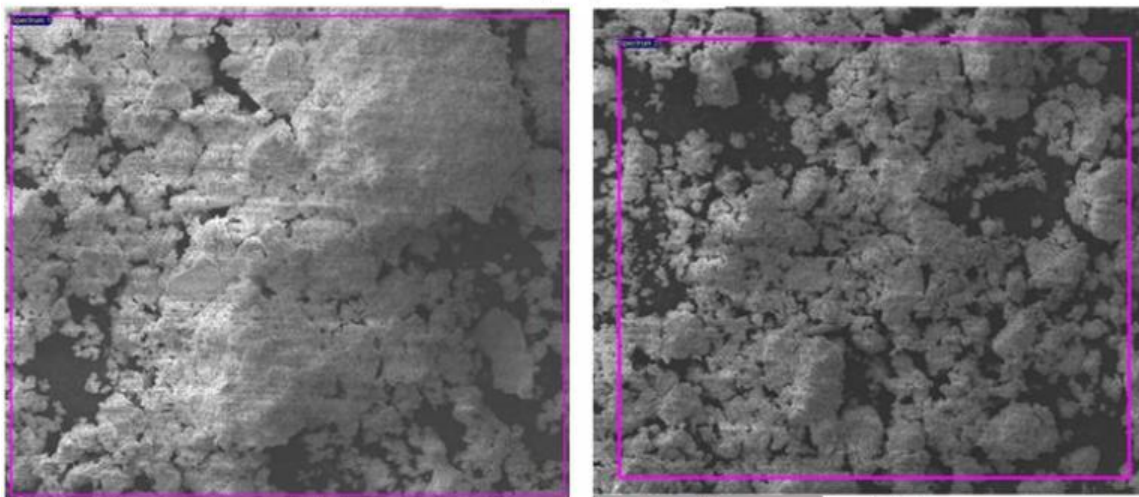


Spectrum	In stats.	O	Al	Si	Cl	Ca	Total
Spectrum 2	Yes	49.14	1.27	7.40	13.77	28.42	100.00

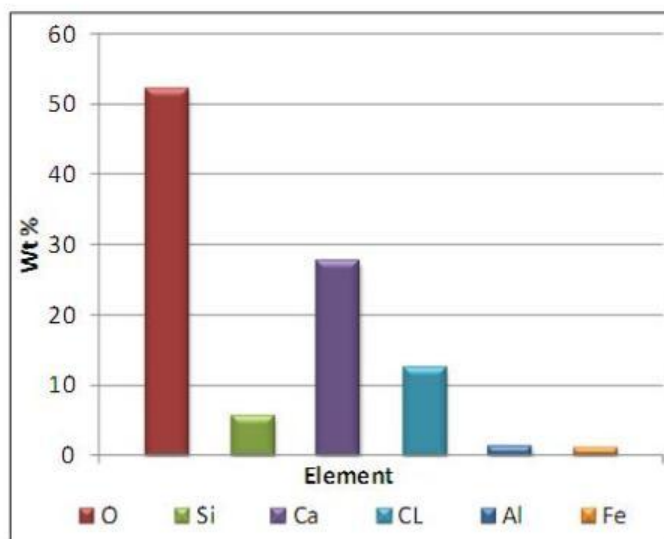
Spectrum	In stats.	O	Al	Si	Cl	Ca	Fe	Total
Spectrum 2	Yes	50.49	1.10	6.12	15.26	25.84	1.20	100.00



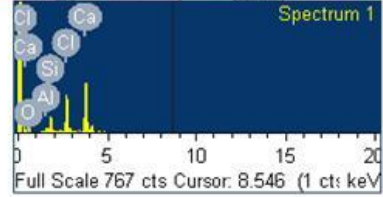
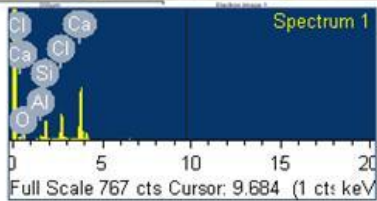
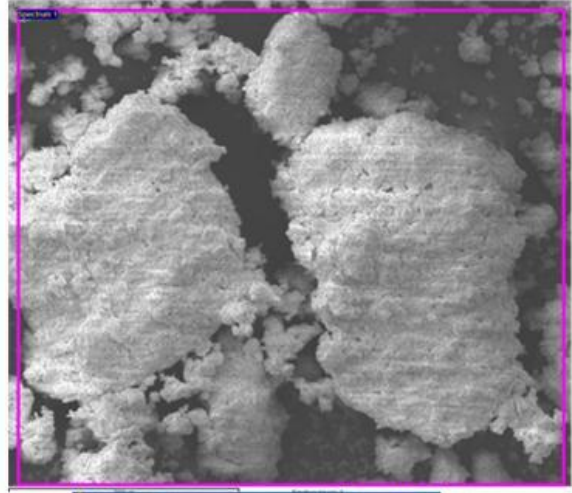
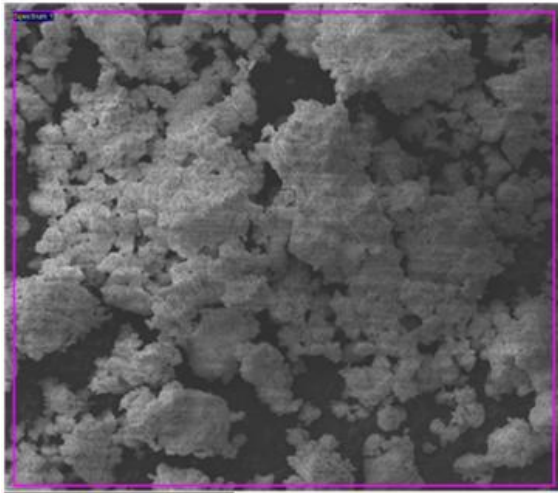
Sample 6 (7700 ft)



Spectrum	In stats.	O	Al	Si	Cl	Ca	Fe	Total
Spectrum 1	Yes	50.54	1.01	5.81	13.56	26.98	2.10	100.00
Spectrum 2	Yes	53.75	1.42	5.27	11.31	28.24		100.00

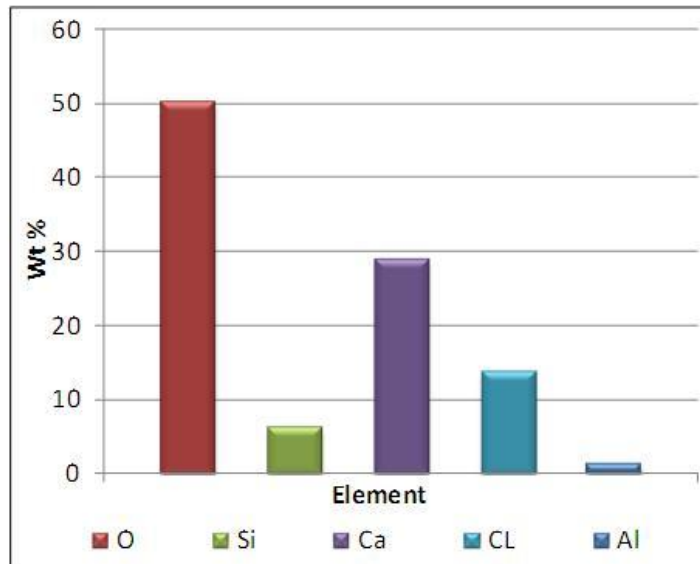


Sample 7 (7900 ft)

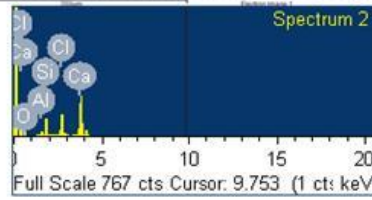
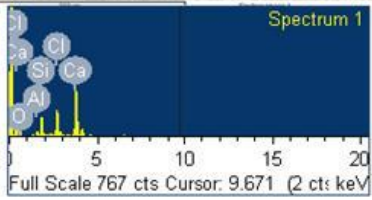
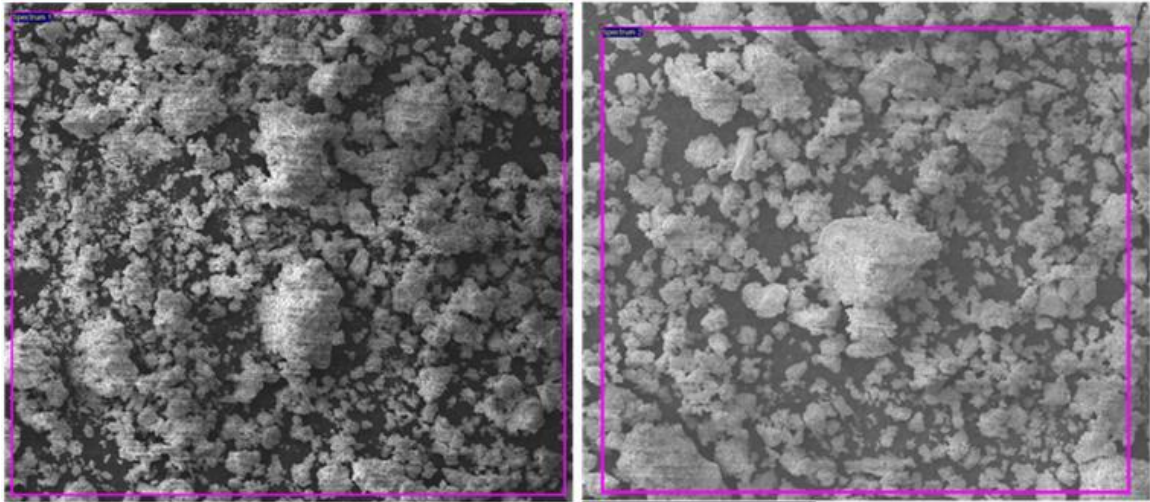


Spectrum	In stats.	O	Al	Si	Cl	Ca	Total
Spectrum 1	Yes	49.73	1.31	6.97	12.05	29.94	100.00

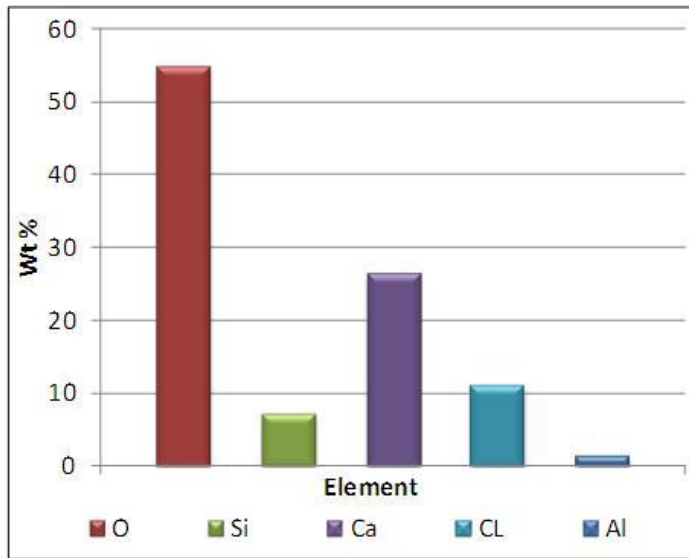
Spectrum	In stats.	O	Al	Si	Cl	Ca	Total
Spectrum 1	Yes	50.39	1.20	5.35	15.15	27.91	100.00



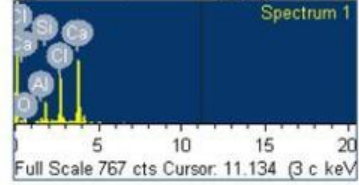
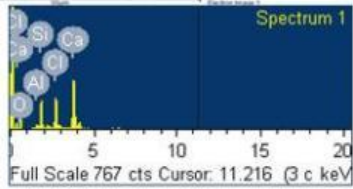
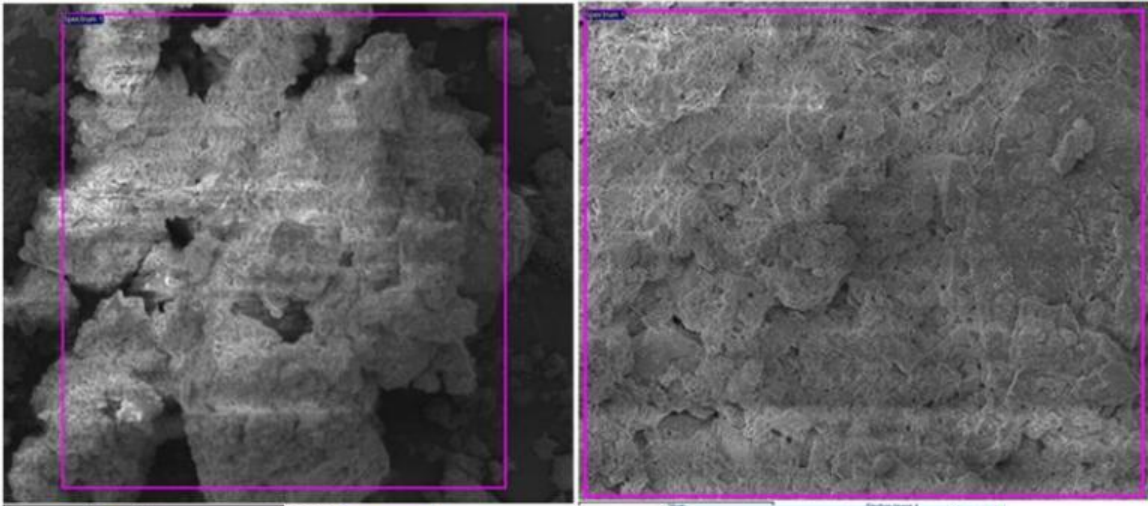
Sample 8 (8100 ft)



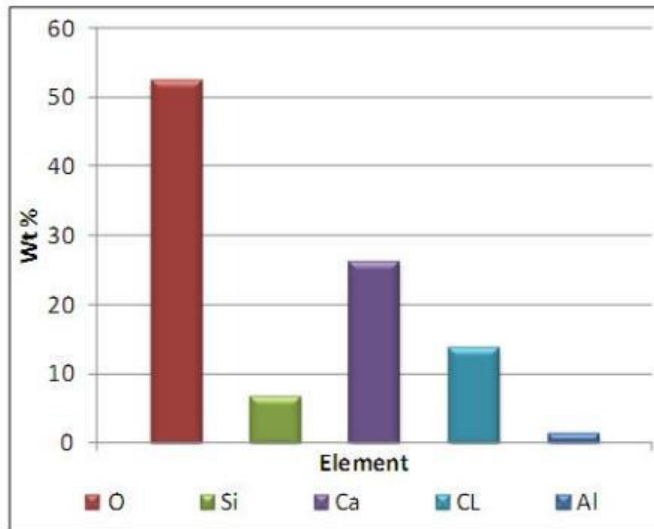
Spectrum	In stats.	O	Al	Si	Cl	Ca	Total
Spectrum 1	Yes	54.28	1.18	6.88	10.87	26.79	100.00
Spectrum 2	Yes	55.02	1.25	7.14	10.86	25.73	100.00



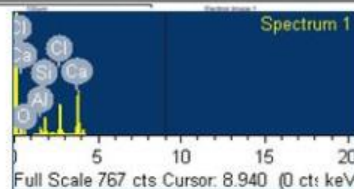
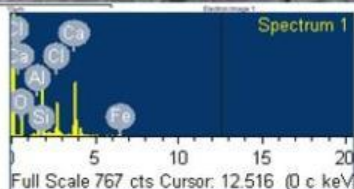
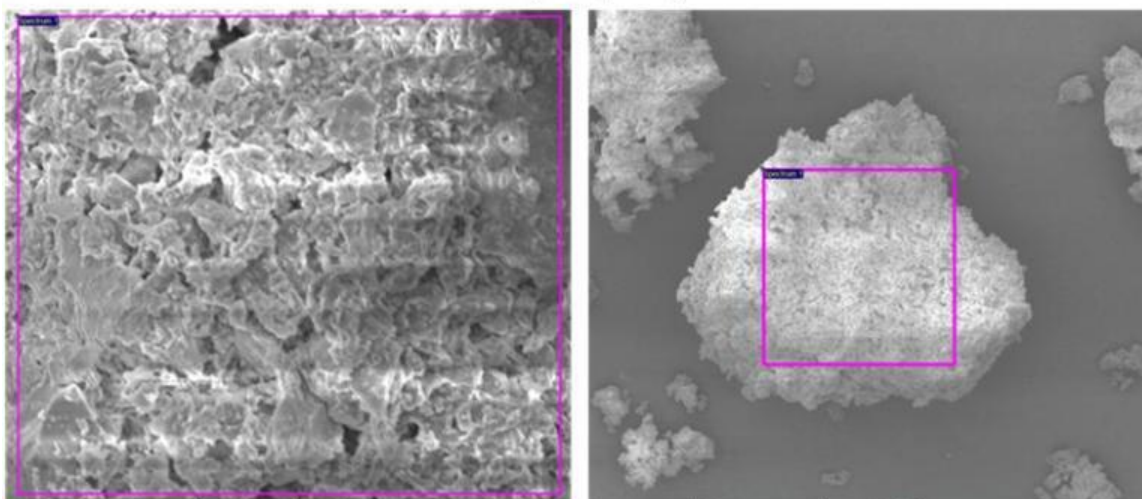
Sample 9 (8300 ft)



Spectrum	In stats.	O	Al	Si	Cl	Ca	Total
Spectrum 1	Yes	53.13	1.20	8.16	12.46	25.05	100.00
Spectrum	In stats.	O	Al	Si	Cl	Ca	Total
Spectrum 1	Yes	51.32	1.39	5.00	14.95	27.34	100.00

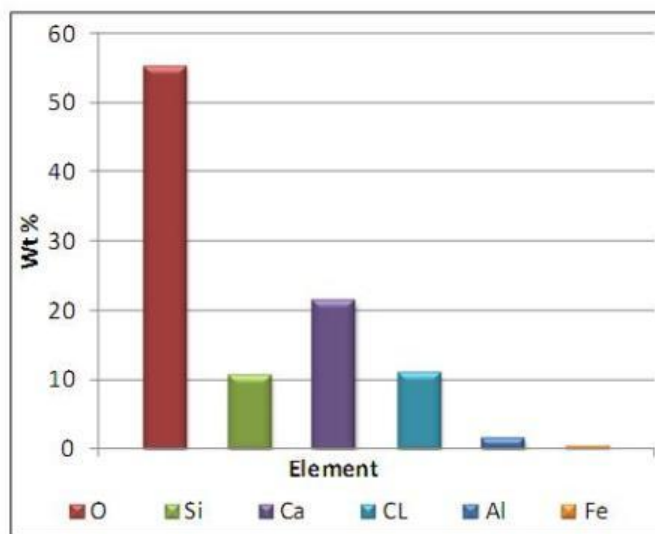


Sample 10 (8500 ft)

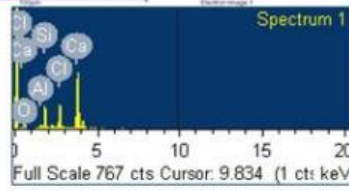
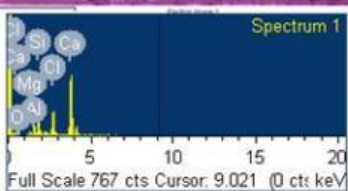
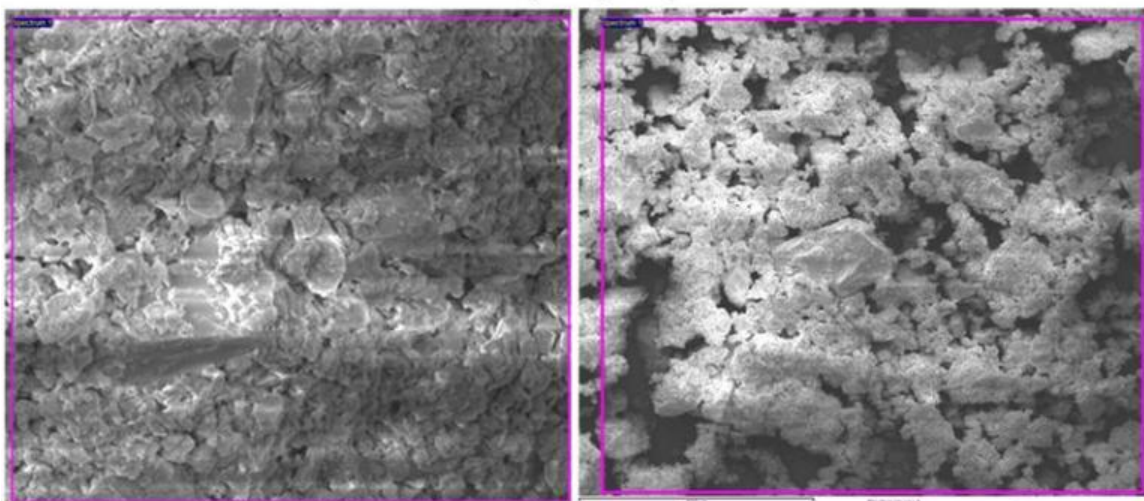


Spectrum	In stats.	O	Al	Si	Cl	Ca	Fe	Total
Spectrum 1	Yes	55.16	1.13	14.52	9.44	18.86	0.90	100.00

Spectrum	In stats.	O	Al	Si	Cl	Ca	Total
Spectrum 1	Yes	55.17	1.88	6.37	12.51	24.07	100.00

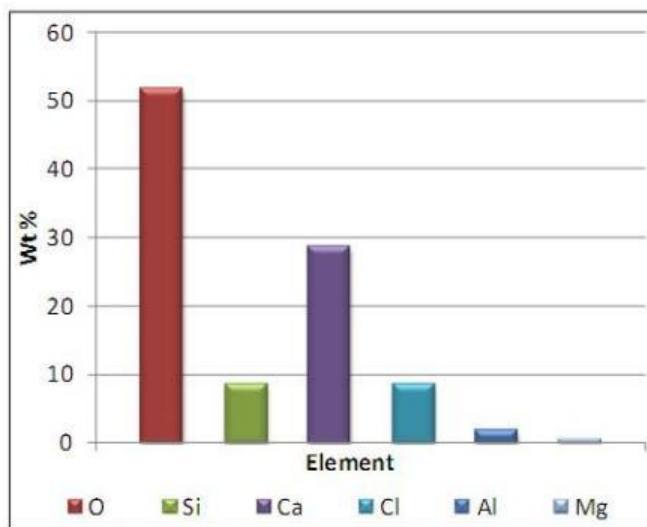


Sample 11 (8700 ft)

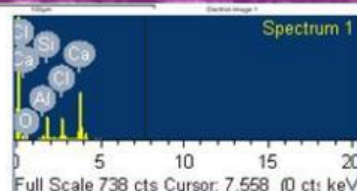
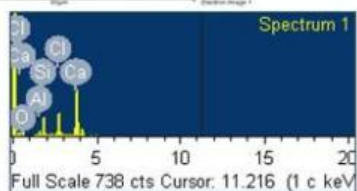
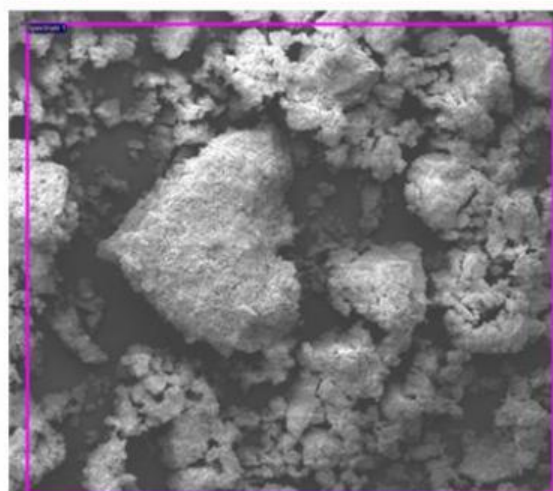
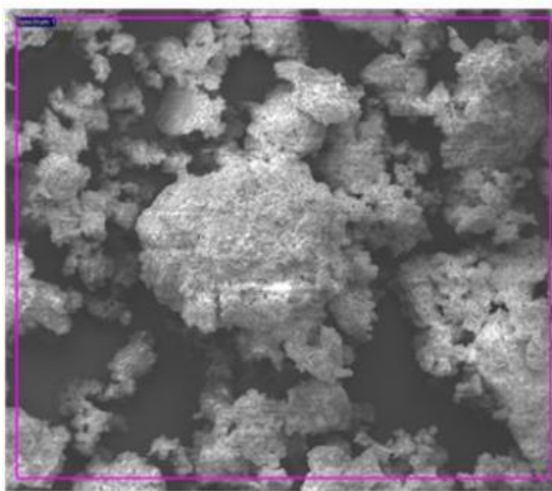


Spectrum	In stats.	O	Mg	Al	Si	Cl	Ca	Total
Spectrum 1	Yes	52.66	1.29	2.30	10.09	7.39	26.27	100.00

Spectrum	In stats.	O	Al	Si	Cl	Ca	Total
Spectrum 1	Yes	50.83	1.28	7.15	9.81	30.93	100.00

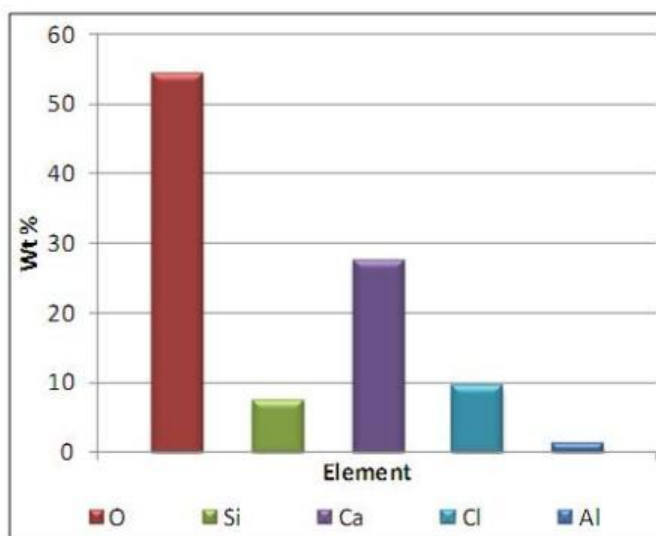


Sample 12 (8900 ft)

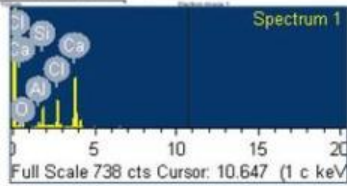
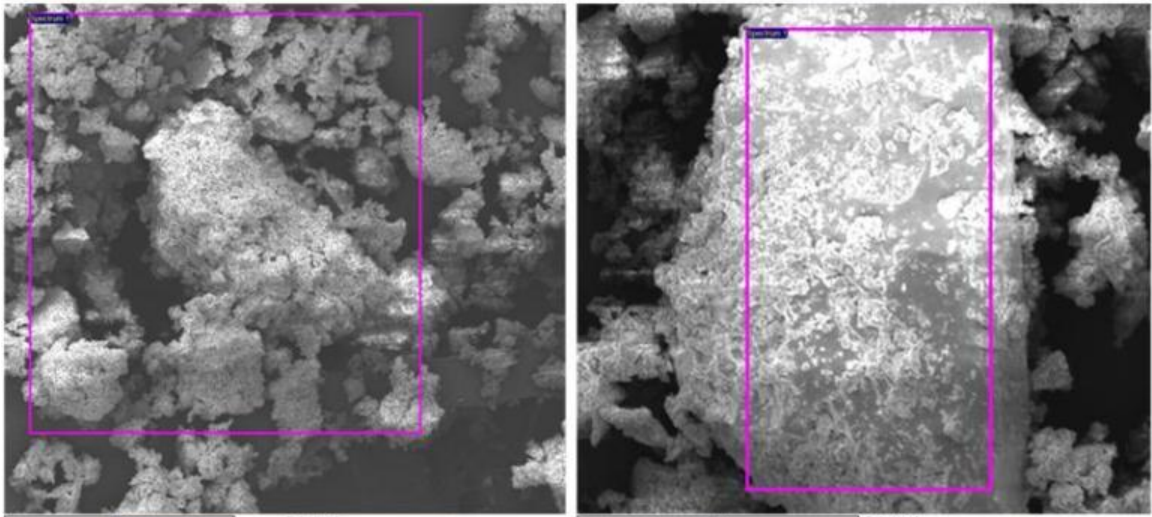


Spectrum	In stats.	O	Al	Si	Cl	Ca	Total
Spectrum 1	Yes	54.48	1.30	6.85	9.83	27.55	100.00

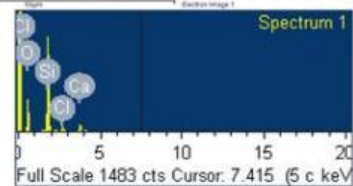
Spectrum	In stats.	O	Al	Si	Cl	Ca	Total
Spectrum 1	Yes	54.06	1.35	8.03	9.07	27.49	100.00



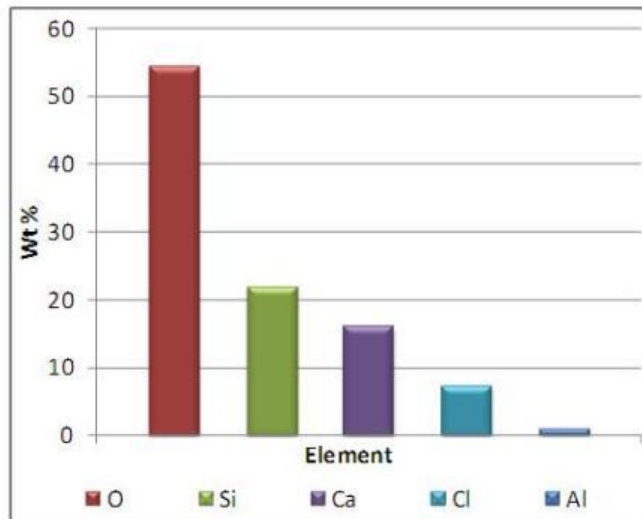
Sample 13 (9100 ft)



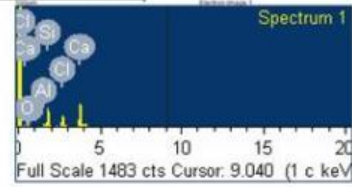
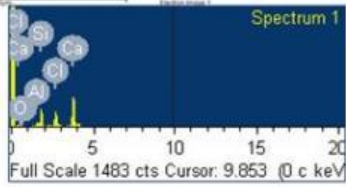
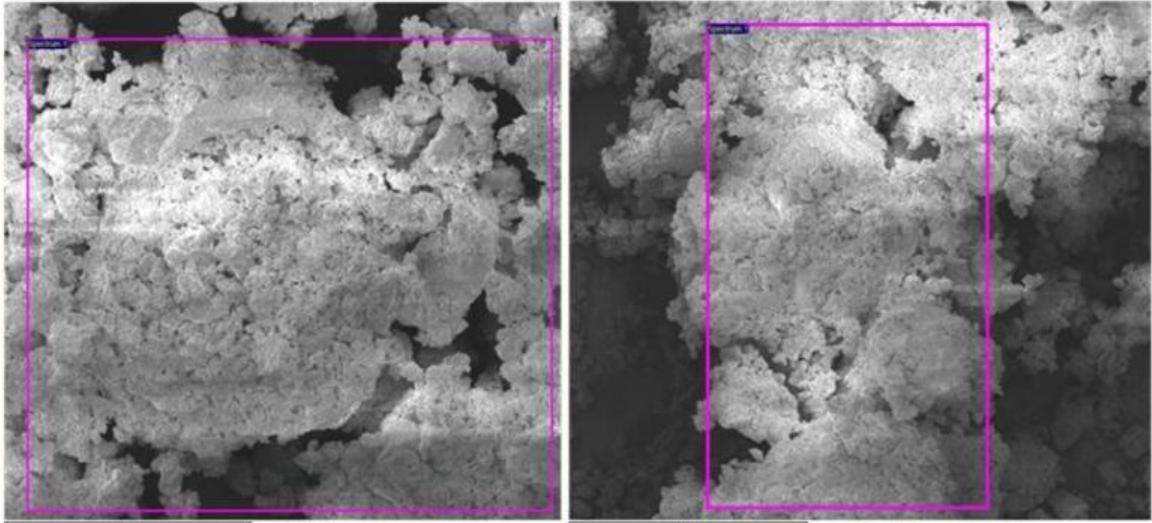
Spectrum	In stats.	O	Al	Si	Cl	Ca	Total
Spectrum 1	Yes	52.31	1.59	6.30	11.71	28.09	100.00



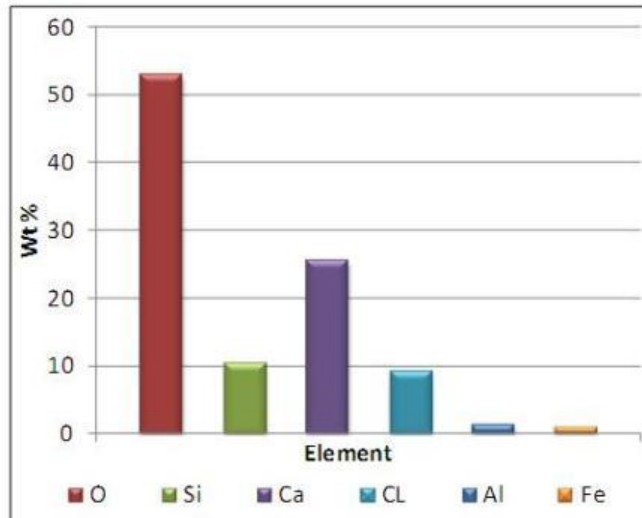
Spectrum	In stats.	O	Si	Cl	Ca	Total
Spectrum 1	Yes	56.08	37.30	2.76	3.85	100.00



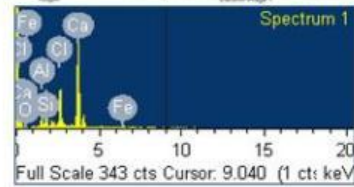
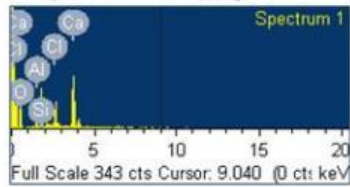
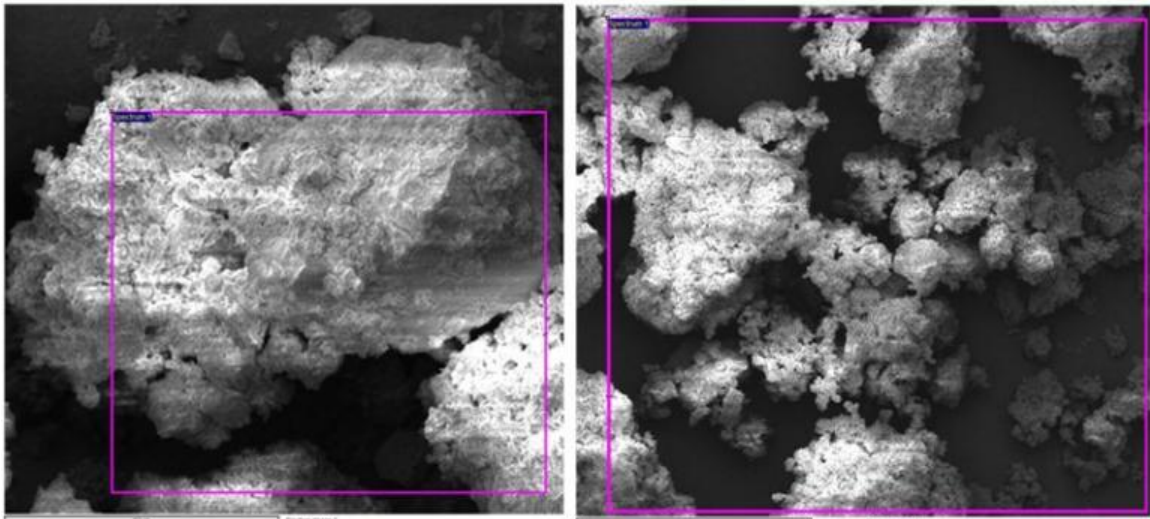
Sample 14 (9300 ft)



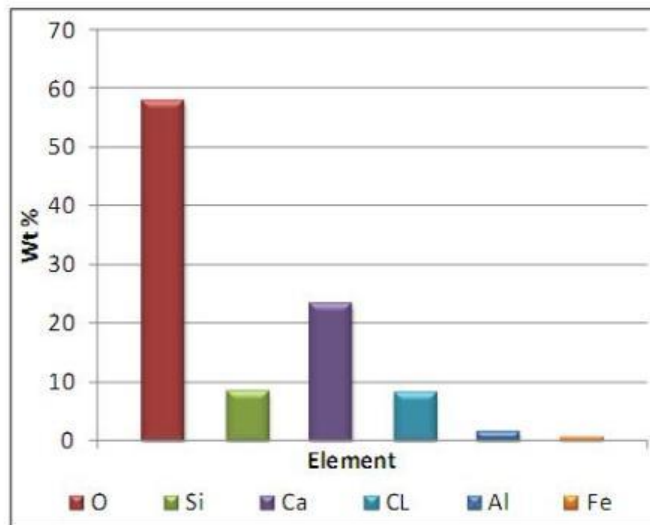
Spectrum	In stats.	O	Al	Si	Cl	Ca	Fe	Total
Spectrum 1	Yes	50.61	1.43	9.58	9.79	27.51	1.08	100.00
Spectrum	In stats.	O	Al	Si	Cl	Ca	Fe	Total
Spectrum 1	Yes	55.04	1.08	10.90	8.65	23.41	0.91	100.00



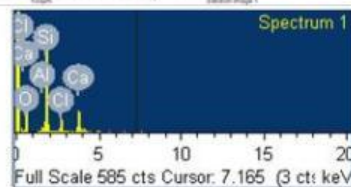
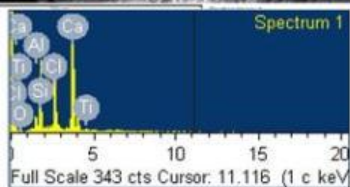
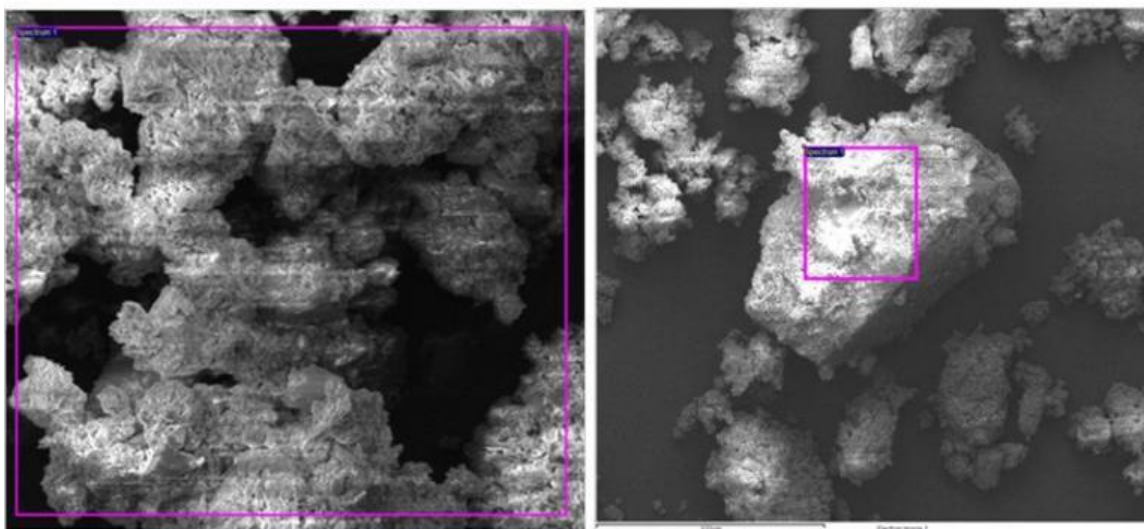
Sample 15 (9500 ft)



Spectrum	In stats.	O	Al	Si	Cl	Ca	Total	
Spectrum 1	Yes	60.57	1.48	9.05	7.37	21.53	100.00	
Spectrum	In stats.	O	Al	Si	Cl	Ca	Fe	Total
Spectrum 1	Yes	55.28	1.45	7.87	8.99	25.17	1.25	100.00

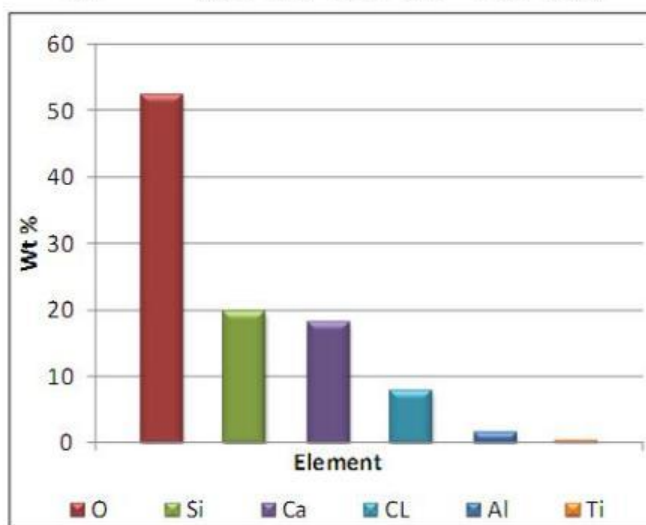


Sample 16 (96750 ft)



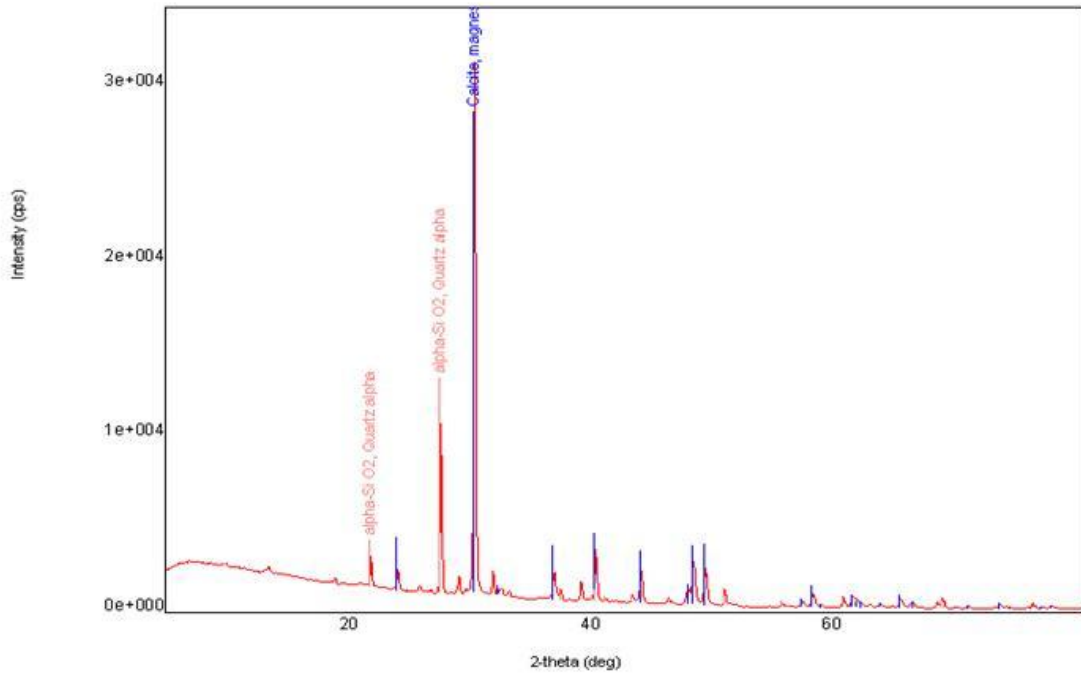
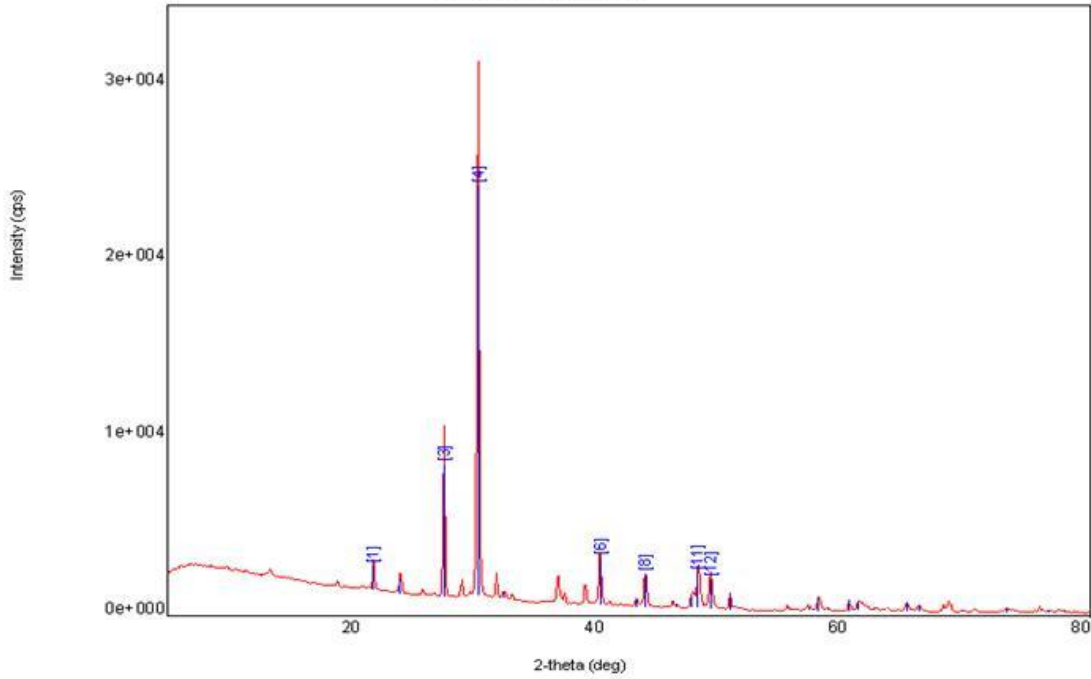
Spectrum	In stats.	O	Al	Si	Cl	Ca	Ti	Total
Spectrum 1	Yes	53.72	1.61	9.13	9.89	24.91	0.73	100.00

Spectrum	In stats.	O	Al	Si	Cl	Ca	Total
Spectrum 1	Yes	50.94	1.40	30.41	5.85	11.39	100.00



APPENDIX-B (XRD RESULTS)

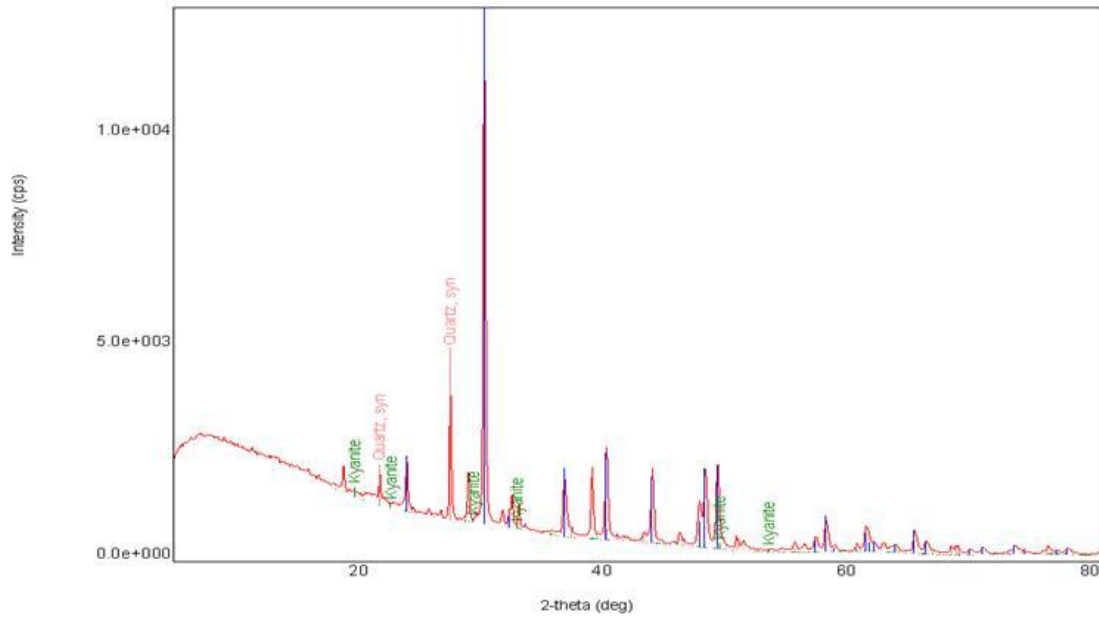
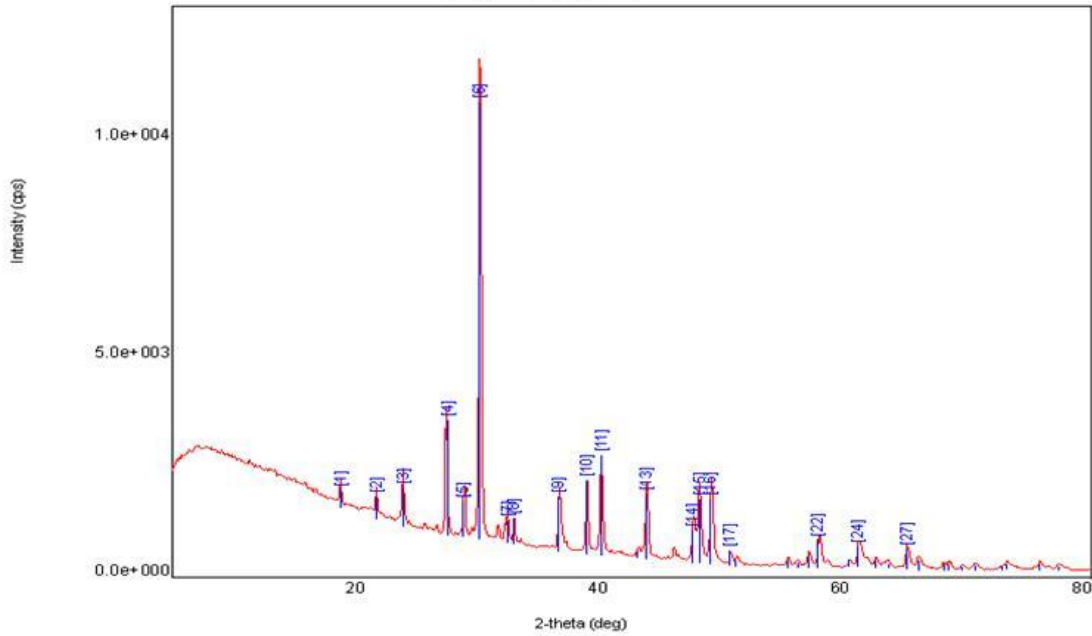
Sample 1 (6700 ft)



Quantitative analysis results (WPPF)

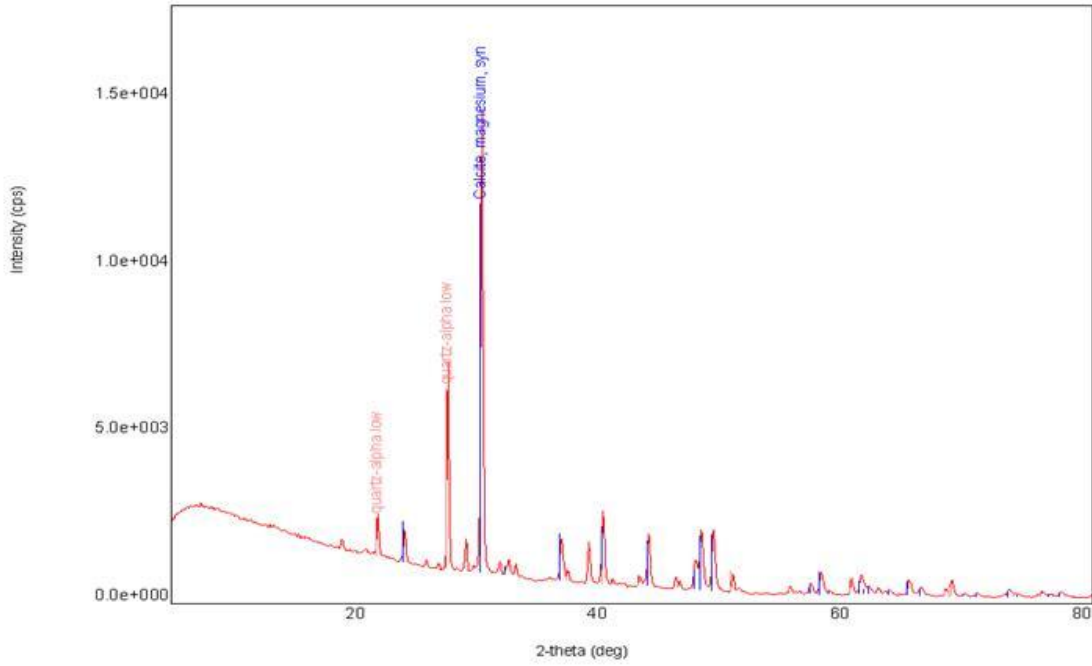
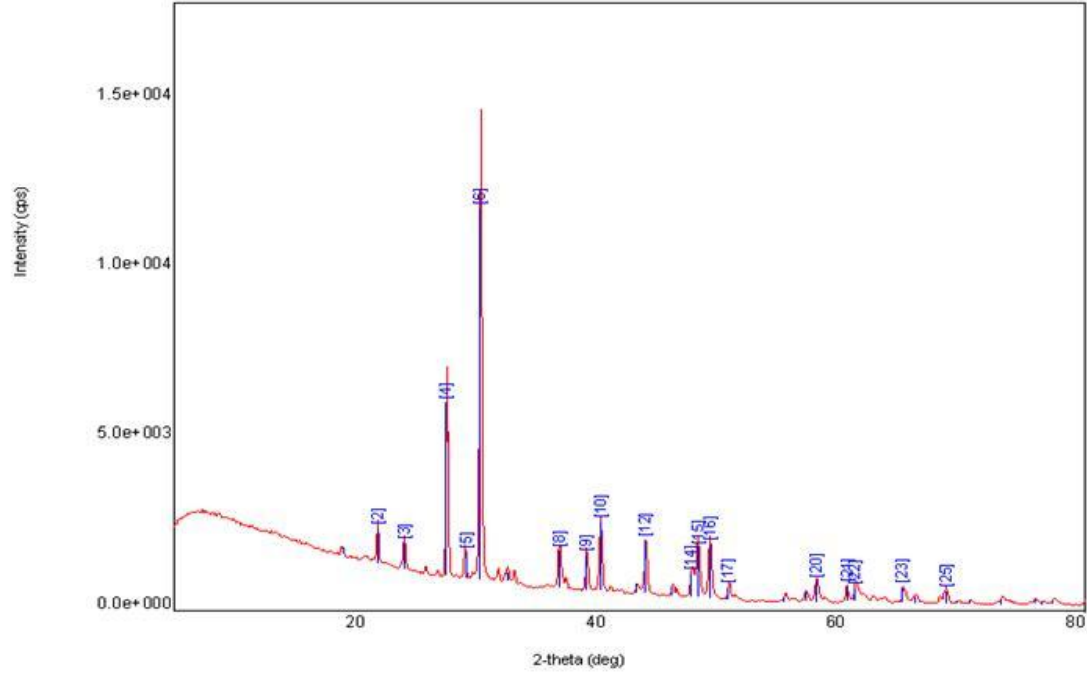
Phase name	Content(%)
Calcite	78
Quartz	22

Sample 2 (6900 ft)



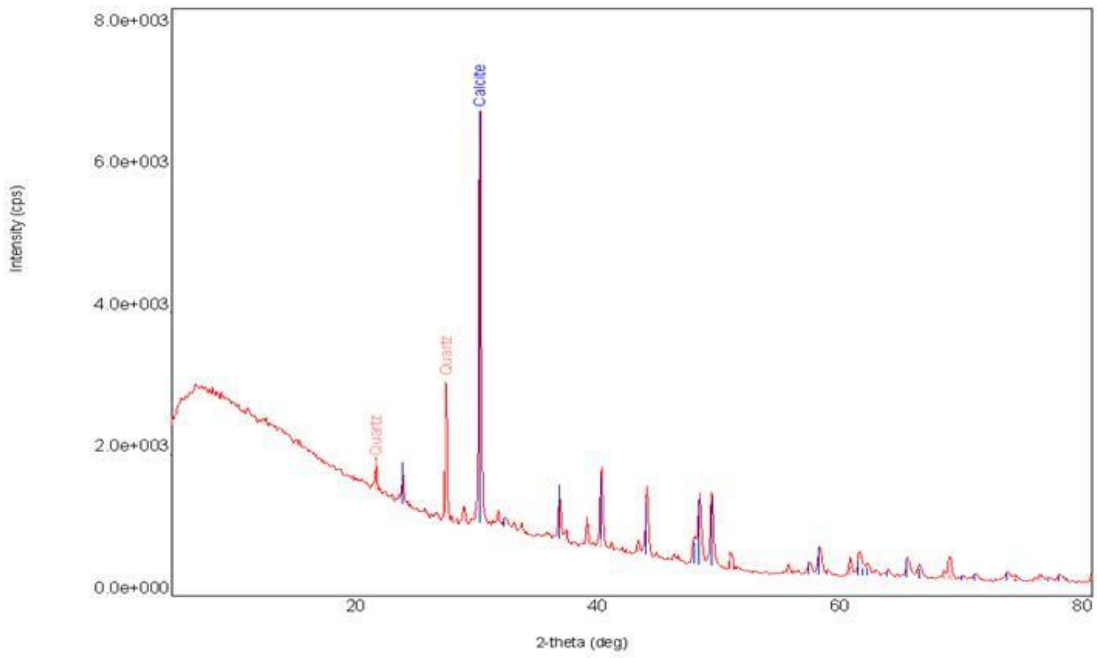
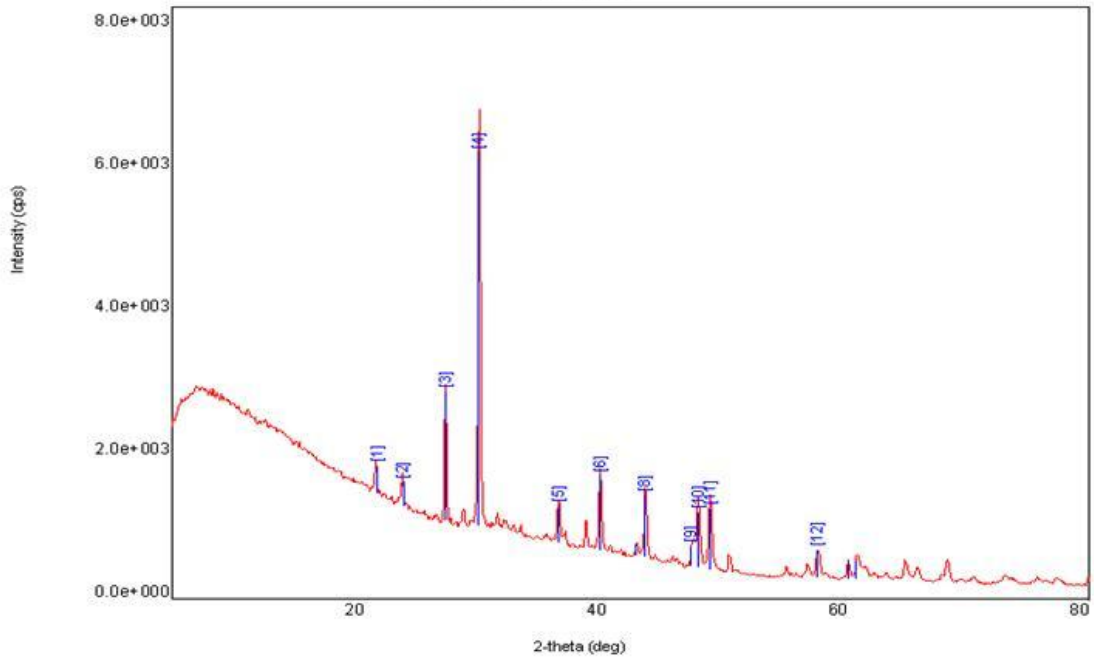
Quantitative analysis results (WPPF)	
Phase name	Content(%)
Calcite	85
Quartz	11.4
Kyanite	3

Sample 3 (7100 ft)



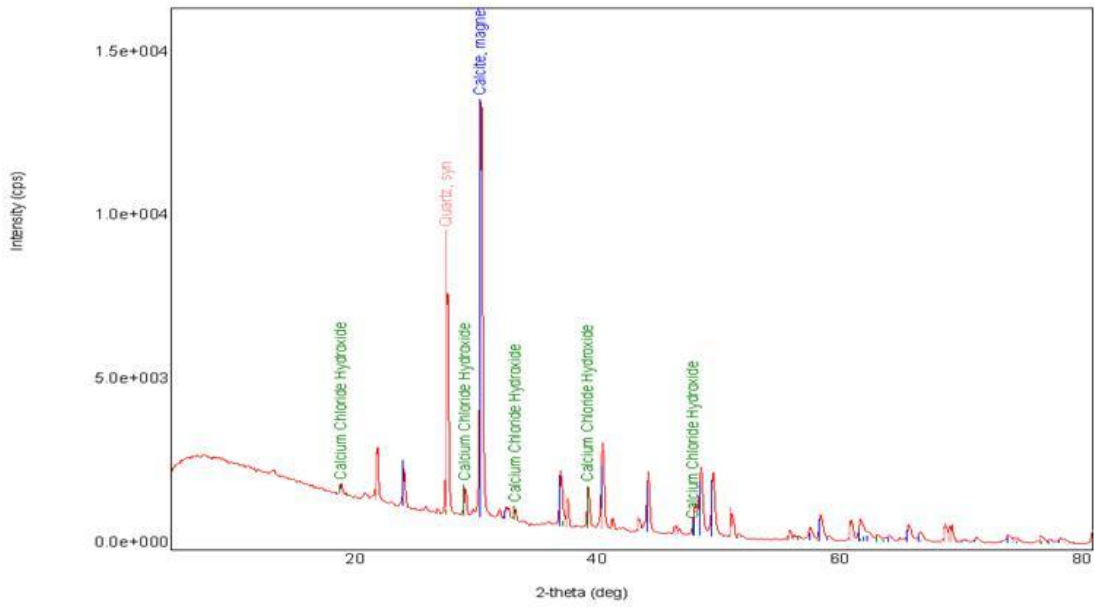
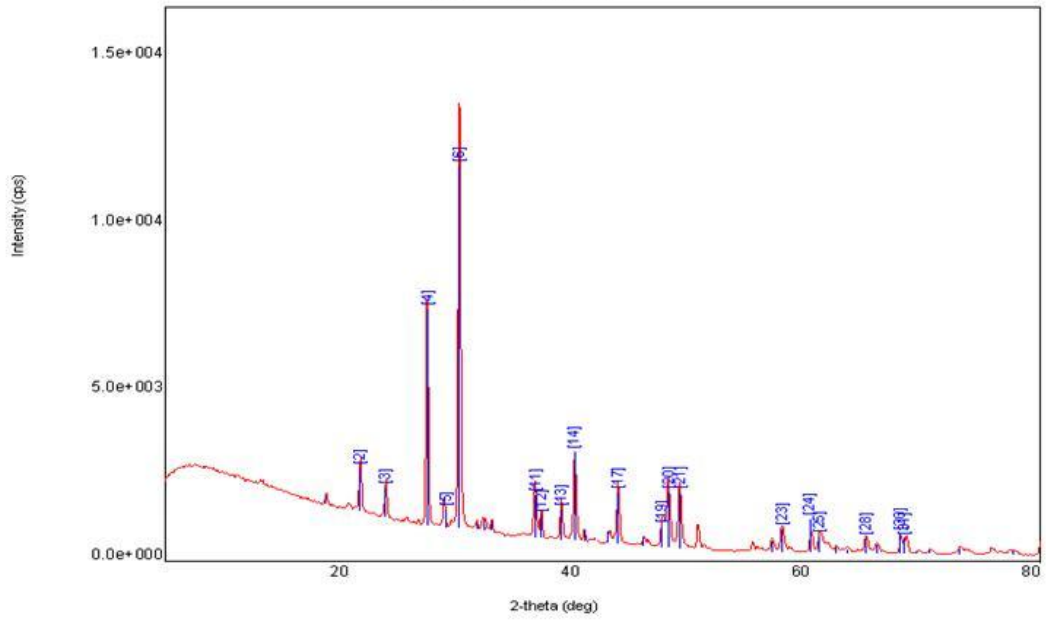
Quantitative analysis results (WPPF)	
Phase name	Content(%)
Calcite	73
Quartz	26.9

Sample 4 (7300 ft)



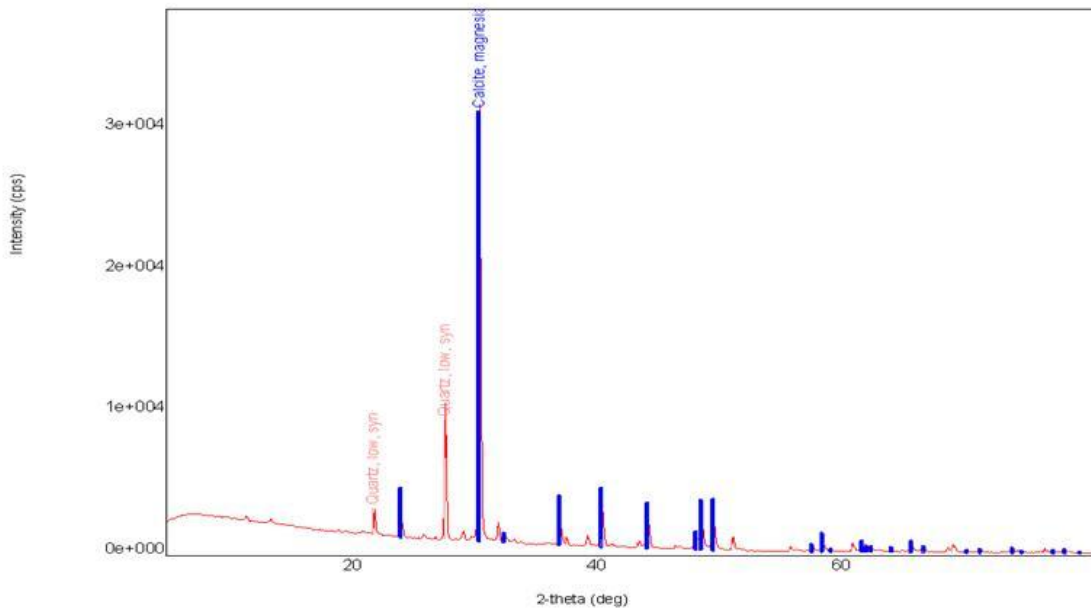
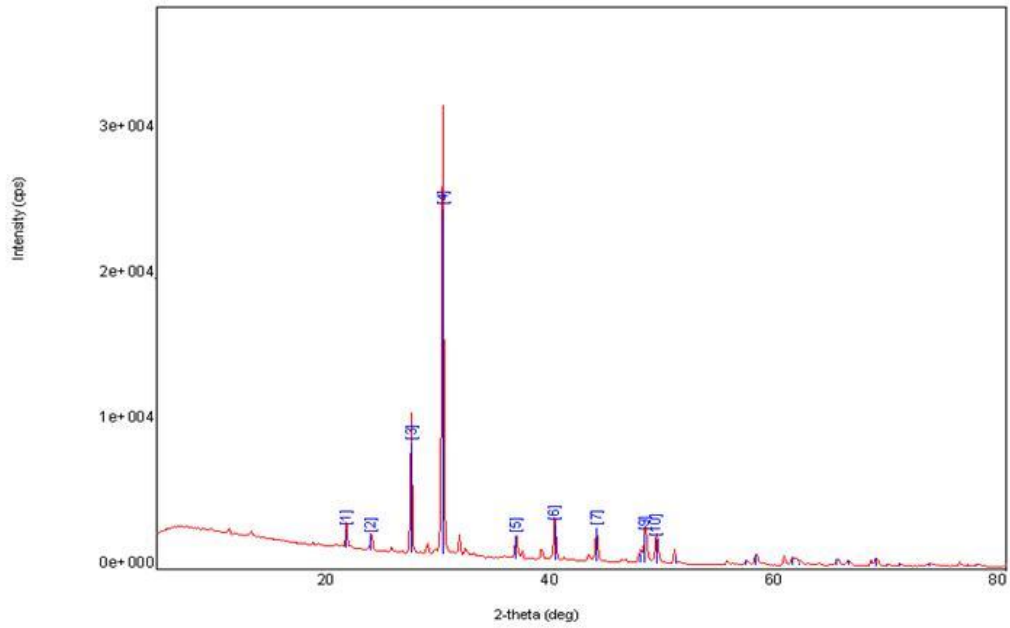
Quantitative analysis results (WPPF)	
Phase name	Content(%)
Calcite	77
Quartz	23

Sample 5 (7500 ft)



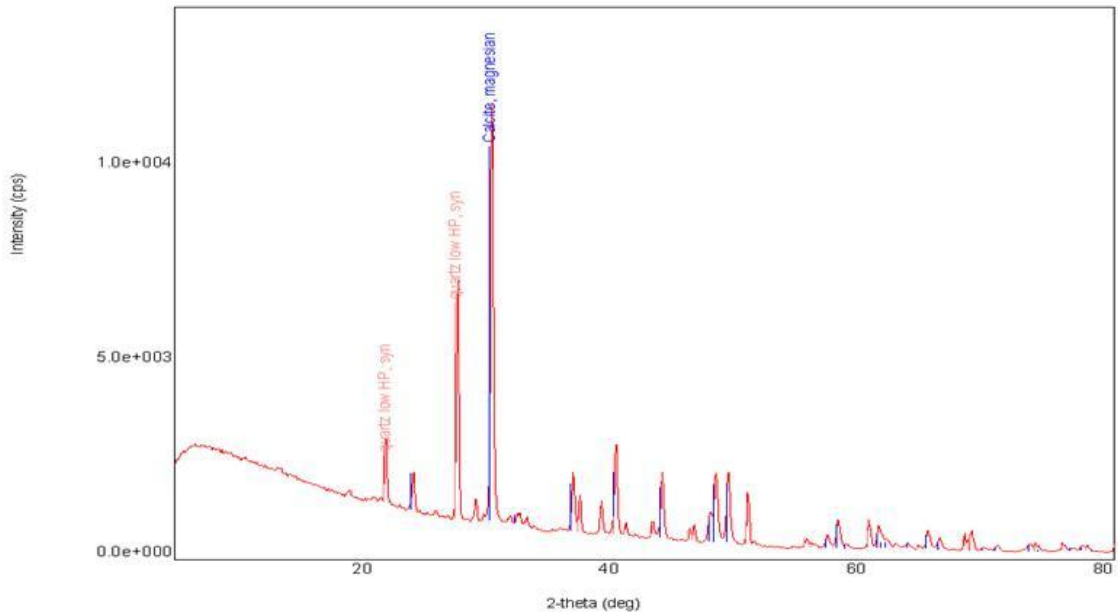
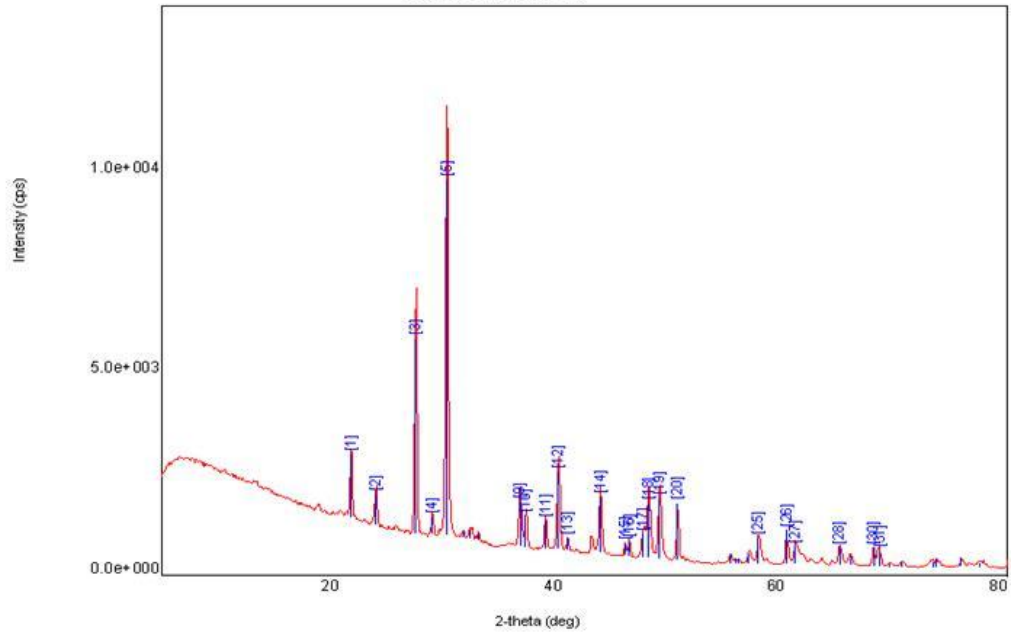
Quantitative analysis results (WPPF)	
Phase name	Content(%)
Calcite	66.9
Quartz	31.1
Calcium Chloride Hydroxide	2

Sample 6 (7700 ft)



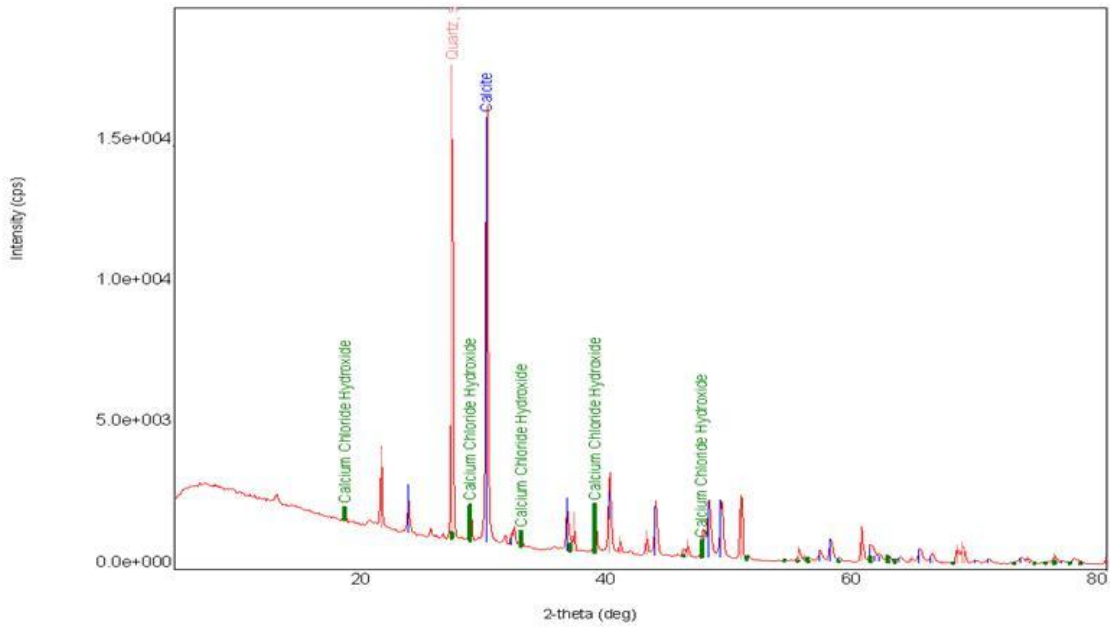
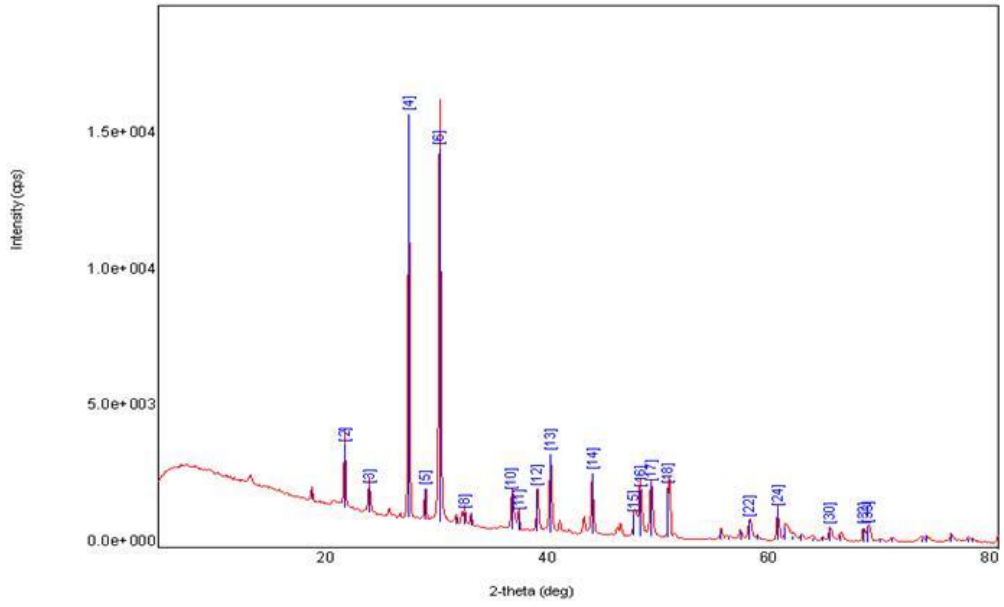
Quantitative analysis results (WPPF)	
Phase name	Content(%)
Calcite	81
Quartz	19.3

Sample 7 (7900 ft)



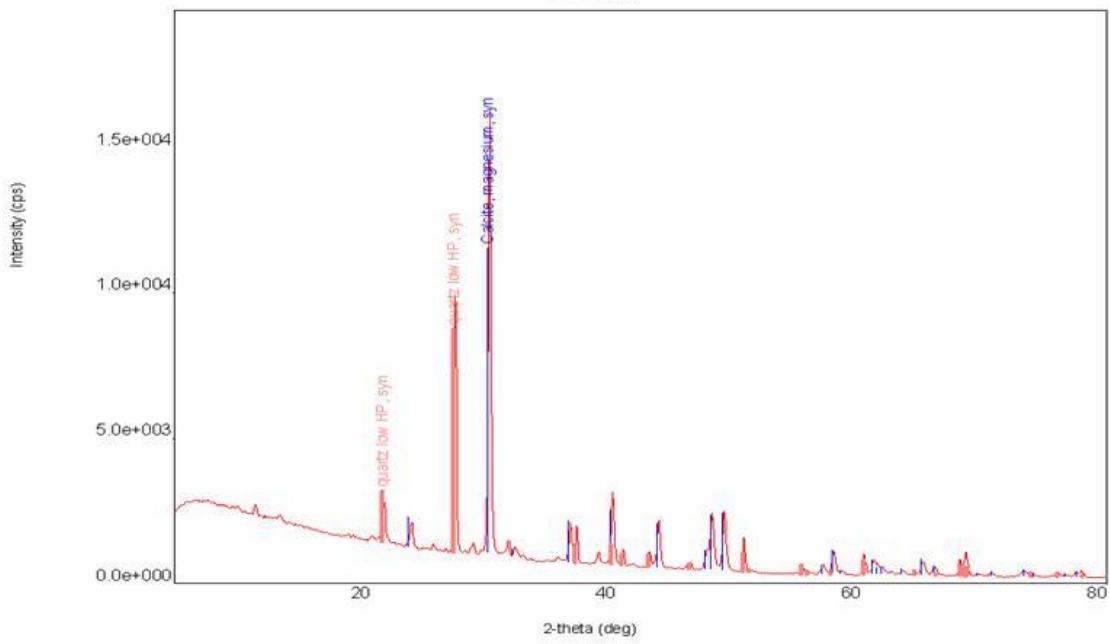
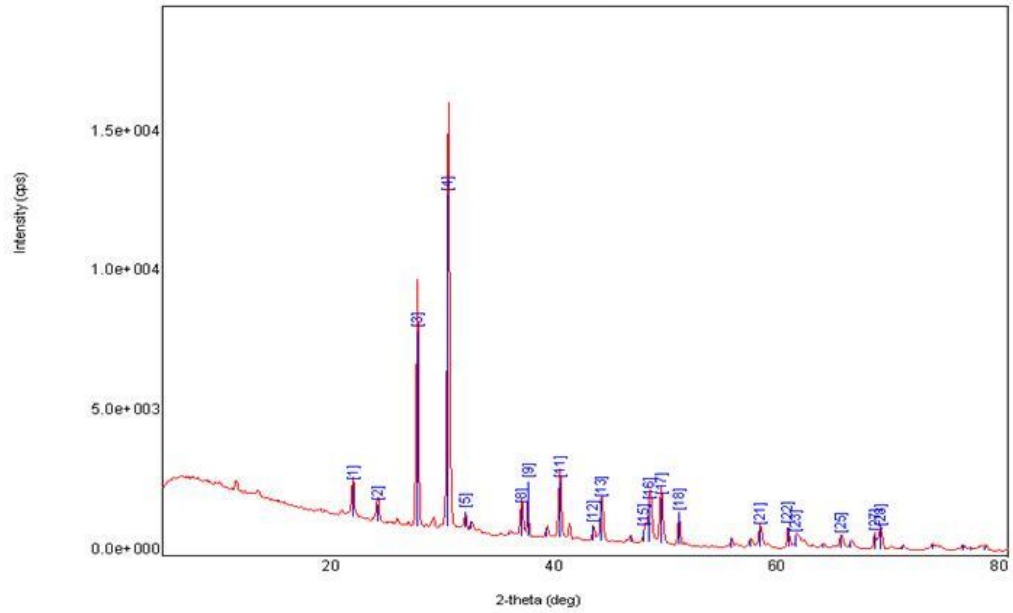
Quantitative analysis results (WPPF)	
Phase name	Content(%)
Calcite	68.3
Quartz	31.7

Sample 9 (8300 ft)



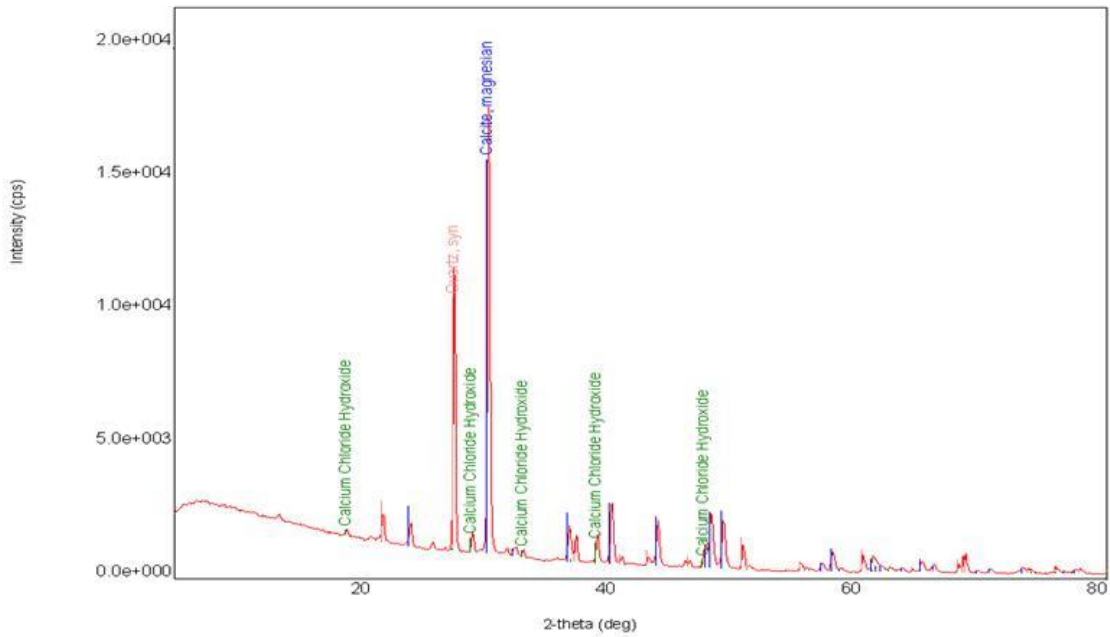
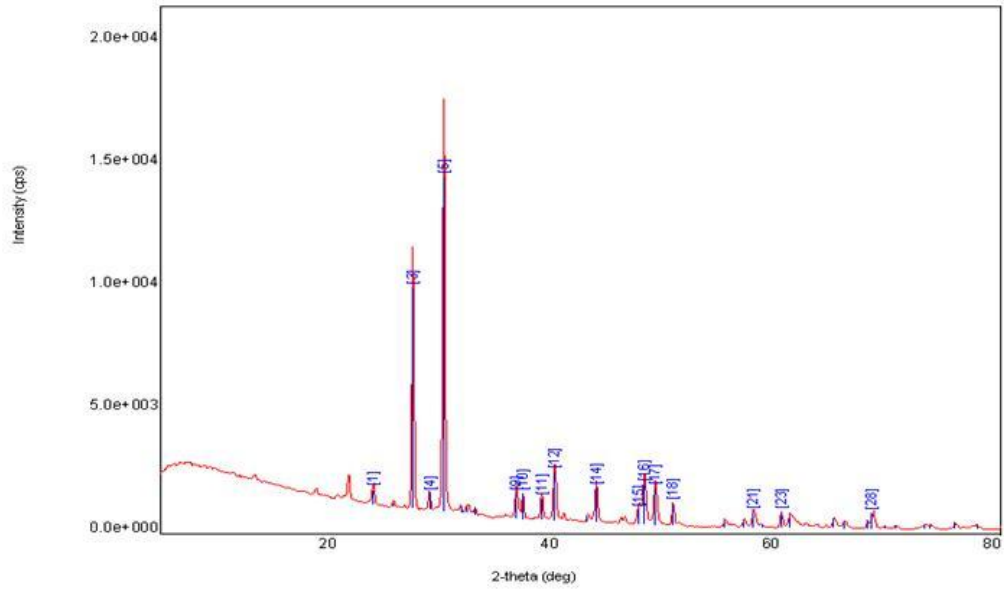
Quantitative analysis results (WPPF)	
Phase name	Content(%)
Calcite	59.3
Quartz	40.7

Sample 10 (8500 ft)



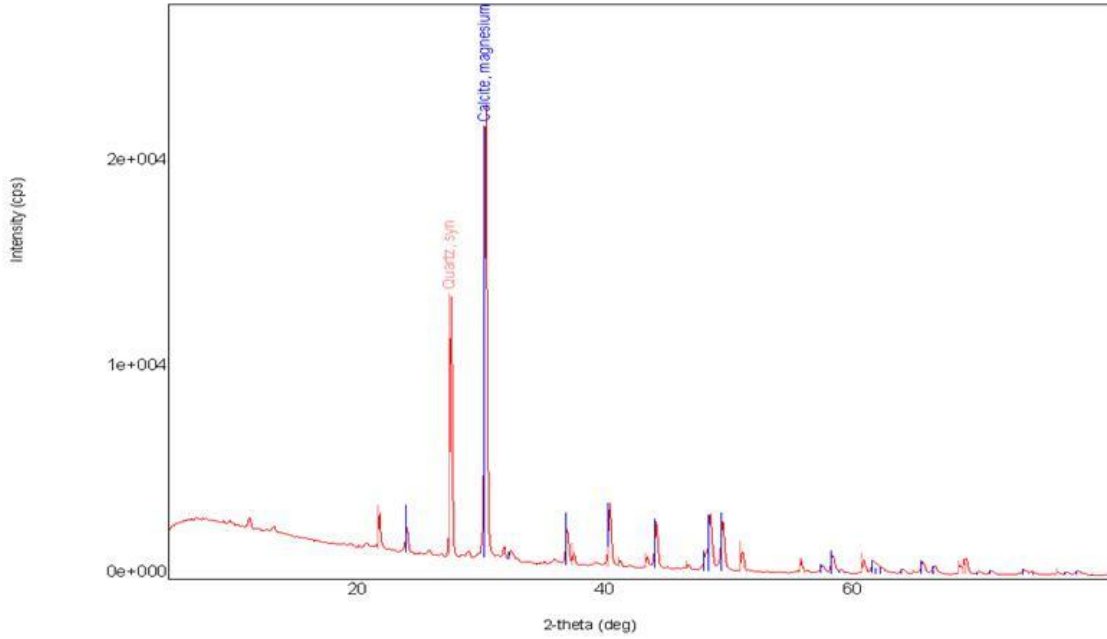
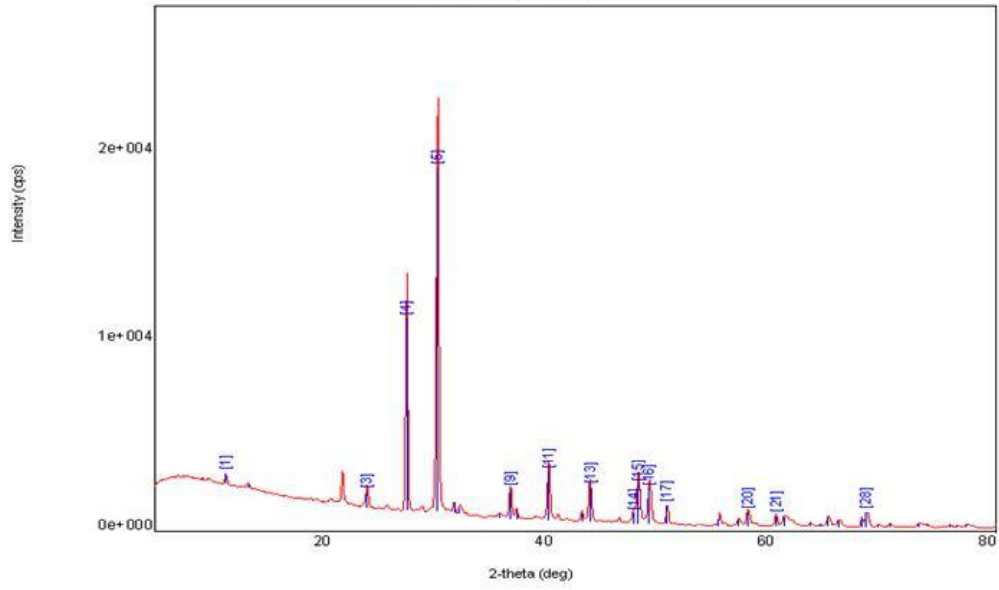
Quantitative analysis results (WPPF)	
Phase name	Content(%)
Calcite	63.9
Quartz	36.1

Sample 11 (8700 ft)



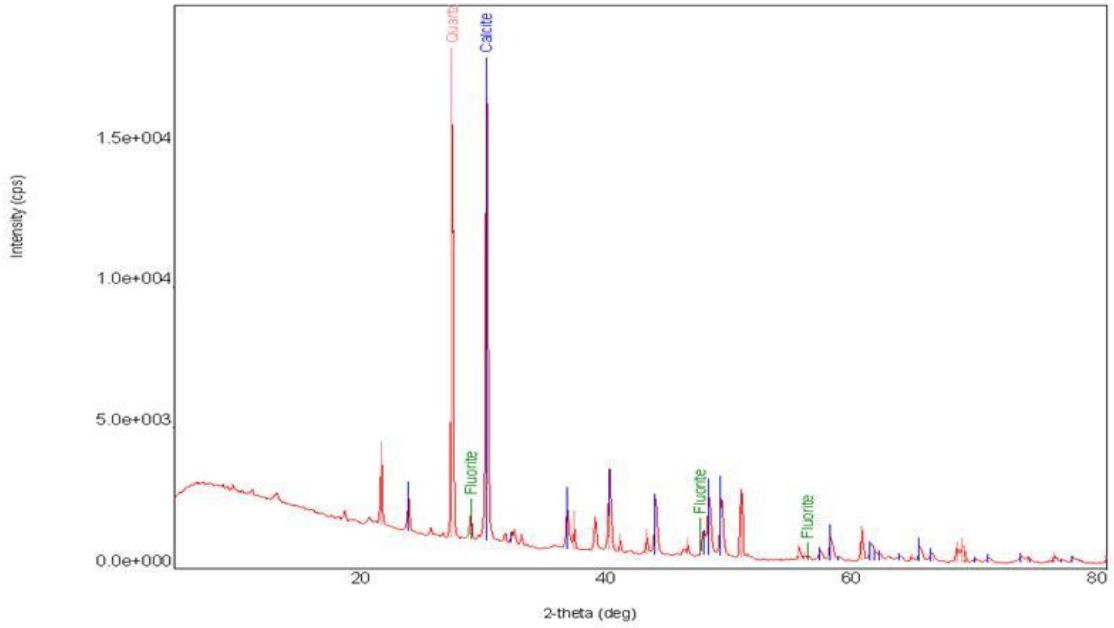
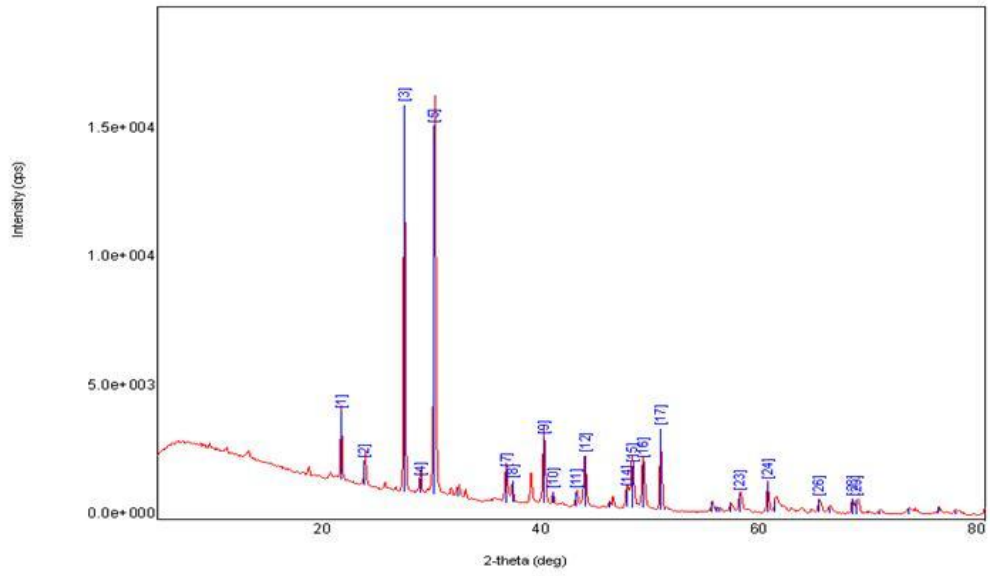
Quantitative analysis results (WPPF)	
Phase name	Content(%)
Calcite	64.8
Quartz	31.2
Calcium Chloride Hydroxide	5

Sample 12 (8900 ft)



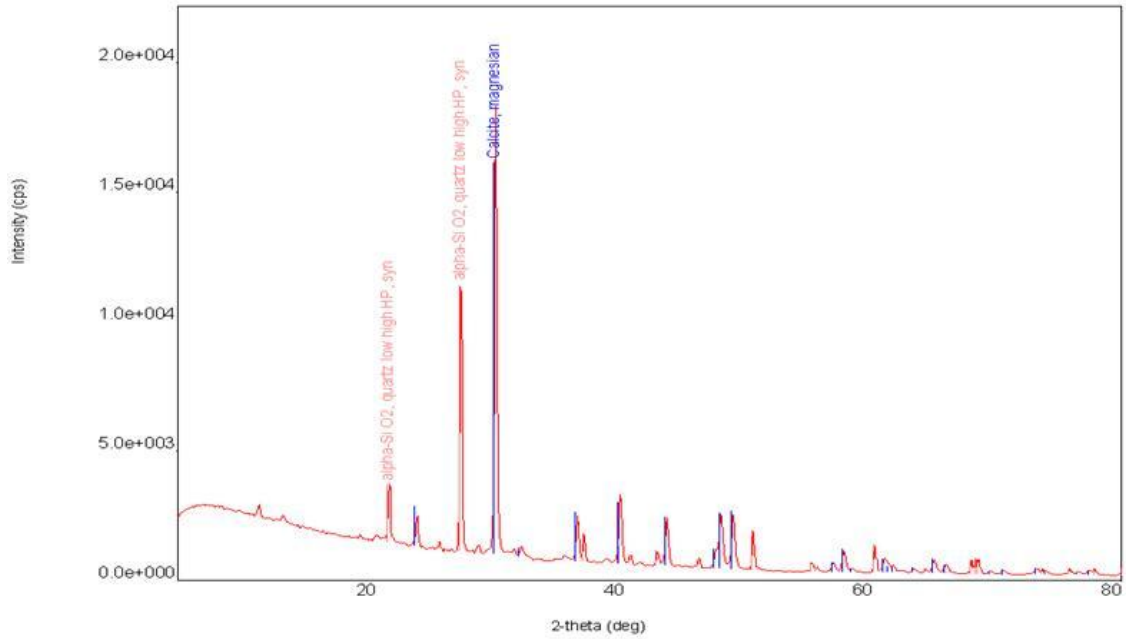
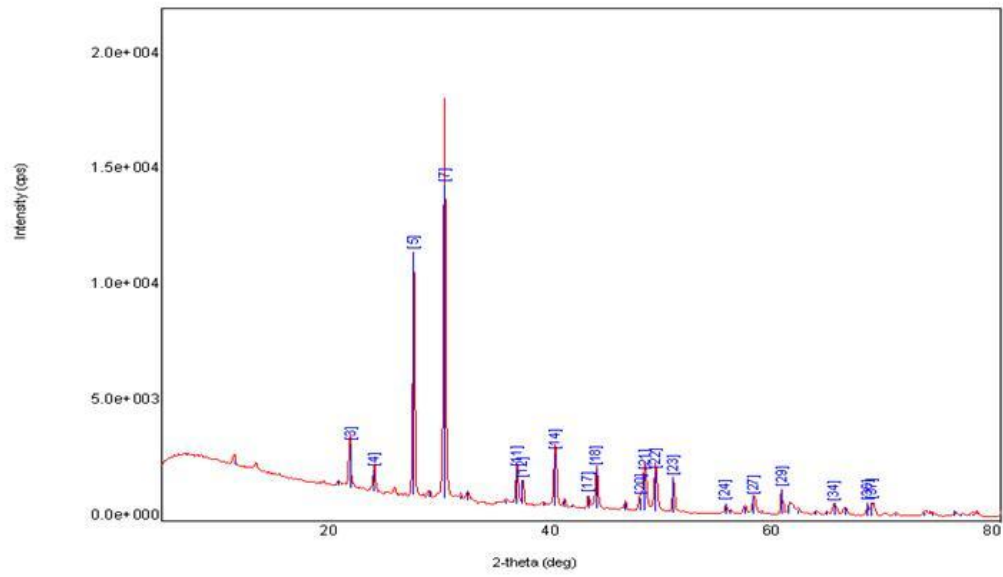
Quantitative analysis results (WPPF)	
Phase name	Content(%)
Calcite	69.5
Quartz	30.5

Sample 13 (9100 ft)



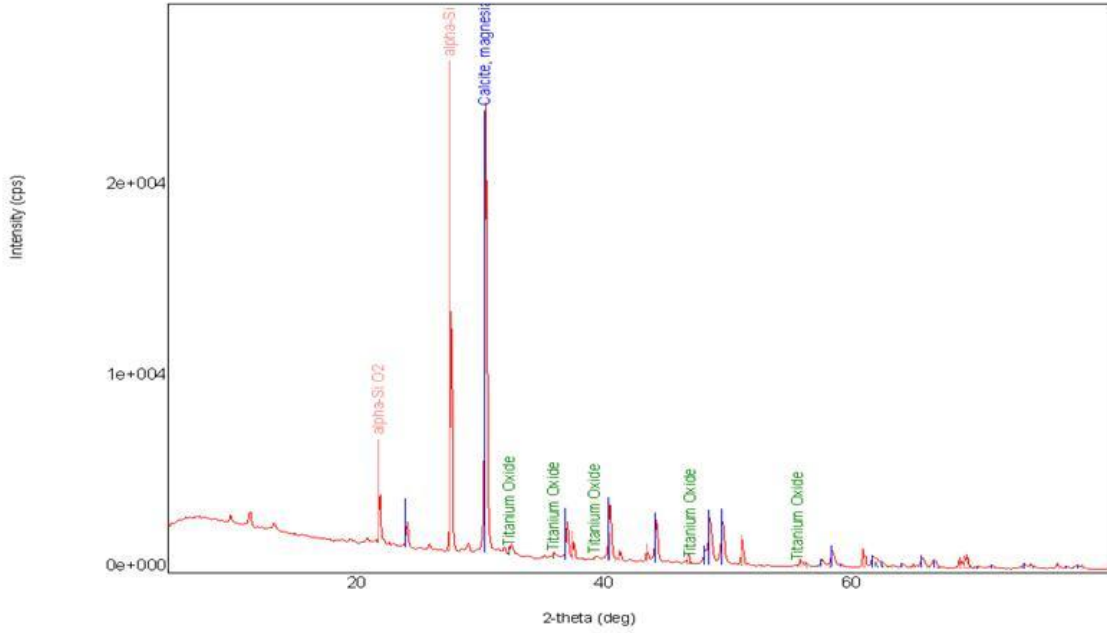
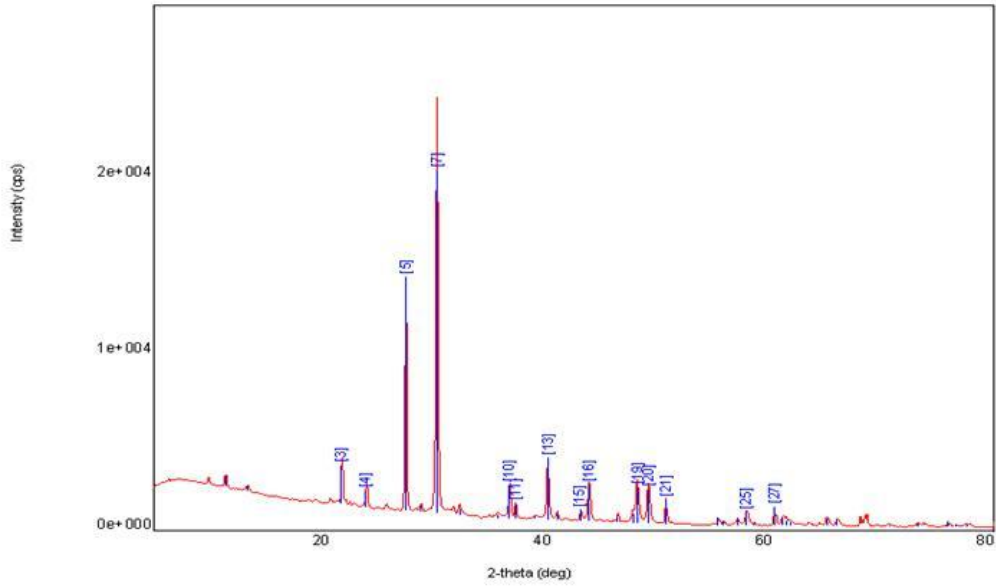
Quantitative analysis results (WPPF)	
Phase name	Content(%)
Calcite	48
Quartz	42
Fluorite	10

Sample 14 (9300 ft)



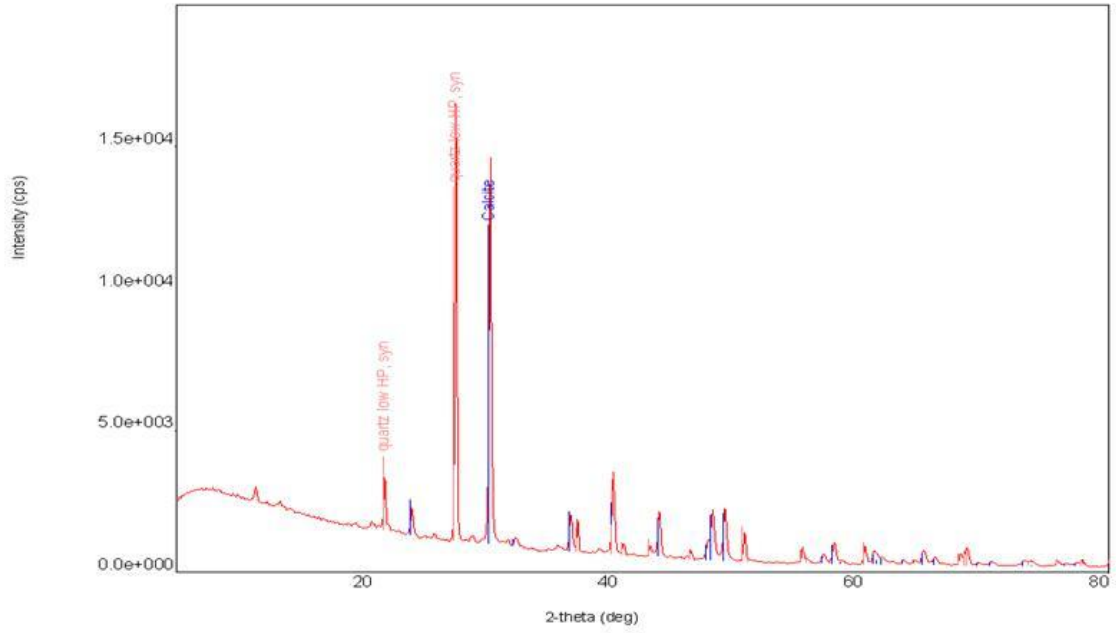
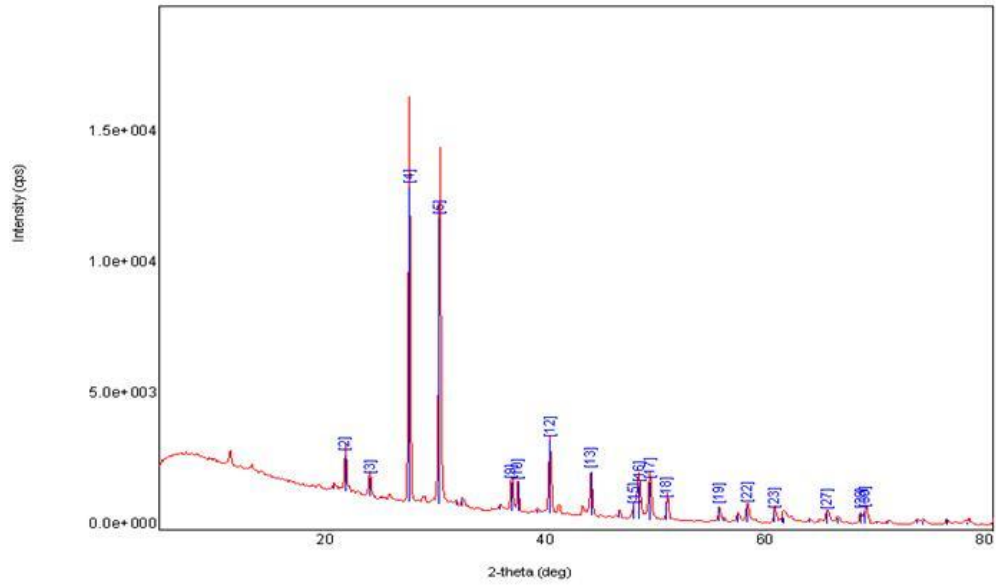
Quantitative analysis results (WPPF)	
Phase name	Content(%)
Calcite	64.1
Quartz	35.9

Sample 15 (9500 ft)



Quantitative analysis results (WPPF)	
Phase name	Content(%)
Calcite	40.1
Quartz	56
Titanium Oxide	4

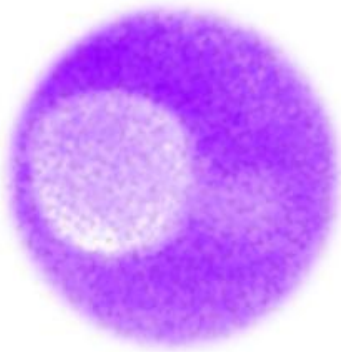
Sample 16 (9675 ft)



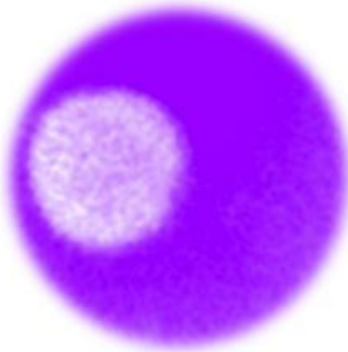
Quantitative analysis results (WPPF)	
Phase name	Content(%)
Calcite	54.2
Quartz	45.8

APPENDIX-C (CT SCAN RESULTS)

Sample 1 (6700 ft)
(sand = 22%)



Layer 1



Layer 2



Layer 3

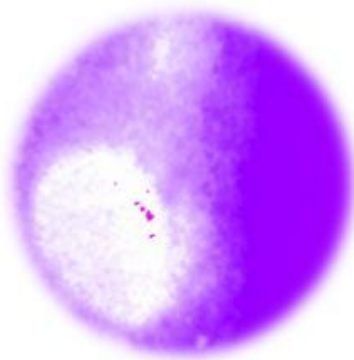


Layer 4



Layer 5

**Sample 2 (6900 ft)
(sand = 11.4%)**



Layer 1



Layer 2



Layer 3

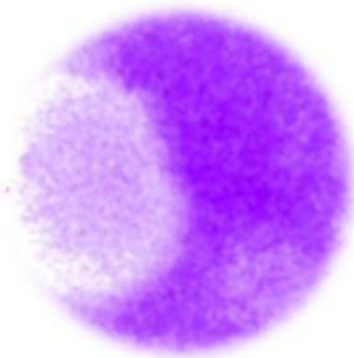


Layer 4

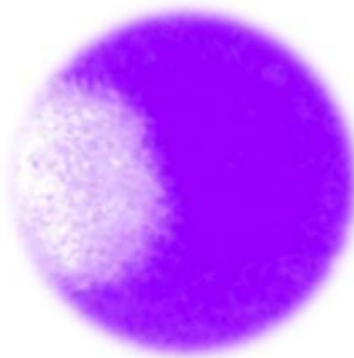


Layer 5

Sample 8 (8100 ft)
(sand = 33%)



Layer 1



Layer 2



Layer 3

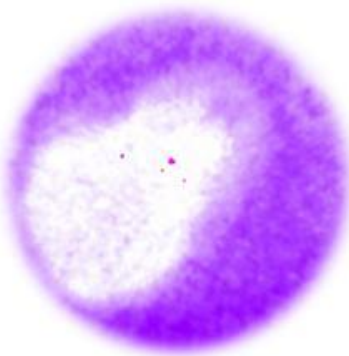


Layer 4

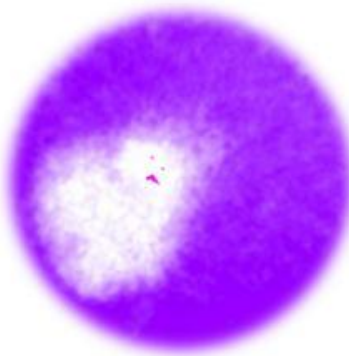


Layer 5

Sample 10 (8500 ft)
(sand = 36.1%)



Layer 1



Layer 2



Layer 3

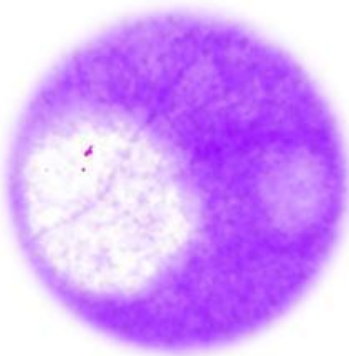


Layer 4



Layer 5

Sample 16 (9675 ft)
(sand = 45.8%)



Layer 1



Layer 2



Layer 3



Layer 4



Layer 5

VITAE

NAME: Badr Salem Ba geri
ADDRESS: Ber Al-Madeni, Bour,
Seyion, Hadramout,
Yemen
E-MAIL: Bageri.b@gmail.com
Mob. No. 00966535101971
DATE OF BIRTH: August, 27 1982
NATIONALITY: Yemeni

EDUCATIONAL QUALIFICATION:

M.S (Petroleum Engineering)

May 2012

King Fahd University of Petroleum and Minerals
Dhahran, Saudi Arabia.

B.S. (Petroleum Engineering)

July 2007.

Hadramout University for Science &Technology
Hadramout, Yemen.